DESIGN AND VALIDATION OF A STRUCTURAL HEALTH MONITORING SYSTEM FOR AERONAUTICAL STRUCTURES

by

Diego Alexander Tibaduiza Burgos

Supervised by

Dr. José Rodellar Benedé
Dr. Luis Eduardo Mujica

DOCTORAL THESIS
Departament de Matemàtica Aplicada III
Universitat Politècnica de Catalunya
Barcelona, Spain
September, 2012

UNIVERSITAT POLITÈCNICA DE CATALUNYA
DEPARTAMENT DE MATEMÁTICA APLICADA III

ABSTRACT

DESIGN AND VALIDATION OF A STRUCTURAL HEALTH MONITORING SYSTEM FOR AERONAUTICAL STRUCTURES

by Diego Alexander Tibaduiza Burgos

ADVISORS:
Dr. José Rodellar
Dr. Luis E. Mujica

September, 2012
Barcelona, Spain

Structural Health Monitoring (SHM) is an area where the main objective is the verification of the state or the health of the structures in order to ensure proper performance and maintenance cost savings using a sensor network attached to the structure, continuous monitoring and algorithms. Different benefits are derived from the implementation of SHM, some of them are: knowledge about the behavior of the structure under different loads and different environmental changes, knowledge of the current state in order to verify the integrity of the structure and determine whether a structure can work properly or whether it needs to be maintained or replaced and, therefore, to reduce maintenance costs. The paradigm of damage identification (comparison between the data collected from the structure without damages and the current structure in order to determine if there are any changes) can be tackled as a pattern recognition problem. Some statistical techniques as Principal Component Analysis (PCA) or Independent Component Analysis (ICA) are very useful for this purpose because they allow obtaining the most relevant information from a large amount of variables.

This thesis uses an active piezoelectric system to develop statistical data driven approaches for the detection, localization and classification of damages in structures. This active piezoelectric system is permanently attached to the surface of the structure under test in order to apply vibrational excitations and sensing the dynamical responses propagated through the structure at different points. As pattern recognition technique, PCA is used to perform the main task of the proposed methodology: to build a base-line model of the structure without damage

and subsequently to compare the data from the current structure (under test) with this model. Moreover, different damage indices are calculated to detect abnormalities in the structure under test. Besides, the localization of the damage can be determined by means of the contribution of each sensor to each index. This contribution is calculated by several different methods and their comparison is performed. To classify different damages, the damage detection methodology is extended using a Self-Organizing Map (SOM), which is properly trained and validated to build a pattern baseline model using projections of the data onto the PCA model and damage detection indices. This baseline is further used as a reference for blind diagnosis tests of structures. Additionally, PCA is replaced by ICA as pattern recognition technique. A comparison between the two methodologies is performed highlighting advantages and disadvantages. In order to study the performance of the damage classification methodology under different scenarios, the methodology is tested using data from a structure under several different temperatures.

The methodologies developed in this work are tested and validated using different structures, in particular an aircraft turbine blade, an aircraft wing skeleton, an aircraft fuselage, some aluminium plates and some composite materials plates.

UNIVERSITAT POLITÈCNICA DE CATALUNYA
DEPARTAMENT DE MATEMÁTICA APLICADA III

RESUMEN

DISEÑO Y VALIDACIÓN DE UN SISTEMA DE MONITORIZACIÓN DE DAÑOS EN ESTRUCTURAS AERONÁUTICAS

por Diego Alexander Tibaduiza Burgos

DIRECTORES:
Dr. José Rodellar
Dr. Luis E. Mujica

Septiembre, 2012
Barcelona, España

La monitorización de daños en estructuras (SHM por sus siglas en inglés) es un área que tiene como principal objetivo la verificación del estado o la salud de la estructura con el fin de asegurar el correcto funcionamiento de esta y ahorrar costos de mantenimiento. Para esto se hace uso de sensores que son adheridos a la estructura, monitorización continua y algoritmos. Diferentes beneficios se obtienen de la aplicación de SHM, algunos de ellos son: el conocimiento sobre el desempeño de la estructura cuando esta es sometida a diversas cargas y cambios ambientales, el conocimiento del estado actual de la estructura con el fin de determinar la integridad de la estructura y definir si esta puede trabajar adecuadamente o si por el contrario debe ser reparada o reemplazada con el correspondiente beneficio del ahorro de gastos de mantenimiento. El paradigma de la identificación de daños (comparación entre los datos obtenidos de la estructura sin daños y la estructura en un estado posterior para determinar cambios) puede ser abordado como un problema de reconocimiento de patrones. Algunas técnicas estadísticas tales como Análisis de Componentes Principales (PCA por sus siglas en inglés) o Análisis de Componentes Independientes (ICA por sus siglas en ingles) son muy útiles para este propósito puesto que permiten obtener la información más relevante de una gran cantidad de variables.

Esta tesis hace uso de un sistema piezoeléctrico activo para el desarrollo de algoritmos estadísticos de manejo de datos para la detección, localización y clasificación de daños en estructuras. Este sistema piezoeléctrico activo está permanentemente adherido a la superficie

de la estructura bajo prueba con el objeto de aplicar señales vibracionales de excitación y recoger las respuestas dinámicas propagadas a través de la estructura en diferentes puntos. Como técnica de reconocimiento de patrones se usa Análisis de Componentes Principales para realizar la tarea principal de la metodología propuesta: construir un modelo PCA base de la estructura sin daño y posteriormente compararlo con los datos de la estructura bajo prueba. Adicionalmente, algunos índices de daños son calculados para detectar anormalidades en la estructura bajo prueba. Para la localización de daños se usan las contribuciones de cada sensor a cada índice, las cuales son calculadas mediante varios métodos de contribución y comparadas para mostrar sus ventajas y desventajas.

Para la clasificación de daños, se amplia la metodología de detección añadiendo el uso de Mapas auto-organizados, los cuales son adecuadamente entrenados y validados para construir un modelo patrón base usando proyecciones de los datos sobre el modelo PCA base e índices de detección de daños. Este patrón es usado como referencia para realizar un diagnóstico ciego de la estructura. Adicionalmente, dentro de la metodología propuesta, se utiliza ICA en lugar de PCA como técnica de reconocimiento de patrones. Se incluye también una comparación entre la aplicación de las dos técnicas para mostrar las ventajas y desventajas. Para estudiar el desempeño de la metodología de clasificación de daños bajo diferentes escenarios, esta se prueba usando datos obtenidos de una estructura sometida a diferentes temperaturas.

Las metodologías desarrolladas en este trabajo fueron probadas y validadas usando diferentes estructuras, en particular un álabe de turbina, un esqueleto de ala y un fuselaje de avión, así como algunas placas de aluminio y de material compuesto.

Contents

Contents v

List of Figures ix

1 INTRODUCTION 1
- 1.1 Introduction . . . 1
- 1.2 Main contribution . . . 5
- 1.3 Objectives . . . 6
- 1.4 General results . . . 6
- 1.5 Research framework . . . 9
- 1.6 Organization . . . 9

2 THEORETICAL BACKGROUND 11
- 2.1 Introduction . . . 11
- 2.2 Waves in plates . . . 11
  - 2.2.1 Sound wave propagation . . . 11
  - 2.2.2 Lamb waves . . . 12
  - 2.2.3 Dispersion curves . . . 13
- 2.3 Principal Component Analysis (PCA) . . . 14
- 2.4 Damage detection indices based on PCA . . . 16
  - 2.4.1 Contribution analysis based on PCA . . . 17
- 2.5 Independent Component Analysis (ICA) . . . 19
- 2.6 Self-Organizing Map (SOM) . . . 20
- 2.7 Discrete Wavelet Transform . . . 21
- 2.8 Remarks and conclusions . . . 23

3 A REVIEW OF STRUCTURAL HEALTH MONITORING AS PATTERN RECOGNITION 25
- 3.1 Introduction . . . 25
- 3.2 Brief review of the Structural Health Monitoring levels . . . 26
  - 3.2.1 Damage detection . . . 26
  - 3.2.2 Damage localization . . . 28
  - 3.2.3 Damage classification . . . 28
  - 3.2.4 Type and extent of damage . . . 30
  - 3.2.5 Damage prognosis (DP) . . . 30
- 3.3 Structural health monitoring using statistical methods . . . 31

3.3.1 Principal Component Analysis (PCA) . . . 31
3.3.2 Independient Component Analysis (ICA) . . . 33
3.3.3 Other approaches . . . 33

4 CASE STUDIES **37**
4.1 Aluminium plate with reversible damages . . . 37
4.2 Aluminium plate with real (non reversible) damage . . . 39
4.3 Composite plate 1 . . . 39
4.4 Composite plate 2 . . . 41
4.5 Aircraft turbine blade . . . 41
4.6 Aircraft wing skeleton . . . 42
4.7 Aircraft fuselage . . . 44
4.8 Aluminium plate with reversible damages and temperature variations . . . 45

5 DAMAGE DETECTION SYSTEM **47**
5.1 Problem statement . . . 47
5.2 Damage detection methodology . . . 47
5.2.1 Overview . . . 47
5.2.2 Experimental setup and data acquisition . . . 48
5.2.3 Preprocessing . . . 48
5.2.4 Baseline model building and calculation of damage indices using PCA . 50
5.3 Generalization of the methodology . . . 51
5.4 Experimental results . . . 52
5.4.1 By using PCA baseline models . . . 52
5.4.2 By using ICA baseline models . . . 62
5.5 Discussion . . . 63

6 DAMAGE LOCALIZATION SYSTEM **65**
6.1 Damage Localization . . . 65
6.2 Damage Localization Methodology . . . 65
6.3 Experimental Results . . . 66
6.3.1 Aircraft turbine blade . . . 66
6.3.2 Aluminum plate . . . 76
6.4 Discussion . . . 79

7 DAMAGE CLASSIFICATION SYSTEM **81**
7.1 Damage classification . . . 81
7.2 Methodology for damage classification . . . 81
7.2.1 General approach . . . 81
7.2.2 Discrete Wavelet Transform as feature extraction . . . 84
7.3 Experimental results . . . 85
7.3.1 Configurating the baseline pattern . . . 86
7.3.2 Using the baseline pattern for diagnosis . . . 89
7.3.3 Analysis and discussion of the results using DWT . . . 90
7.3.4 Damage classification using ICA . . . 97
7.3.5 Analysis of changes in temperature . . . 99

7.4 Discussion 104

8 CONCLUSIONS AND FUTURE RESEARCH 105
8.1 Observations and concluding remarks 105
8.1.1 Instrumentation and data acquisition 105
8.1.2 Data preprocessing 106
8.1.3 Data driven baseline modeling 107
8.1.4 Damage detection 107
8.1.5 Damage localization 108
8.1.6 Damage classification 109
8.2 General conclusions 110
8.3 Future work 110
8.3.1 Tests with different damages 111
8.3.2 Variation of the environmental conditions 111
8.3.3 Sensor distribution Optimization 111
8.3.4 Sensor fault detection 111
8.3.5 Validation using more complex structures 111
8.3.6 Evaluation of different statistical methods 112

A PUBLICATIONS 113
A.1 Book chapters 113
A.2 Journals 113
A.3 Conferences 114

B STRUCTURAL HEALTH MONITORING LABORATORY 117
B.1 Commercial Solutions 117
B.1.1 Sensor and actuator systems 117
B.1.2 Hardware to acquire and pre-processing the collected signals 118
B.1.3 Software 118
B.2 Structural Health Monitoring Laboratory of the CoDAlab Group 125

Bibliography 129

List of Figures

1.1 Comparison of a SHM system with the human nervous system. 2
1.2 Levels in SHM. 3
1.3 Fighter aircraft F-18 E/F. (a) F/A-18F Super Hornet [19] (b)Schematic diagram with the percentage of structural weight [32]. 3
1.4 Utility of composite structures on A380: monolithic CFRP and thermoplastics [197]. 4
1.5 Utility of composite structures on A380: materials distributions (weight breakdown) [197]. 5

2.1 Vibration modes [13]. 12
2.2 Dispersion curves in an aluminium plate with traction free [114]. 14
2.3 Elements in a Self Organizing Map. 21
2.4 DWT Decomposition Tree. 22

4.1 Aluminium plate. 38
4.2 Damage description and location. 38
4.3 Excitation signal. 38
4.4 Aluminum plate and damage description. 39
4.5 CFRP plate and damages positions. 40
4.6 Damage 3 in the CRFP Composite Plate. 40
4.7 Multilayered composite plate. 41
4.8 Aircraft turbine blade. 42
4.9 Damage distribution on the aircraft turbine blade. 42
4.10 Sections tested with the PZT location. 43
4.11 Damage description. 43
4.12 Airbus A320 Fuselage. 44
4.13 Damage distribution in the Airbus A320 Fuselage. 44
4.14 Damage 1 and 2 in the aircraft fuselage. 45
4.15 Damages in the aluminum plate. 45

5.1 Unfolding the collected data in 3D to bi-dimensional matrix (I×JK). 49
5.2 Group scaling pre-processing. 49
5.3 Baseline definition methodology. 50
5.4 Data projection into the PCA models. 51
5.5 Generalization of the methodology for damage detection considering just one actuator phase. 52
5.6 Distribution of the variance in phase 1, 3, 4 and 7 in the aircraft turbine blade. . 53

5.7 Distribution of the variance in phase 1, 3, 5 and 6 in the aircraft wing skeleton. . 54
5.8 Score 1 vs. score 2 in the aircraft turbine blade in the phases 1, 3, 4 and 7. . . . 55
5.9 Score 1 vs. score 2 in the aircraft wing skeleton in the phases 1, 3, 5 and 6. . . . 56
5.10 T^2-index in the aircraft turbine blade. 57
5.11 T^2-index in the aircraft wing skeleton. 57
5.12 Q-index in the aircraft turbine blade. 58
5.13 Q-index in the aircraft wing skeleton. 59
5.14 I^2-index in the aircraft turbine blade. 60
5.15 I^2-index in the aircraft wing skeleton. 60
5.16 ϕ-index in the aircraft turbine blade. 61
5.17 ϕ-index in the aircraft wing skeleton. 61
5.18 ICA score plots in the aircraft wing skeleton. 62

6.1 Damage Localization Methodology. 66
6.2 Contributions of each PZT transducer to the Q-index. 67
6.3 Contributions of each PZT to T^2-index. 68
6.4 Contributions of each PZT to ϕ-index. 68
6.5 Contributions of each PZT to I^2-index. 69
6.6 Comparison between methods of contribution using PZT 1 as actuator to (a)I^2-index and (b)ϕ-index. 70
6.7 Comparison between methods of contribution using PZT 2 as actuator to (a)I^2-index and (b)ϕ-index. 70
6.8 Comparison between methods of contribution using PZT 3 as actuator to (a)I^2-index and (b)ϕ-index. 71
6.9 Comparison between methods of contribution using PZT 4 as actuator to (a)I^2-index and (b)ϕ-index. 71
6.10 Comparison between methods of contribution using PZT 5 as actuator to (a)I^2-index and (b)ϕ-index. 72
6.11 Comparison between methods of contribution using PZT 6 as actuator to (a)I^2-index and (b)ϕ-index. 72
6.12 Comparison between methods of contribution using PZT 7 as actuator to (a)I^2-index and (b)ϕ-index. 73
6.13 Data fusion in the damage localization methodology. 74
6.14 Interface for damage localization. 75
6.15 Localization of the damage 3 using CDC to Q-index. 75
6.16 Damage localization for damage 1 using CDC to Q-index. 76
6.17 Damage localization with Q-index for the damage 1 using (a) DC, (b) CDC, (c) PDC, (d) ABC, (e) RBC. 77
6.18 Comparison between the methods using Q-index. 77
6.19 Damage localization with T^2-index for the damage 2 using (a) DC, (b) CDC, (c) PDC, (d) ABC, (e) RBC. 78
6.20 Comparison between the methods using $T^2 - index$. 79

7.1 Methodology for damage classification. 82
7.2 SOM training. 83
7.3 Final baseline damage pattern. 84

7.4 Damage detection and classification including the DWT within the Phase 1. . . 85
7.5 Classification of damages using eight scores, both damage indices (T^2 and Q-statistic) and normalization type (a) $histC$, (b) $histD$, (c) var. 87
7.6 Classification of damages using eight scores, Q-statistic and normalization type (a)$histC$, (b)$histD$, (c)var. 87
7.7 Classification of damages using Q-statistic, normalization type $histC$ and (a) 2 scores, (b) 7 scores, (c) 8 scores. 88
7.8 Classification of damages using Q-statistic, normalization type $histD$ and (a) 2 scores, (b) 7 scores, (c) 8 scores. 88
7.9 Classification of damages using Q-statistic, normalization type var and (a) 2 scores, (b) 7 scores, (c) 8 scores. 89
7.10 Tested map using $histC$ normalization, 7 scores and Q-index. 90
7.11 Percentage of cumulative variance in the actuator phase 8 in the aircraft fuselage. 91
7.12 Wavelet decomposition. 92
7.13 Cluster maps varying the number of scores in the aircraft fuselage with the direct signals. 93
7.14 Cluster map for damage classification in the aircraft fuselage, using: (a) direct signals, (b) approximation coefficients and (c) detail coefficients. 95
7.15 U-matrix for damage classification in the aircraft fuselage using: (a) direct signals, (b) approximation coefficients and (c) detail coefficients. 95
7.16 Cluster map for damage classification in the CFRP Plate using: (a) direct signals, (b) approximation coefficients and (c) detail coefficients. 96
7.17 U-matrix for damage classification in the CFRP plate using: (a) direct signals, (b) approximation coefficients and (c) detail coefficients. 97
7.18 Damage classification using 3 Scores and Q-statistic. Figures (a) and (b) show the Cluster Map and the U-matrix using approximation coefficients from DWT and PCA. 98
7.19 Damage classification using 3 Scores and SPE. Figures (a) and (b) show the Cluster Map and the U-matrix using approximation coefficients from DWT and ICA. 98
7.20 Classification of the different baselines at different temperatures using 2 scores and the Q-index. 99
7.21 Classification of the different baselines at 24 C using 2 scores and the Q-index. 100
7.22 Classification of the different baselines at 30 C using 2 scores and the Q-index. 101
7.23 Classification of the different baselines at 35 C using 2 scores and the Q-index. 102
7.24 Classification of the different baselines at 40 C using 2 scores and the Q-index. 102
7.25 Classification of the different baselines at 45 C using 2 scores and the Q-index. 103
7.26 Classification of the different baselines at 50 C using 2 scores and the Q-index. 103

B.1 Smart Layer sensors [3]. 118
B.2 Smart Layer sensors [3]. 118
B.3 Composite Damage Detection System [3]. 119
B.4 Impact Monitoring System [3]. 120
B.5 Hot-Spot Monitoring [3]. 120
B.6 Digitexx SHM system [9]. 120
B.7 Digitexx software for SHM [9]. 121

B.8 SensorRope [8] 121
B.9 SensorRope application [8]. 121
B.10 Robo®Control mageba [12]. 122
B.11 Robo®Control mageba [12]. 122
B.12 Robo®Control general scheme [12]. 122
B.13 Diagnostic & Dynamic Testing Systems[7]. 123
B.14 Long Term Data Collection systems[7]. 123
B.15 Fiber Bragg Grating Interrogation (FBGI) [11]. 123
B.16 Embedded corrosion monitoring [20]. 124
B.17 Stressalert software [15]. 124
B.18 Sensor Highway II [14]. 125
B.19 Laboratory in SHM. 127

Chapter 1

INTRODUCTION

1.1 Introduction

The currently daily passengers flow, merchandise and operations in airports in a global scale suggest increasing the safety in the daily operations in all the elements involved. According to the International Civil Aviation Organization (ICAO) in 2010 the total world volume of scheduled commercial flights began to edge over 30 million per year [89] and still increasing. To ensure the safety, the ICAO promote the systematic implementation of Standards and Recommended Practices (SARPs) for the aviation safety through the following activities:

- Policy and Standardization initiatives
- Monitoring of key safety trends and indicators
- Safety analysis
- Implementing programmes to address safety issues

At airports level, Safety Management Systems (SMS) are defined in order to contribute to the airports to detect and correct safety problems before they result in aircraft accidents or incidents [10], [89]. These management systems are very important because the risk and the probability of an accident are presented in the daily tasks. In addition, there is an increment in this factor due to the higher number of operations which are significative and still rising. As example, in Spain airports during 2011, the total number of passengers was 204.373.288 and the number of merchandise transportation was 671.722.190 according to AENA ("Aeropuertos Españoles y Navegación Aérea") [4]. These quantities associated with value of what is transported daily, provide important reasons for increasing the safety in airport operations and in the involved elements (airplanes, helicopters, etc.). In a low level, each flight company requires to ensure the reliability of its aircrafts during the different phases of the flight (pre-flight, departure and climb, enroute, cruise, descent and landing). To do that, the company needs to guarantee the proper performance of their aircraft structures, navigation systems, communication systems, among other elements. According to [6]: "when an aircraft is being designed and produced, the aviation authority, the manufacturer, and selected industry participants form groups called Maintenance Steering Groups (MSG) and industry steering committees (ISC). These groups, through numerous meetings determine the frequency and scope of aircraft inspections to be peformed. This information is provided to another group called the Maintenance Review Board

(MRB) which will issue their final recommendations to the manufacturer on how an aircraft should be maintained". In general, the inspection of all civil aircraft is determined by the type of operation. The aircraft must also be maintained in an airworthy condition (referred to as continued airworthiness) between those required inspections [6]. Additionally, a preflight inspection is conducted before each flight in ramp, this consists of checking the aircraft by visual examinations and operational tests to detect defects and maladjustments [5]. Many times these inspections have revealed faults and damages in the structures. Recently, for instance some small cracks were discovered in the world's biggest passenger aircraft (Airbus A380) during a routine inspection. To correct this possible problem 20 aircrafts were inspected and according to the vice-president of AIRBUS (Tom Williams): "This is not a fatigue problem, but a problem during the manufacturing process" [1]. Unfortunately, failures of this type have traditionally been detected during routine inspection periods and normally with the use of various non-destructive techniques, but in the case of visual inspections, it is sometimes impossible to detect small structural damages (for instance between each flight). In this sense, Structural Health Monitoring (SHM) borns as a solution to provide tools for early structural damage detection using non-destructive techniques and algorithms.
In a general way, it is possible to compare a SHM system with the human nervous system as in Figure 1.1. In both cases a sensor network is connected to a central system which allows to apply excitation signals and sense the responses from the sensors distributed along the structure. Additionally there is a system for processing the data, which defines the state or the health of the structure.

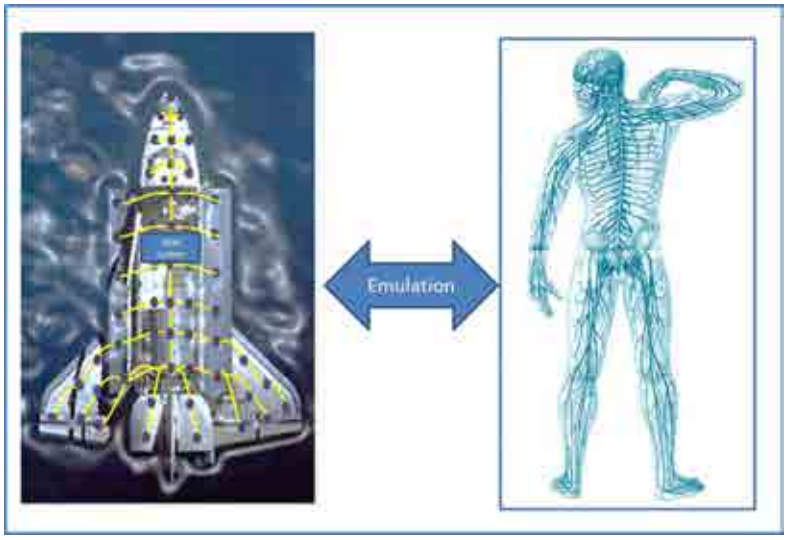

Figure 1.1: Comparison of a SHM system with the human nervous system.

In SHM different levels exist for damage diagnosis [148] in a general way, which can be grouped in four levels (Figure 1.2). The first level corresponds to the damage detection. In this level it is important to know whether there is any change in the structure and if this change is due to a damage. In second level, after detecting a damage, using proper techniques, the position of the damage can be determined. The third level considers the definition of the type of damage and its size. Finally, in the level 4, the remaining lifetime is determined. Recently, an extra level is considered in order to include the capability of auto-healing in smart structures [90].

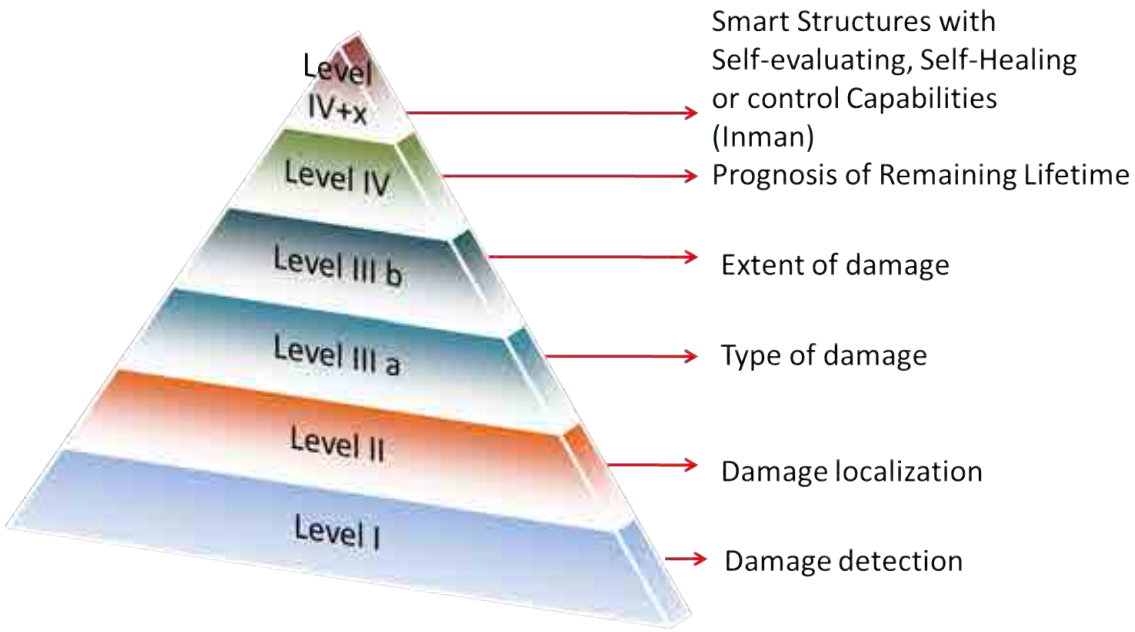

Figure 1.2: Levels in SHM.

Most common applications in SHM are concentrated in the first three levels and there are many applications using different techniques (see Chapter 3). The majority of these implementations include the use of Non-Destructive inspections by means of sensors attached to the structure. These experimental setups normally require to know the structure in order to define which sensor can be used and their distributions in the structure. The variety of sensors and configurations for data acquisition is quite broad as will be shown in the literature review.

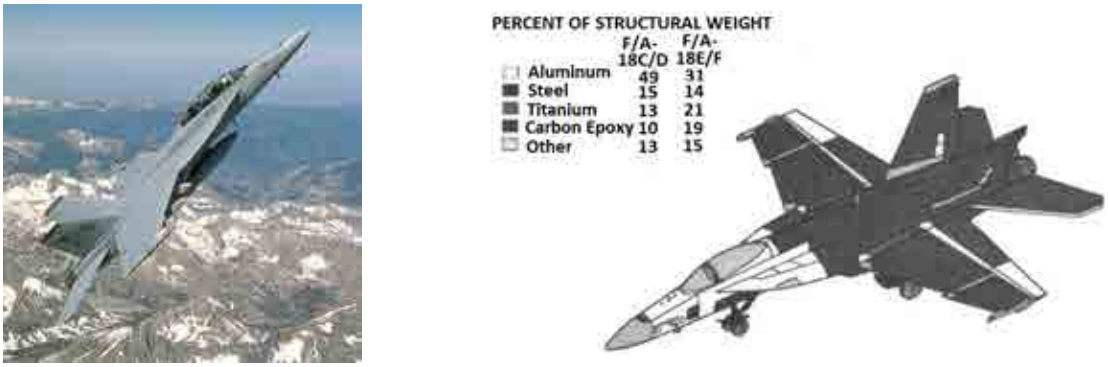

Figure 1.3: Fighter aircraft F-18 E/F. (a) F/A-18F Super Hornet [19] (b)Schematic diagram with the percentage of structural weight [32].

In aeronautic and astronautic areas it is very common the use of aluminium and composite materials for building the structures [197]. Since some years ago (probably since the first introduction into commercial use in 1944 as fuselage skin for Vultee BT-15 trainer plane [85] [197]), the trend in the design of the structures has been directed towards the use of composite materials because the advantages compared with traditional materials as the aluminum allowing the weight-saving among others benefits. There are many examples very useful to show the diversity of the materials currently used in military and commercial applications among others.

For instance, in the U.S. Navy, the F-18 E/F fighter has 31 % of aluminium of the total weight, while the carbon epoxy has the 19 % as can be seen in the Figure 1.3. Other example can be found in the AIRBUS A380, which is one of the biggest commercial aircraft. Although the use of composite materials has increased, the aluminum is still widely used (Figures 1.4 and 1.5).

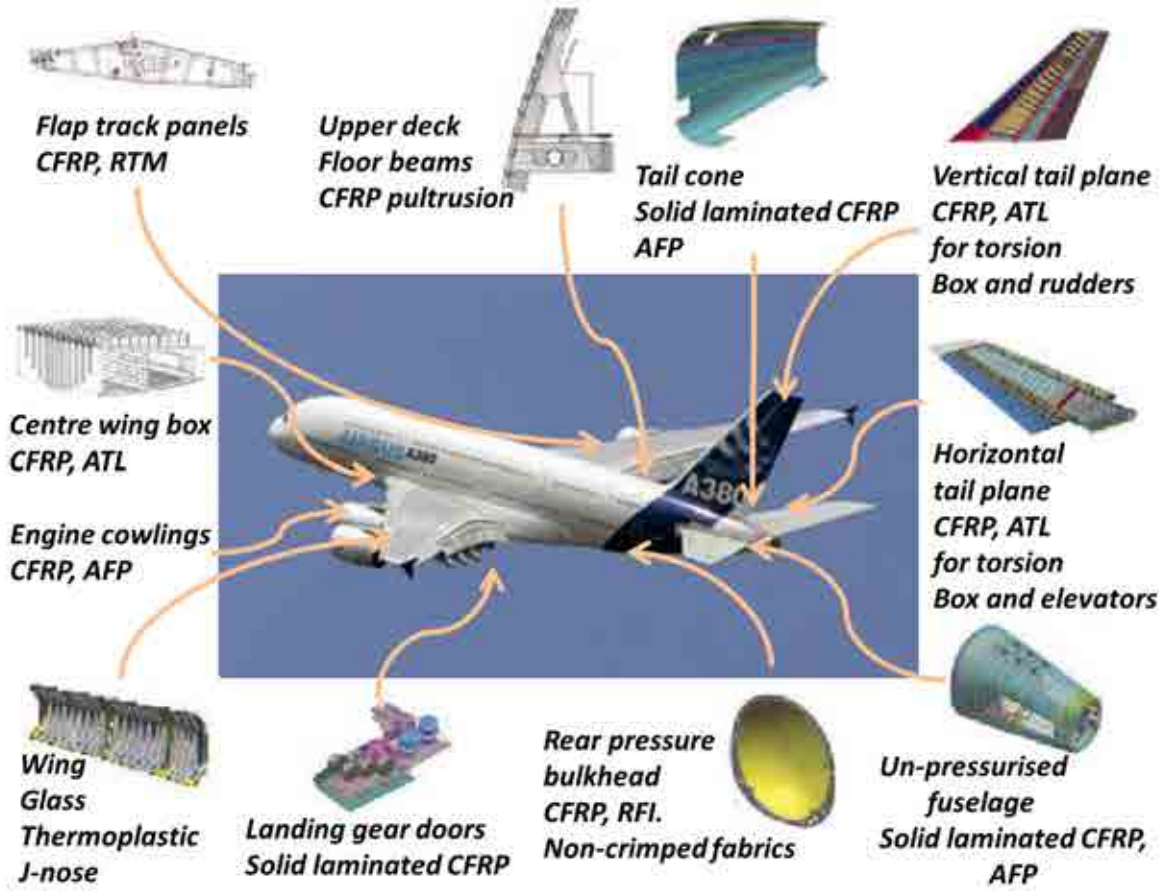

Figure 1.4: Utility of composite structures on A380: monolithic CFRP and thermoplastics [197].

The SHM systems are currently in state of development and the majority of the applications are available in a research level, specially in the aeronautic and astronautic areas. To perform the inspection of the structures in the majority of applications, the structure is isolated and the monitoring is performed under special conditions. In areas as aeronautical and aerospace it is really important to evaluate the health of the structures in normal operational conditions when the element is integrated into the system (aircraft, helicopters, satellites, space shuttle, among others). This reason has motivated the development of new methodologies. An additional motivation is the reduction in the cost of maintenance to avoid that the aircraft goes out of operation for periodical maintenance and to increase the security in the normal operation of the structures.

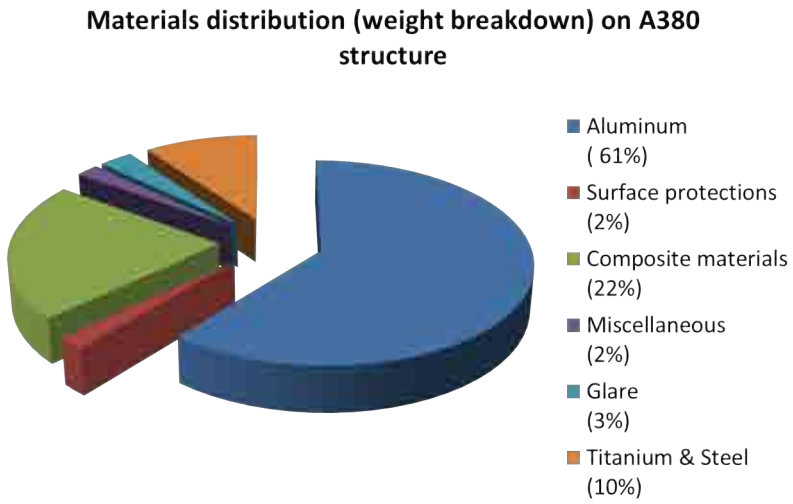

Figure 1.5: Utility of composite structures on A380: materials distributions (weight breakdown) [197].

1.2 Main contribution

As a contribution to the damage detection, localization and classification tasks in SHM, this thesis presents the development of some methodologies that make use of a piezoelectric active system and data driven approaches for the damage identification. The paradigm of damage identification (comparison between the data collected from the structure without damages and the current structure in order to determine if there are any changes) is tackled as a pattern recognition application, where, some statistical techniques and some damage indices are used for data processing and pattern recognition.

In general, a data acquisition system is used to inspect the structures using a BURST signal in different phases. Each phase corresponds to the use of one PZT transducer as actuator and others as sensors. Signals collected from experiments are preprocessed and techniques as Principal Component Analysis (PCA) and Independent Component Analysis (ICA) are used for the analysis and the calculation of some indices in order to define if exist or not any damage, where is it located, and which kind of damage is presented in the structure under test by each phase. Data fusion is applied in the localization and the classification tasks in order to obtain a final result by the combination of the particular analysis in each phase.

The developed methodologies have been subjected to extensive experimental validations: an aircraft wing skeleton, an aircraft turbine blade, an aircraft fuselage, some aluminum plates and some composite materials plates. All the results are included and discussed to demonstrate the validity of the approaches.

1.3 Objectives

The main goal of the current doctoral thesis is to develop a methodology for the detection, localization and classification of damages in aeronautical structures using the paradigm that any damage in the structure produces changes in the vibrational responses. These changes are detected by means of the comparison between the data from the healthy and the current structure under test using statistical techniques. To achieve this goal, the following specific objectives are proposed:

1. To study the problem of monitoring and damage detection in structures.
2. To study the application of statistical techniques as tools for pattern recognition to detect changes in vibrational responses of aircraft structures
3. To propose, implement and evaluate different statistical indices for the detection of damages in aircraft structures
4. To propose, implement and evaluate different methods based on the contributions of each sensor to each index for the localization of damages in aircraft structures
5. To propose, implement and evaluate different methods for the classification of damages in aircraft structures.
6. To validate the methodologies using aircraft and aerospace structures in real-scale as well as small scale structures.

1.4 General results

According to each specific objective, some comments about the results are summarized below. Most extensive descriptions are included in the document.

1. **To study the problem of monitoring and damage detection in structures.**

   The Structural Health Monitoring problem, its applications and current developments were studied and discussed in various scenarios. First, the author participated as assistant in a European course: " Advanced course: Structural Health Monitoring" performed in 2009 in Barcelona-Spain, where some of the most relevant topics and its applications were presented by some of the relevant researchers in the area.

2. **To study the application of statistical techniques as tools for pattern recognition to detect changes in vibrational responses of aircraft structures**

   Several references on these topics were reviewed and organized in Chapter 3. This review makes emphasis on the applications in Structural Health Monitoring that involve statistical methods including PCA, ICA and damage indices.
   Based on the previous works of the advisors of this thesis, the previous review and studies by the author in the first stage of its doctoral studies, Principal Component Analysis is defined as one of the methods used for data driven analysis. Additionally, the

author includes the use of Independent Component Analysis(ICA) in order to compare the results obtained with PCA and generalize the methodologies for the detection, localization and classification.

3. **To propose, implement and evaluate different statistical indices for the detection of damages in aircraft structures**

   The damage detection problem was addressed by means of a general methodology that allows to obtain some damage detection plots by each actuator phase. This methodology is evaluated using two statistical methods. The first one makes use of Principal Component Analysis or the Independent Component Analysis to build the models using the data from the undamaged structure in different phases. In each phase, a PZT transducer is used as actuator and the signals from the other sensors are collected and organized in a matrix for representing the vibrational responses of the structure in different points due to this actuator. To perform the detection, the data from the structure in different states is projected into the models and after these projections are depicted. This methodology was introduced previously by the advisors of this thesis using PCA and now it is extended and applied using ICA as second statistical method for pattern recognition. The methodology was also extended by using four damage indices which are obtained from the models and the projections calculated through PCA.

   Results from the application of this methodology were published in:

   - D.A. Tibaduiza, L.E. Mujica, M. Anaya, J. Rodellar, A. Güemes. Independent Component Analysis for Detecting Damage on Aircraft Wing Skeleton. Presented in: EACS 2012-5th European Conference on Structural Control. Genoa-Italy, June 2012.
   - D.A. Tibaduiza, L.E. Mujica, M. Anaya, J. Rodellar, A. Güemes. Principal Component Analysis vs Independent Component Analysis for Damage Detection. Presented in: The 6th European Workshop on Structural Health Monitoring. Dresden-Germany, July 2012.
   - D.A. Tibaduiza, L.E. Mujica, J. Rodellar. Structural Health Monitoring based on principal component analysis: damage detection, localization and classification. In: Advances in Dynamics, Control, Monitoring and Applications, Universitat Politècnica de Catalunya, Departament de Matemàtica Aplicada III, p. 8-17, 2011.

4. **To propose, implement and evaluate different methods based on the contributions of each sensor to each index for the localization of damages in aircraft structures**

   For damage localization, a methodology was developed using the contributions of each variable to each index. In each index five contribution methods were tested in order to compare the results in the localization of damages and to show the capabilities of the approaches. The results obtained were published in:

   - D.A. Tibaduiza, L.E. Mujica, J. Rodellar. Comparison of Several Methods for Damage Localization Using Indices and Contributions Based on PCA. Presented to: The

9th International Conference on Damage Assessment of Structures. Oxford-UK, July 2011.

- D.A. Tibaduiza, L.E. Mujica, J. Rodellar. Comparison of several methods for damage localization using indices and contributions based on PCA. Journal of Phisycs: Conference Series, 305 012013 doi:10.1088/1742-6596/305/1/012013, 2011.
- D.A. Tibaduiza, L.E. Mujica, M. Anaya, J. Rodellar. Combined and I indices based on Principal Component Analysis for damage detection and localization. Presented to: The 8th International Workshop on Structural Health Monitoring. Stanford-USA, September 2011.
- L.E. Mujica, D.A. Tibaduiza, J. Rodellar. Data-Driven Multiactuator Piezoelectric System for Structural Damage Localization. Presented in: The Fifth World Conference on Structural Control and Monitoring (5WCSCM). Tokyo-Japan, July 2010.

5. **To propose, implement and evaluate different methods for the classification of damages in aircraft structures.**

   In the damage classification task, a methodology was developed by combining the use of PCA or ICA, some damage indices and a Self Organizing Map to perform a generalized analysis of the structure using data fusion with the results from each phase to classify the different structural states of a structure. The results showed that the methodology allows also to perform detection tasks.
   Applications of this methodology were published in:

   - D.A. Tibaduiza, L.E. Mujica, J. Rodellar. Damage Classification in Structural Health Monitoring using Principal Component Analysis and Self Organizing Maps. Accepted for publication in Structural Control and Health Monitoring.
   - D.A. Tibaduiza, M.A. Torres Arredondo, L.E. Mujica, J. Rodellar, C.P. Fritzen. A study of Two Unsupervised Data Driven Statistical Methodologies for Detecting and Classifying Damages in Structural Health Monitoring. Submitted to Mechanical Systems and Signal Processing.
   - M.A. Torres Arredondo, D.A. Tibaduiza, L.E. Mujica, J. Rodellar, C.P. Fritzen. Data Driven Multivariate Algorithms for Damage Detection and Classification: Evaluation and Comparison. Submitted to Structural Health Monitoring An International Journal.
   - D. A. Tibaduiza, L. E. Mujica, A. Güemes, J. Rodellar. Active Piezoelectric System using PCA. Presented in: The Fifth European Workshop on Structural Health Monitoring. Sorrento-Italy, June 2010.

6. **To validate the methodologies using aircraft and aerospace structures in real-scale as well as small scale structures.**

   Different structures were tested and used for the validation of the approaches. In specific terms, three real-scale specimens were studied, the first two corresponds to an aircraft wing skeleton and an aircraft turbine blade which were tested in the Center of

Composites Materials and Smart Structures in the "Universidad Politécnica de Madrid" in Madrid-Spain. The third structure corresponds to an aircraft fuselage which was tested in a research visit in the Siegen University. More details of these structure can be found in the Chapter 4 (case studies). The small-scale validation was performed by means of simplified structures. Specifically, aluminum and composite plates in different configurations were used.

1.5 Research framework

This thesis has been supported in general through the projects: DPI2008-06564 and DPI2011-28033 funded by the Spain Government. The first is: "Smart aircraft structures: Development and validation of a system for monitoring and damage detection (EstAIn)" which is a coordinated project with the Laboratory of Composite Materials and Smart Structures (LCMSS) from "Universidad Politécnica de Madrid" which is leaded by Professor Alfredo Guemes and had as main objective the development and the validation of a experimental monitoring system for damage detection in aeronautical structures based on advanced signal processing and pattern recognition. The second project is a continuation of the first one and included a new partner, IKERLAN, a technological research center from the Vasc Country in Spain. The project is: "Smart Structures: Development and Validation of Monitoring and Damage Identification Systems with Application in Aeronautics and Offshore Wind Energy Plants (AEROLICA)". Its main objective is the development of new monitoring systems and data processing methodologies for damage identification in smart structures, with emphasis in two key industrial sectors: aeronautics and offshore wind energy plant. The project integrates basic research on sensors and model-free, data-driven identification approaches with development of practical algorithms and numerical and experimental validations.

The author was supported by the "Agència de Gestió dAjust Universitaris i de Recerca (AGAUR) of Generalitat de Catalunya by means of a FI-contract for 3 years (Jul-2009 to Jul 2012). Additionally, to perform the research stay at Siegen University, the author was supported by the Spain government by means of the plan: "Movilidad de estudiantes en programas de doctorado con mención hacia la excelencia".

1.6 Organization

In general, the present thesis is organized in seven chapters starting with this introduction where the objectives, general results and research framework and the organization are described. The second chapter includes a theoretical background which covers a brief definition of all the methods used into the proposed methodologies. Afterwards, in the third chapter, a literature review about SHM is presented in order to show the originality of the approaches proposed in the following chapters. The review covers selected aspects of Structural Health Monitoring focusing in statistical methods for pattern recognition. Fourth chapter presents a description of all the structures used to validate the methodologies. The following three chapters are concerning to the development of the methodologies for damage detection, localization and

classification respectively. In detection, the methodology developed makes use of PCA or ICA in order to build a model of the structure by each actuator-phase using data from the structure when it is known as healthy. In a later stage, the data from the structure in different states is projected into the models and these projections and some damage indices are used for the detection. This chapter also includes a comparison between the results obtained by PCA and ICA. In the damage localization chapter, the damage detection methodology is extended using five contribution methods and data fusion to determine the position of the damage in the structure. Each contribution method allows to calculate the contributions of each transducer in the sensor network to each damage index.
For damage classification, in Chapter 7 the damage detection methodology is again extended for classifying different states of a structure using a classifier. For this purpose a Self Organizing Map is used to merge the results of each phase and perform a generalized analysis based on all the data from the sensor network. Finally, the last chapter presents the conclusions and some comments about the methodologies developed and the results obtained.

Chapter 2

THEORETICAL BACKGROUND

2.1 Introduction

The methodologies presented in this thesis are based on data driven analysis. This means that all the information and the analysis is performed by using directly data gathered from experiments. No physical models are used to achieve the damage detection, classification and localization tasks, some statistical techniques for pattern recognition are adapted and applied in order to identify changes in the structures based on their vibrational responses. In particular, the experiments performed to the structures and the methodologies were performed by using a multiactuator system. Lamb waves are produced into the structures through of vibrational excitation signals generated by an active piezoelectric network. A brief description of this kind of waves, the statistical methods and the different tools used in the methodologies are included in this chapter. More details about how these methods are used are presented in the following chapters.

2.2 Waves in plates

2.2.1 Sound wave propagation

Since molecules in solids can vibrate in different directions, there are different kinds of sound waves. These can be characterized in space by oscillatory patterns that are capable of maintaining their shape and propagating in a stable manner. These propagations are also called wave modes [13]. There are different wave types in solids [147] [13] that can be summarized in Table 2.1.

In ultrasonic inspection, the longitudinal and transverse modes are used. These modes can show different types of elliptical or complex vibrations of the particles. Some examples can be seen in [27], [176]. The use of Lamb waves in SHM is very common due to the advantages for detection and the interaction with the structure. Some examples of its use can be found in [142], [72]. For inspecting large structures, this kind of waves are potentially a good solution compared with the conventional ultrasonic inspection. The advantage lies in that lamb waves can be generated in one single point by means of a transducer such as a piezoelectric (PZT). Besides, they can propagate by considerable distances. On the other hand, the use of a piezoelectric

Wave Types in Solids	Particle Vibrations
Longitudinal	Parallel to wave direction
Transverse (Shear)	Perpendicular to wave direction
Surface-Rayleigh	Elliptical orbit-symmetrical mode
Plate Wave-Lamb	Component perpendicular to surface (extensional wave)
Plate Wave-Love	Parallel to plane layer, perpendicular to wave direction
Stoneley(Leaky Rayleigh Waves)	Wave guided along interface
Sezawa	Antisymetric mode

Table 2.1: Wave types in solids [13].

sensor network permanently attached to the structure allows to inspect any time all the structure, while, ultrasonic inspection needs to scan over each point of the structure to assess[24].

2.2.2 Lamb waves

According to [13]: "Lamb waves are complex vibrational waves that propagate parallel to the test surface throughout the thickness of the material. Propagation of Lamb waves depends on the density and the elastic material properties of a component. They are also influenced a great deal by the test frequency and material thickness. Lamb waves are generated at an incident angle in which the parallel component of the velocity of the wave in the source is equal to the velocity of the wave in the test material. Lamb waves will travel several meters in steel and so are useful to scan plate, wire, and tubes".

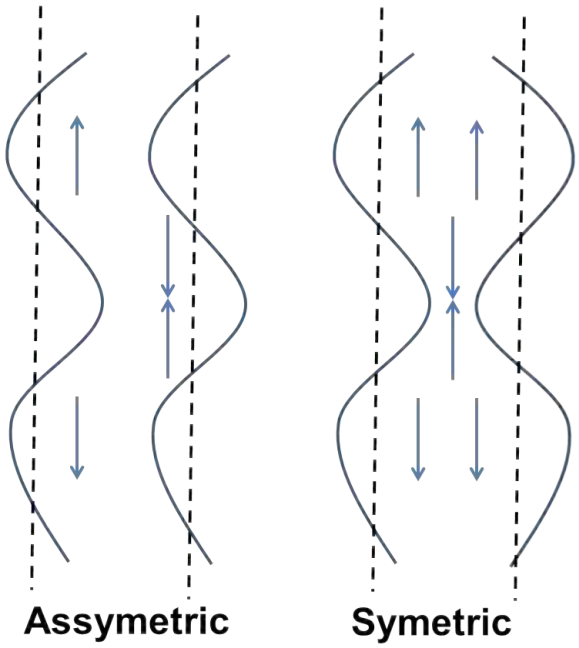

Figure 2.1: Vibration modes [13].

Different vibration modes are possible with lamb waves, the most common are the symmetrical and asymmetrical modes (Figure 2.1). These modes describe elliptical orbits for surface waves [13] and mathematically are defined by the equations 2.1 and 2.2 for the traction free boundary conditions at the surface [94]:

$$\frac{tan(qh)}{tan(ph)} = -\frac{4k^2pq}{(q^2-k^2)^2} \tag{2.1}$$

$$\frac{tan(qh)}{tan(ph)} = -\frac{(q^2-k^2)^2}{4k^2pq} \tag{2.2}$$

where, p, q and k are defined as:

$$p^2 = \left(\frac{w}{c_L}\right)^2 - k^2 \tag{2.3}$$

$$q^2 = \left(\frac{w}{c_T}\right)^2 - k^2 \tag{2.4}$$

and c_L is the longitudinal wave velocity, c_T the shear wave velocity, h is the half of the plate thickness, $w = 2\pi f$ and k is $\frac{2\pi}{\lambda}$ where λ corresponds to the wavelength. The propagation of this kind of waves can be described by the phase velocity and group velocity as shown in the following section.

2.2.3 Dispersion curves

The velocity of propagation of the lamb waves depends of the frequency and other constants of the material where these are propagated. By these reasons the lamb waves are considered as dispersive. To represent the dispersion curves are used, this kind of plots shows how the velocity changes according to the frequency and how the pulses tend to become stretched or dispersed as they propagate [146]. Additionally, it can be used to determine the features about the excitation conditions, such as frequency and angle of incidence, of a desired mode [94]. These features can be calculated solving the wave equation with boundary conditions (Equations 2.1 and 2.2). In addition, they have the advantage that can be generated for all types of structures [146]. As example, Figure 2.2 shows the dispersion curves of one aluminium plates as the described in the section: case studies. The dimensions of this plate are $250mm \times 250mm \times 2mm$. In the Figure, the dispersion curves are labeled as S0, A0, S1, A1 and so forth, depending on whether the mode is symmetric or antisymmetric.

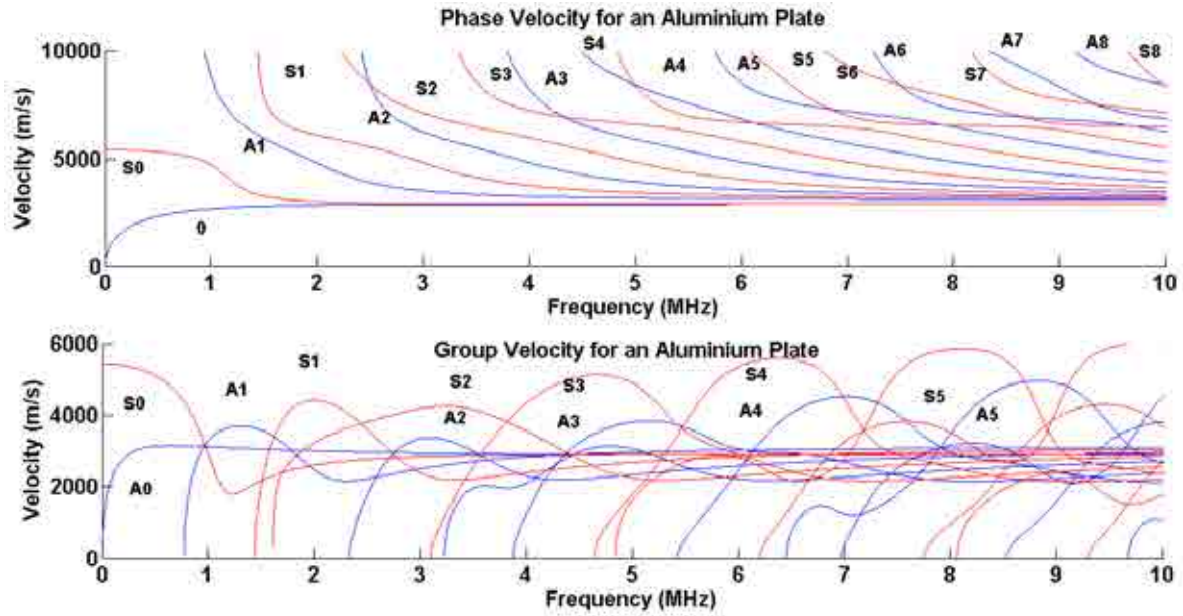

Figure 2.2: Dispersion curves in an aluminium plate with traction free [114].

2.3 Principal Component Analysis (PCA)

Principal Component Analysis (PCA) is a technique of multivariable and megavariate analysis [96] which may provide arguments for how to reduce a complex data set to a lower dimension and reveal some hidden and simplified structure/patterns that often underlie it. It was developed by Karl Pearson in 1901 and integrated to the mathematical statistics in 1933 by Harold Hotelling [123]. The goal of PCA is to discern which dynamics are more important in the system, which are redundant and which are just noise. This goal is essentially achieved by determining a new space (coordinates) to re-express the original data filtering that noise and redundancies based on the variance-covariance structure of the original data. PCA can be also considered as a simple, non-parametric method for data compression and information extraction, which finds combinations of variables or factors that describe major trends in a confusing data set. Among their objectives it can be mentioned: to generate new variables that could express the information contained in the original set of data, to reduce the dimensionality of the problem that is studied and to eliminate some original variables if its information is not relevant. In order to develop a PCA model it is necessary to arrange the collected data in a matrix $\mathbf{X}$. This $n \times m$ matrix contains information from m sensors and n experimental trials [124]. Since physical variables and sensors have different magnitudes and scales, each data-point is scaled using the mean of all measurements of the sensor at the same time and the standard deviation of all measurements of the sensor. Once the variables are normalized, the covariance matrix $\mathbf{C}_x$ is calculated as follows:

$$\mathbf{C}_x = \frac{1}{n-1}\mathbf{X}^T\mathbf{X} \tag{2.5}$$

It is a square symmetric $m \times m$ matrix that measures the degree of linear relationship within the data set between all possible pairs of variables (sensors). The subspaces in PCA are defined

by the eigenvectors and eigenvalues of the covariance matrix as follows:

$$\mathbf{C}_x\widetilde{\mathbf{P}} = \widetilde{\mathbf{P}}\Lambda \tag{2.6}$$

where the eigenvectors of $\mathbf{C}_x$ are the columns of $\widetilde{\mathbf{P}}$ and the eigenvalues are the diagonal terms of Λ (the off-diagonal terms are zero). Columns of matrix $\widetilde{\mathbf{P}}$ are sorted according to the eigenvalues by descending order and they are called as (by some authors) Principal Components of the data set or loading vectors. The eigenvectors with the highest eigenvalue represents the most important pattern in the data with the largest quantity of information. Choosing only a reduced number $r < n$ of principal components, those corresponding to the first eigenvalues, the reduced transformation matrix could be imagined as a model for the structure. In this way, the new matrix $\mathbf{P}$ ($\widetilde{\mathbf{P}}$ sorted and reduced) can be called as PCA model. Geometrically, the transformed data matrix $\mathbf{T}$(score matrix) represents the projection of the original data over the direction of the principal components $\mathbf{P}$:

$$\mathbf{T} = \mathbf{XP} \tag{2.7}$$

In the full dimension case (using $\widetilde{\mathbf{P}}$), this projection is invertible (since $\widetilde{\mathbf{P}}\widetilde{\mathbf{P}}^T = \mathbf{I}$) and the original data can be recovered as $\mathbf{X} = \mathbf{T}\widetilde{\mathbf{P}}^T$. In the reduced case (using $\mathbf{P}$), with the given $\mathbf{T}$, it is not possible to fully recover $\mathbf{X}$, but $\mathbf{T}$ can be projected back onto the original m-dimensional space and obtain another data matrix as follows:

$$\hat{\mathbf{X}} = \mathbf{TP}^T = (\mathbf{XP})\mathbf{P}^T \tag{2.8}$$

Therefore, the residual data matrix (the error for not using all the principal components) can be defined as the difference between the original data and the projected back.

$$\mathbf{E} = \mathbf{X} - \hat{\mathbf{X}} \tag{2.9}$$

$$\mathbf{E} = \mathbf{X} - \mathbf{XPP}^T \tag{2.10}$$

$$\mathbf{E} = \mathbf{X}(\mathbf{I} - \mathbf{PP}^T) \tag{2.11}$$

To perform PCA is simple in practice through the basic steps [124]:

1. Organize the data set as an $n \times m$ matrix, where m is the number of measured variables and n is the number of trials.

2. Normalize the data to have zero mean and unity variance.

3. Calculate the eigenvectors - eigenvalues of the covariance matrix.

4. Select the first eigenvectors as the principal components.

5. Transform the original data by means of the principal components (projection).

2.4 Damage detection indices based on PCA

PCA is a well known statistical technique that has been used as a pattern recognition technique by several years with excellent result. Its use allows to obtain pattern that often underlie from the data by calculating the principal components and re-expressing the information in a new space. In this thesis, PCA allows to define patterns from the structure when it is known as healthy to define the baseline by each actuator phase as will be shown in the following chapters.

A comparison between dynamical responses of the structure to analyze and a baseline (pattern) allows to determine if exist some changes and, besides, whether these changes can be considered as a damage or not. Transforming or projecting data from different states of the structure by using PCA would permit an easy comparison between them. Sometimes these projections are not enough and it is necessary the use of some statistical measurements that can be considered as damage indices.

There are several kinds of fault detection indices [23]. Two well-known indices are commonly used to this aim: the $Q - index$ (or $SPE - index$), the Hotelling's $T^2 - statistic$ ($D - statistic$). The first one is based on analyzing the residual data matrix $\widetilde{X}$ to represent the variability of the data projection in the residual subspace [124]. The second method is based on analyzing the score matrix **T** to check the variability of the projected data in the new space of the principal components.

There exist another types of indices reported in the literature as combined index ($\phi - index$) [198] and $I^2 - index$ [84], which have been used in control process and clinical studies. The first one is a combination of the $Q - index$ and $T^2 - index$ and was proposed as a convenient alternative for merging information from both into a single value [198]. The second one is used in meta-analysis and can be interpreted as a percentage of heterogeneity. In a general way, it is possible to define any index [23] in the form:

$$\textbf{Index} = \boldsymbol{x}^T \mathbf{M} \boldsymbol{x} \tag{2.12}$$

where the column vector $\boldsymbol{x}$ represents measurements from all the sensors at a specific experiment trial (a row of $\boldsymbol{x}$). Matrix **M** is a $m \times m$ squared matrix and depends of the type of index as follows:

$$Q - index = \boldsymbol{x}^T \mathbf{M}_Q \boldsymbol{x} = \boldsymbol{x}^T (\mathbf{I} - \mathbf{P}\mathbf{P}^T) \boldsymbol{x} \tag{2.13}$$

$$T^2 - index = \boldsymbol{x}^T \mathbf{M}_T \boldsymbol{x} = \boldsymbol{x}^T (\mathbf{P}\Lambda^{-1}\mathbf{P}^T) \boldsymbol{x} \tag{2.14}$$

$$\phi - index = (Q - index) + (T^2 - index) = \boldsymbol{x}^T \mathbf{M}_\phi \boldsymbol{x} = \boldsymbol{x}^T (\mathbf{I} - \mathbf{P}\mathbf{P}^T + \mathbf{P}\Lambda^{-1}\mathbf{P}^T) \boldsymbol{x} \tag{2.15}$$

$$I - index = \boldsymbol{x}^T \mathbf{M}_I \boldsymbol{x} \tag{2.16}$$

where:

$$\mathbf{M}_I = \begin{cases} 0, & \text{for } \mathbf{Q} \leq \text{(k-1)}; \\ \frac{\mathbf{Q} - (k-1)}{\mathbf{Q}} * 100\%, & \text{for } \mathbf{Q} > \text{(k-1)}. \end{cases} \tag{2.17}$$

2.4.1 Contribution analysis based on PCA

All the indices presented in the previous section can determine whether there are damages and distinguish between them. However, they do not provide more useful information. Contribution analysis tries to find which variable or variables are the responsible of this distinction. The main idea is to calculate the contribution of each sensor to each index.
In general, any index can be decomposed in the form:

$$Index = \sum_{j=1}^{n} (Contributions) \tag{2.18}$$

where n is the number of sensors

According to [23], five methods can be used for fault detection in process monitoring. In this thesis, these methods are used for damage localization in structures. These methodologies are used to calculate the contribution of each sensor to each index in each experiment test. In this way, it is expected that the damage is located between the actuator and the sensor that contains the largest contribution.

1. Complete Decomposition Contributions (CDC)
   Complete Decomposition Contributions, also called contribution plots by some authors, are well known diagnostic tools for fault identification in processes [123]. In each index indicate the significance of the effect of each variable on the index. In general, this is based on the idea that the variables with the largest contribution to the damage detection index defines the presence of abnormalities. The contribution of the variable (or sensor) j to the index is defined as:

$$Index = \boldsymbol{x}^T \mathbf{M} \boldsymbol{x} = \|\mathbf{M}^{\frac{1}{2}} \mathbf{x}\|^2 \tag{2.19}$$

$$Index = \sum_{j=1}^{n} (\xi_j^T \mathbf{M}^{\frac{1}{2}} \boldsymbol{x})^2 = \sum_{j=1}^{n} \mathbf{CDC}_j^{Index} \tag{2.20}$$

$$\mathbf{CDC}_j^{Index} = \boldsymbol{x}^T \mathbf{M}^{\frac{1}{2}} \xi_j \xi_j^T \mathbf{M}^{\frac{1}{2}} \boldsymbol{x} \tag{2.21}$$

   where ξ_j is the j^{th} column of the identity matrix.

2. Partial Decomposition Contributions (PDC)
   This method decomposes a damage detection index as the summation of variable contributions.

$$\mathbf{PDC}_j^{Index} = \boldsymbol{x}^T \mathbf{M} \xi_j \xi_j^T \boldsymbol{x} \tag{2.22}$$

3. Diagonal Contributions(DC)
   The diagonal contribution remove the cross-talk among variables. The DC is defined as:

$$\mathbf{DC}_j^{Index} = \boldsymbol{x}^T \xi_j \xi_j^T \mathbf{M} \xi_j \xi_j^T \boldsymbol{x} \tag{2.23}$$

4. Reconstruction Based Contributions (RBC)
   The Reconstruction-Based Contribution [22] is an approach that uses the amount of reconstruction of a damage detection index along a variable direction as the contribution of that variable to the index. The RBC is defined as:

$$\mathbf{RBC}_j^{Index} = \boldsymbol{x}^T\mathbf{M}\xi_j(\xi_j^T\mathbf{M}\xi_j)^{-1}\xi_j^T\mathbf{M}\boldsymbol{x} \tag{2.24}$$

$$\mathbf{RBC}_j^{Index} = \frac{(\xi_j^T\mathbf{M}\mathbf{x})^2}{(\xi_j^T\mathbf{M}\xi_j)} \tag{2.25}$$

5. Angle-Based Contributions (ABC)

$$\overline{\xi}_j = \mathbf{M}^{\frac{1}{2}}\xi_j \tag{2.26}$$

$$\overline{x} = \mathbf{M}^{\frac{1}{2}}\mathbf{x} \tag{2.27}$$

   The ABC of Variable j is the squared cosine of the angle between

$$\mathbf{ABC}_j^{Index} = (\frac{\xi_j^T\overline{\boldsymbol{x}}}{\|\overline{\xi}_j\|\|\overline{\boldsymbol{x}}\|})^2 = \frac{(\xi_j^T\mathbf{M}\boldsymbol{x})^2}{\xi_j^T\mathbf{M}\xi_j\boldsymbol{x}^T\mathbf{M}\boldsymbol{x}} \tag{2.28}$$

$$\mathbf{ABC}_j^{Index} = \frac{\mathbf{RBC}_j^{Index}}{Index(x)} \tag{2.29}$$

Table 2.2 summarizes the contributions obtained by the above 5 methods to the four indices(Equations 2.21-2.29).

	Q	T^2	ϕ	I^2
CDC	$\boldsymbol{x}^T\mathbf{M}_Q^{\frac{1}{2}}\xi_j\xi_j^T\mathbf{M}_Q^{\frac{1}{2}}\boldsymbol{x}$	$\boldsymbol{x}^T\mathbf{M}_T^{\frac{1}{2}}\xi_j\xi_j^T\mathbf{M}_T^{\frac{1}{2}}\boldsymbol{x}$	$\boldsymbol{x}^T\mathbf{M}_\phi^{\frac{1}{2}}\xi_j\xi_j^T\mathbf{M}_\phi^{\frac{1}{2}}\boldsymbol{x}$	$\boldsymbol{x}^T\mathbf{M}_I^{\frac{1}{2}}\xi_j\xi_j^T\mathbf{M}_I^{\frac{1}{2}}\boldsymbol{x}$
PDC	$\boldsymbol{x}^T\mathbf{M}_Q\xi_j\xi_j^T\boldsymbol{x}$	$\mathbf{x}^T\mathbf{M}_T\xi_j\xi_j^T\boldsymbol{x}$	$x^T\mathbf{M}_\phi\xi_j\xi_j^T\boldsymbol{x}$	$\boldsymbol{x}^T\mathbf{M}_I\xi_j\xi_j^T\boldsymbol{x}$
DC	$\boldsymbol{x}^T\xi_j\xi_j^T\mathbf{M}_Q\xi_j\xi_j^T\boldsymbol{x}$	$\boldsymbol{x}^T\xi_j\xi_j^T\mathbf{M}_T\xi_j\xi_j^T\boldsymbol{x}$	$\boldsymbol{x}^T\xi_j\xi_j^T\mathbf{M}_\phi\xi_j\xi_j^T\boldsymbol{x}$	$\boldsymbol{x}^T\xi_j\xi_j^T\mathbf{M}_I\xi_j\xi_j^T\boldsymbol{x}$
RBC	$\frac{(\xi_j^T\mathbf{M}_Q\boldsymbol{x})^2}{(\xi_j^T\mathbf{M}_Q\xi_j)}$	$\frac{(\xi_j^T\mathbf{M}_T\boldsymbol{x})^2}{(\xi_j^T\mathbf{M}_T\xi_j)}$	$\frac{(\xi_j^T\mathbf{M}_\phi\boldsymbol{x})^2}{(\xi_j^T\mathbf{M}_\phi\xi_j)}$	$\frac{(\xi_j^T\mathbf{M}_I\boldsymbol{x})^2}{(\xi_j^T\mathbf{M}_I\xi_j)}$
ABC	$\frac{RBC_j^{\textbf{Index Q}}}{\boldsymbol{x}^T\mathbf{M}_Q\boldsymbol{x}}$	$\frac{RBC_j^{\textbf{Index T}}}{\boldsymbol{x}^T\mathbf{M}_T\boldsymbol{x}}$	$\frac{RBC_j^{Index\phi}}{\boldsymbol{x}^T\mathbf{M}_\phi\boldsymbol{x}}$	$\frac{RBC_j^{\textbf{Index I}}}{\boldsymbol{x}^T\mathbf{M}_I\boldsymbol{x}}$

Table 2.2: Damage diagnosis methods.

According to [23] it is possible to group CDC and PDC in General Decompositive Contributions.

The complete and partial decomposition can be defined as special cases of this formulation. The General Decomposition Contribution (GDC) is defined as:

$$\mathbf{GDC}_j^{Index} = \boldsymbol{x}^T\mathbf{M}^{1-\beta}\xi_j\xi_j^T\mathbf{M}^{\beta}\boldsymbol{x}, \qquad 0 \leq \beta \leq 1 \tag{2.30}$$

When $\beta = 0$ $PDC = GDC$ as is shown in the equations 2.31 -2.34.

$$\mathbf{GDC}_j^{Index} = \boldsymbol{x}^T\mathbf{M}^{1-0}\xi_j\xi_j^T\mathbf{M}^{0}\boldsymbol{x} \tag{2.31}$$

$$\mathbf{GDC}_j^{Index} = \boldsymbol{x}^T \mathbf{M}^1 \xi_j \xi_j^T (I) \boldsymbol{x} \tag{2.32}$$

$$\mathbf{GDC}_j^{Index} = \boldsymbol{x}^T \mathbf{M}^1 \xi_j \xi_j^T \boldsymbol{x} = PDC_j^{Index}, \tag{2.33}$$

When $\beta = 1$:

$$\mathbf{GDC}_j^{Index} = \boldsymbol{x}^T \mathbf{M}^{1-1} \xi_j \xi_j^T \mathbf{M}^1 \boldsymbol{x}, \qquad if \beta = 1 \tag{2.34}$$

Here, $\mathbf{I} = \Sigma_(j = 1)^n \xi_j \xi_j^T$, then is possible to reorganize the equation to obtain:

$$\mathbf{GDC}_j^{Index} = \boldsymbol{x}^T \mathbf{M} \xi_j \xi_j^T \boldsymbol{x} = PDC_j^{Index} \tag{2.35}$$

In the same way, when $\beta = \frac{1}{2}$ is possible to obtain CDC.

$$\mathbf{GDC}_j^{Index} = \boldsymbol{x}^T \mathbf{M}^{1-\frac{1}{2}} \xi_j \xi_j^T \mathbf{M}^{\frac{1}{2}} \boldsymbol{x} \tag{2.36}$$

$$\mathbf{GDC}_j^{Index} = CDC_j^{Index} \tag{2.37}$$

Since ABC is a scaled version of RBC, it is possible to use RBC as a general case for both diagnosis methods.

2.5 Independent Component Analysis (ICA)

Independent Component Analysis is a statistic technique whose objective is to decompose a data set **X** into factors by searching for components which are as statistically independent as possible and not only uncorrelated, i.e. the values of one component provide no information about the values of other components. This is a stronger condition than the pure non-correlation condition in PCA, where the values of one component can still provide information about the values of another component in case of non-Gaussian distributions [152]. In general terms, ICA can be expressed as

$$\mathbf{X} = \mathbf{AS} \tag{2.38}$$

where **X** is a $n \times m$ matrix that contains n observations in m variables, **A** is a $n \times r$ mixing matrix with r statistically independent sources and **S** is the Independent Component matrix with dimensions $n \times r$, where each column is the vector of latent variables of each original variable. Since **A** and **S** are unknown, it is necessary to find these two matrixes considering that only the **X** matrix is known. The ICA algorithm finds the independent components by minimizing or maximizing some measure of statistical independence [88]. To perform ICA, the first step includes the application of pre-whitening to the input data **X**. The main idea is to use a linear transformation to produce a new data matrix **Z=VX** whose elements are mutually uncorrelated and their variances equal unity. A popular method to obtain the whitening matrix **V** is by means of Singular Value Decomposition (SVD), such as the one used in Principal Component Analysis (PCA). To perform PCA, as was explained in the Section 2.3, the first step is to calculate the covariance matrix as follows:

$$\mathbf{C}_x = \frac{1}{n-1} \mathbf{X}^T \mathbf{X} \tag{2.39}$$

It is a square symmetric $m \times m$ matrix that measures the degree of linear relationship within the data set between all possible pairs of variables (sensors). The subspaces in PCA are defined by the eigenvectors and eigenvalues of the covariance matrix as follows:

$$\mathbf{C}_x\tilde{\mathbf{P}} = \tilde{\mathbf{P}}\Lambda \tag{2.40}$$

where the eigenvectors of $\mathbf{C}_x$ are the columns of $\widetilde{\mathbf{P}}$ and the eigenvalues are the diagonal terms of Λ (the off-diagonal terms are zero). Columns of matrix $\widetilde{\mathbf{P}}$ are sorted according to the eigenvalues by descending order. Choosing only a reduced number of eigenvalues the data reduction can be performed. Now, it is possible to express the PCA transformation [199] as follows:

$$\tilde{\mathbf{X}} = \Lambda^{-1}\tilde{\mathbf{P}}^T\mathbf{X} \tag{2.41}$$

where $\tilde{\mathbf{X}}$ is the data obtained by the projection in the PCA model. In this way, the whitening transformation ($\mathbf{V}$) corresponds to:

$$\mathbf{V} = \Lambda^{-1}\widetilde{\mathbf{P}}^T \tag{2.42}$$

and $\mathbf{Z}$ can be calculated as:

$$\mathbf{Z} = \Lambda^{-1}\widetilde{\mathbf{P}}^T\mathbf{X} \tag{2.43}$$

The second step is to define a separating matrix $\mathbf{W}$ using the the fixed-point algorithm to transform the matrix $\mathbf{Z}$ to the matrix $\mathbf{S}$ whose variables are non-Gaussian and statistically independent:

$$\mathbf{S} = \mathbf{W}^T\mathbf{Z} \tag{2.44}$$

There are several approaches to reach this goal. Maximizing the non-Gaussianity of $\mathbf{W}^T\mathbf{Z}$ give us the independent components. On the other hand, minimizing the mutual information between the columns of $\mathbf{W}^T\mathbf{Z}$ is equal to minimize the dependence between them. The non-Gaussianity can be measured by different methods, kurtosis and negentropy being the most commonly used. From this step, the $\mathbf{W}$ and $\mathbf{S}$ matrix are obtained. Finally, to calculate the mixing matrix $\mathbf{A}$, equation (2.38) can be used.

2.6 Self-Organizing Map (SOM)

A Self-Organizing Map (SOM) is a special kind of Artificial Neural Network (ANN) converting the relationships between high-dimensional data into simple geometric relationships of their image points on a low dimensional display [101]. This type of network has the special property of generating one organized map in the output layer based on the inputs allowing the grouping of the input data with similar characteristics into clusters. To do that, the SOM internally organizes the data based on features and their abstractions from input data. In order to aid the user in understanding the cluster structure, additional visualization techniques such as the U-Matrix [179], cluster connections [121], or local factors [98] have been developed. In particular, these maps have been used in practical speech recognitions, robotics, process control, and telecommunications, among others [103]. In general, the SOM works by assigning weights to each relation between the input data and the each cluster in the map. The SOM algorithm starts working with a random initialization of these weights. The training is done by comparing the input data set with the weight vectors calculating their Euclidean distance in order to find

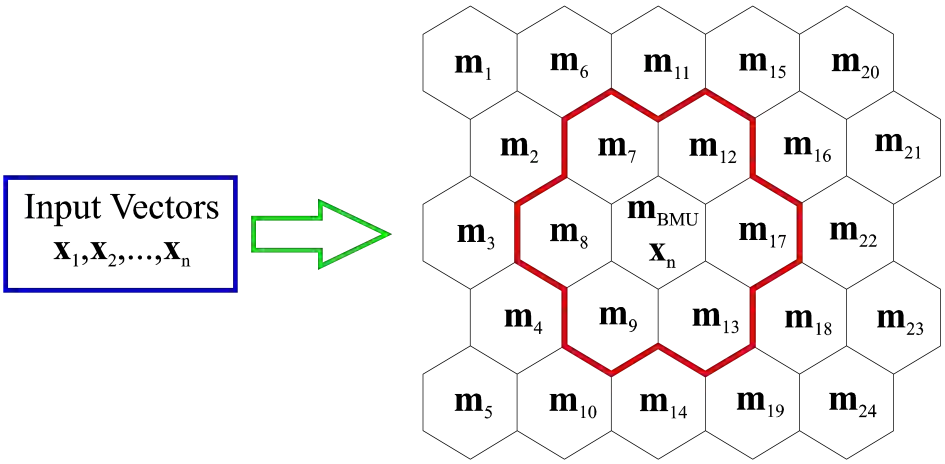

Figure 2.3: Elements in a Self Organizing Map.

the best matching unit (BMU). The updating process takes into consideration a neighbourhood set N_c around the cell $\mathbf{m}_{BMU}$, and by each learning step just the cells within N_c are updated (Figure 2.3). This updating process is defined by equation (2.45).

$$\begin{cases} \mathbf{m}_i(t+1) = \mathbf{m}_i(t) + \alpha(t)(\mathbf{x}(t) - \mathbf{m}_i(t)) & \text{if} \quad i \in N_c(t) \\ \mathbf{m}_i(t) & \text{if} \quad i \notin N_c(t) \end{cases} \tag{2.45}$$

where t denotes current iteration, m_i is the current weight vector, x is the target input vector, and $\alpha(t)$ is a scalar called adaptation gain which is between 0 and 1, and it is reduced by each time. Finally, each incoming dataset could be presented to the map followed by the updating process or all datasets are compared to the map before executing any updating. These methods are known as the sequential and batch algorithms, respectively. After the training phase, different groups will normally form in the map which can be distinguished according to their location on the map. The U-Matrix, showing the average distance of a cell to its neighbouring cells, can be used to depict the difference between the groups. The U-Matrix will normally contain visible boundaries separating the different groups providing an idea of the extent of their difference. The training algorithm used here is implemented in a Matlab-Toolbox created by [180].

2.7 Discrete Wavelet Transform

Wavelet analysis has proved to be a powerful tool in areas dealing with the analysis of transient signals. The concept of wavelet analysis is not new and has been the scope of considerable research over the past 30 years. The wavelet transform is a linear transformation that decomposes a given function $x(t)$ into a superposition of elementary functions derived from an analyzing wavelet by scaling and translation [34]. The continuous wavelet transform (CWT) is defined as

$$W(a,b) = \frac{1}{\sqrt{a}} \int_{-\infty}^{\infty} x(t)\varphi^* \left(\frac{t-b}{a} \right) dt \tag{2.46}$$

where a is the dilation or scale parameter, b is a translation indicating the time locality, φ is the analysing mother wavelet and the asterisk superscript denotes complex conjugation. It is well

known that the CWT is a highly redundant transformation representation. However, the discrete wavelet transform (DWT), on the other hand, provides sufficient information for both the analysis and synthesis of the original signal with a significant reduction in the computation time [191]. Loosely speaking, the variability of the given function at a specified time and scale is represented by the transformation coefficients. In other words, each wavelet coefficient represents time and frequency information of the regarded signal. The DWT analysis can be performed by means of a fast, pyramidal algorithm related to a two-channel subband coding scheme using a special class of filters called quadrature mirror filters as proposed by Mallat [116]. In this algorithm, the signal is analyzed at different frequency bands with different resolution by decomposing the signal into a coarse approximation and detail information. This is achieved by successive high-pass and low-pass filtering of the input signal. One of the most important advantage of DWT is the ability to compute and manipulate data in compressed parameters which are often called features [178]. The extracted wavelet coefficients give a compact rep-

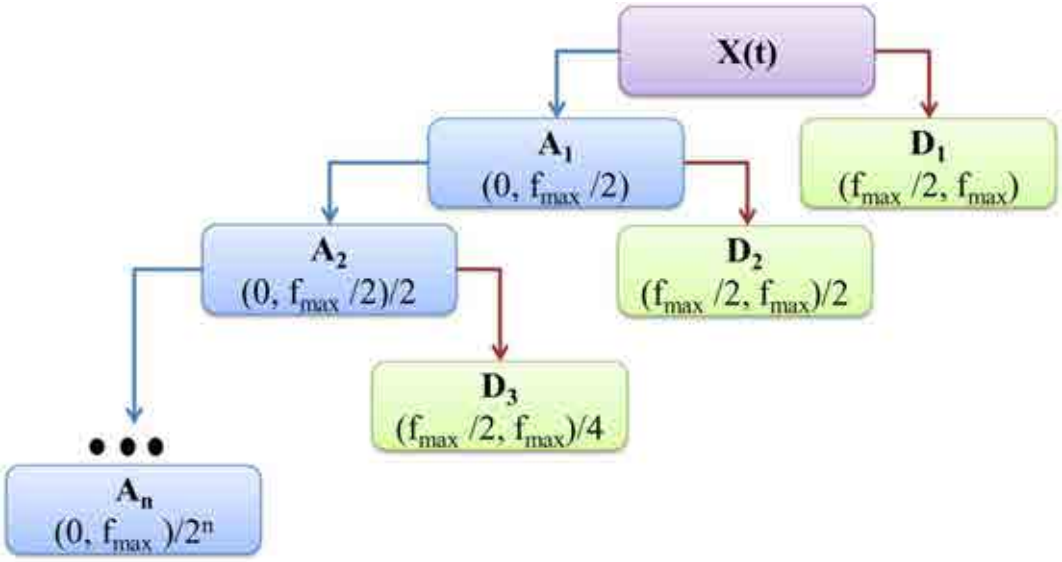

Figure 2.4: DWT Decomposition Tree.

resentation that shows the energy distribution of the structural dynamic responses in time and frequency [166]. The optimum number of level decompositions could be determined for example based on a minimum-entropy decomposition algorithm [45]. Figure 2.4 shows the structure of decomposing the signal and the corresponding frequency bandwidths for the details (Di) and approximations (Ai). The approximations represent the high-scale, low-frequency components of the signal. The details are the low-scale, high-frequency components. The frequency f_{max} represents the maximum frequency contained in the recorded signal and n is the decomposition level. The approximation and details coefficients can be calculated as follows:

$$A_{n,k} = 2^{-n/2}\Sigma_{i=1}^{j} x(i)\gamma(2^{-n}j - k) \tag{2.47}$$

$$D_{n,k} = 2^{-n/2}\Sigma_{i=1}^{j} x(i)\varphi(2^{-n}j - k) \tag{2.48}$$

where γ is called the scaling function, j is the number of discrete points of the input signal, n and k are considered to be the scaling (dilation) index and the translation index, respectively.

Each value of n allows analyzing a different resolution level of the input signal. Scaling functions are similar to wavelet functions except that they have only positive values and are designed to smooth the input signal [115],[116]. It can be seen from the Figure 2.4 that the DWT allows the decomposition of the input signal into several resolution scales. The idea behind is to analyze the signal at different resolutions, i.e. coarse resolution to get a general signal representation and fine resolution to get specific details [116].

2.8 Remarks and conclusions

This chapter has shown a brief description of waves in solids in order to introduce the concept of Lamb Waves and its vibration modes. Also it has been briefly described the use of the dispersion curves to represent the dispersive nature of the lambwaves including an application in an aluminium plate. The chapter has also given a brief description of the methods that will be used in the methodologies developed in this thesis. As will be shown in the next chapter, each of these methods have been used separately and there is no references that show their use together as is developed in this thesis for damage detection, localization and classification.

Chapter 3

A REVIEW OF STRUCTURAL HEALTH MONITORING AS PATTERN RECOGNITION

3.1 Introduction

The problem of structural monitoring can be tackled from different points of view. Some authors have built physical models to describe the characteristics of the structure. In this kind of approaches, a high-fidelity model of the structure is required to perform a reliable damage identification. On the other hand, other authors use techniques based on data gathered by experiments or by numerical simulations. These approaches usually require a statistical model representation of the system to perform the structural state analysis [188]. In this case, the system do not use physical models and the problem of damage identification can be approached as a pattern recognition application, where some features of the collected signals are used as pattern. In general, it exploits the fact that the vibrational response of a damaged and undamaged structure are different. In this way, if some defect exists in the structure, its vibrational response will change and these changes can be analyzed.

Several reviews have been carried out in Structural Health Monitoring (SHM). Among them, in 2005, Fritzen presented an overview of the developments of vibration based methods. The next year, Chang et al. [42] presented a review of SHM for civil infrastructures. Also in 2006, Lynch and Loh presented a summary review of wireless sensors and sensor networks [113]. Farrar and Worden [57] in 2007 performed a brief historical review of SHM technology development. The same year Brownjohn [39] presented a review of SHM applications to various forms of civil infrastructure including a discussion about the damage diagnosis procedure in terms of instrumentation, data acquisition, communication systems and data mining. The next year, Ciang et al. [43] presented a review focused in damage detection methods for a wind turbine system. In 2010, Mujica et al. [126] performed a review of impact damage detection in structures using strain data which included sensors, specimens and impact sources used for developing and testing strategies. Recently, in 2011 Fan and Qiao [53] presented a review and comparative study of vibration-based damage identification methods. The review included methods based on modal parameters, natural frequencies, mode shapes as well as

curvature/strain mode and shape-based methods. These reviews have proved that the interest in the development of algorithms and methodologies in SHM have been growing. As result of this interest, SHM has been applied in different areas that include applications in civil, aeronautics and astronautics structures. Many works has been reported for more than three decades [42] with excellent results, for instance, tests in bridges ([31], [108], [145], [99], [137]), buildings ([70], [153]), wind turbine blades ([140], [51]) and other structures ([80], [131], [158], [93]).

This review, provide in Section 3.2 a brief overview of the SHM levels ([148]) in order to show from a general point of view the wide range of methods and applications developed in SHM. Later on, in Section 3.3 the review is focused on approaches using data driven methods and specifically in pattern recognition applications. In this step, special sections are devoted to the literature review of statistical approaches including Principal Component Analysis (PCA) and Independent Component Analysis (ICA). Particular emphasis has been placed on these two techniques because they are the most involved in the methodologies developed in this thesis.

3.2 Brief review of the Structural Health Monitoring levels

As was mentioned in the introduction, SHM includes different levels starting by the detection of the damage and following with the localization, classification, identification and the prognosis of damages (prediction) [188]. This section is organized according to these levels in order to show some of the applications that have been developed at each level in different fields.

3.2.1 Damage detection

The damage detection corresponds to the first level in SHM, whose goal is to detect defects or damages in structures when they are still in their nascent state using non-destructive techniques and algorithms. As was previously introduced, the damage can be defined as changes in the structure when it is compared with a baseline obtained from the structure in a healthy state. These changes include variations in the material or in the geometric properties.

The need of damage detection a damage to prevent an accident is an essential factor to ensure the proper work of a structure in service. There are many applications in different areas but it is necessary to note that in some areas as aeronautical and aerospace engineering is very important the continuous monitoring of the structural health to guarantee its proper performance. Probably, the use of SHM in these two areas is more important than the applications in others areas due that normally in areas as civil engineering some damages are really dangerous when they start to have a considerable size. In aeronautical and aerospace engineering, some damages that are imperceptible when are subjected to extreme changes in their working conditions can cause catastrophes. In the aeronautical industry, for instance, the majority of inspections are performed visually [38],[126]. However, many research groups around the world are focusing efforts to develop techniques that allow the inspection of structures in service. These investigations are focused on developing techniques for making the best detection of the different possible damages. Some developments at the damage detection level are reviewed below:

In 1992, Kudva et al. [104], in 1993 Gunther et al. [79] and Hahn et al. [82], Sirkis et al. [156] in 1994 and Schindler et al. [151] in 1995 worked on impact damage detection by using advanced signal processing with Artificial Neural Networks (ANN).
Friswell et al. [65] in 1998 used a genetic algorithm for damage detection in vibration based data in order to identify the position of one or more damage sites in a structure and to estimate the extent of the damage at these sites. In the same year, Yap and Zimmerman [196] used genetic algorithms for damage detection. In difference with the classical coding of the genetic algorithm, this work proposed the use of two coding enhancement strategies.

In 2001, Ganguli [69] showed a fuzzy logic system for health monitoring of a helicopter rotor blade when this is on ground. The rules of the fuzzy system were defined in order to define four different levels of damages in the output. The measurements used were the first four flap (transverse bending) frequencies of the rotor blade.

Hao and Xia [83] in 2002 used a genetic algorithm with real number encoding to identify the structural damage by minimizing the objective function, which directly compares the changes in the measurements before and after damage. They used three different criteria, namely, the frequency changes, the mode shape changes and a combination of both. This methodology was tested in a cantilever beam and a frame. The same year, Staszewski et al. [163] used passive acousto-ultrasonic sensors to impact damage detection in composite structures. In this work, a study of different signal processing methods for passive damage monitoring is performed.

In 2004, Sun et al. [167] presented a methodology to classify some statistics patterns using the wavelet packet transform (WPT). The vibration signal collected from the structure were decomposed into wavelet packets. Later on, the signal energy of the packets were calculated and ordered according to the magnitudes. The most important magnitudes were considered and the rest were rejected, using these magnitudes and defining some thresholds and confidential limits to detect abnormal behaviors the damage detection was performed. This methodology is tested in a beam and four damage cases were applied involving line cuts of different severities in the flanges at one cross section.

In 2006, Menéndez et al. [120] used an active piezoelectric system and Fibre Bragg Grating (FBG) to detect de-bonding of subcomponents in monolithic composite parts. In the methodology, the power spectrum was used to find the damage. In the piezoelectric active system the maximum of amplitude of every piezoelectric sensor is used in order to measure the energy loss of the input pulse. The same year, Fernández et al. [62] performed a comparison between the use of FBG and piezoelectric sensors for damage detection. To do that, the Hankel matrix is used to obtain the damage indicator values. They proposed as alternative the use of a combined hybrid piezoelectric/FBG sensors. Wildy et al. in 2007 [185] proposed a passive method of damage detection based on the concept of strain field. Huang et al. in 2008 [87] used acoustic emission in thin glass/epoxy composites plates in order to detect damages. The same year, Mujica et al. [134] used a hybrid methodology which combined Case Base Reasoning (CBR), wavelet transform and Self Organizing Maps (SOM) in order to detect impact damages in a wing flap. Piezoceramic sensors attached over the surface of the flap in order to collect time varying strain response data were used.

In 2009 Chandrashekhar et al. [40], applied a fuzzy logic system with a sliding window defuzzifier using modal curvatures for damage detection. The methodology fuzzified the changes due to a damage in modal curvature using Gaussian fuzzy sets and mapped to damage location and size. This methodology was applied to a cantilever beam. Recently, Dervilis et al. [47], presented a scheme for damage detection in carbon fiber materials using novelty detection methods. These methods were applied to FRF measurements from a stiffened composite plate which was subjected to incremental levels of impact damage.

3.2.2 Damage localization

The localization of damages is the next task after damage detection. Its complexity depends on the structure, the type of sensors and their distribution. Some of the most common strategies for the location of damages include triangulation processes [126]. According to Salehian [150], three sensors are enough for determining impact location for isotropic materials, but in anisotropic materials as composite materials these approaches must be different [126]. Other researches have combined different strategies combined with the processing of sensor data for locating damages. Some of them are discussed below.

Staszewski et al.[165] and Worden and Staszewski[190] in the year 2000, used ANNs as regressor to predict the impact location and energy in composite materials. The approach used a multilayer perceptron which was trained with experimental data using back propagation. Additionally, these works presented the combined use of the genetic algorithms and ANN to find near-optimal sensor distributions for damage detection.

In 2001, Chou and Ghaboussi [44] presented a methodology based on genetic algorithm which uses static measures of displacement for damage localization. In 2003 Coverley and Staszewski [46] showed a methodology for damage locating using triangulation methods and genetic algorithms. In [76] Gorinevsky et al. presented the design as a subsystem to the Integrated Vehicle Health Management (IVHM) system of an aircraft. This system used SMART Layer® sensors from Acellent Technologies. Using the signals obtained from the sensors, the mean signal amplitude was calculated and compared with the scatter signal to obtain a damage Index for each actuator-sensor path. Using these values they obtained a representation of the location structural changes and one measure of the damage size. In 2010 Mujica et al. [130] used Principal Component Analysis and some statistic indices to localize different damages using contribution plots in an aircraft turbine blade. Recently, Hackmann et al. [81] in 2012, presented a holistic approach for damage localization which integrated a decentralized computing architecture using wireless sensor networks. In the approach the damage localization algorithm used post-processed natural frequency data.

3.2.3 Damage classification

The damage classification corresponds to the level which, according to some characteristics obtained from the structure in different structural states and some algorithms, a classification of each state can be performed according to its features. In general, a typical classifier is used to define which damage is present in the structure. Some examples are shown below.

Using a combination of time series analysis, neuronal networks and statistical inference techniques, Sohn et al. in 2002 [159] classifies damages under environmental changes. First, an AR-ARX model is developed in order to extract damage-sensitive characteristics, then a neural network was used to normalize the data and to separate the effect caused by the environmental changes. Finally, a sequential probability ratio test was performed to define the state of the system. The methodology was tested using a numerical example of a computer hard disk and an experimental study of an eight degree-of-freedom spring-mass system.

In 2007 and 2008 Mujica et al. [125], [134] used Wavelet Transform in a hybrid methodology to detect, quantify and localize damages. This methodology used the wavelet transform in order to extract different characteristics from the measured signal and subsequently apply a neural network to classify the damages. In 2008, Zhou et al. [202] proposed an algorithm for the classification of structural damage based on the use of continuous hidden Markov modeling (HMM) technique. It was used to model time-frequency damage features extracted from structural data using the matching pursuit decomposition algorithm.

Many works have shown the usefulness of neural networks for classification [33]. For instance, clustering algorithms based on Self-Organizing Maps -SOM- (attempting to organize feature vectors into clusters) have been used for the classification of acoustic emissions [195][74] and for active sensing damage classification [170].

Dua et al. [52] in 2001 used an ANN with backpropagation algorithm and finite element analysis (FEA) to classify impacts on composite plates. A 503,10,3 ANN was used for training and simulating the data: 503 elements in the input layer which are excited by strain profiles obtained from FEA, 10 neurons in the hidden layer and 3 neurons in the output layer. A total of seven classifications groups were performed inspecting the composite plates and the kinetic energy of the falling mass. This classification was coded using Gray Code.
In 2006 Kolakowski et al. [102] presented two approaches for damage identification. One of them was based on Virtual Distortion Method (VDM). The other methodology involved the use of Case Based-Reasoning (CBR) applying wavelet transform in order to extract features and reduce the variables to introduce into a Self-organizing Map (SOM) for damage identification. These techniques were tested in an aluminum beam. In 2007, Bakhary et al. [33] applied a two-stage ANN system for damage location and damage severities. In the first stage an ANN is used to identify the substructures with damage and the secondary ANN identify the damaged elements and its severity. Inputs in the first ANN were modal frequencies and mode shapes of the full structure and the outputs were modal frequencies of substructures, these were the inputs to the second ANN where the final analysis to locate the damage was performed. For testing the approach, a numerical example was used which consisted of a two-span concrete slab. Dobrzanski et al. [48] used a multilayer perceptron 9-6-5 for the classification of internal damages in steel during creep services using metallographic images. Also in 2007 and 2008 Mujica et al. [131], [134] presented a methodology to detect, quantify and localize damages and impacts in several structures, among them a wing aircraft section and an aluminum beam. This methodology used wavelet transforms to extract different characteristics from the collected signal and a SOM to classify them. In 2008, Kabir et al. [97] presented an algorithm for damage classification using a multilayer perceptron. The methodology included the use of analysis of texture of surface deterioration using optical imagery in concrete structures. The dataset in the perceptron

included three different datasets: spatial, spectral and a combination spatial-spectral dataset. Iskandakari [91] in 2010 applied neural networks to classify composite structure conditions. Resin injection molded (RIM) samples response to impact damage was carried out using low frequency tapping, visual imaging, low temperature thermo imaging and tensile strength. Recently, Zhou et al. [203] presented an artificial inmune pattern recognition (AIPR) approach for the damage classification in structures. The approach included the development of an immune learning algorithm and a ARX algorithm to compress the data.

3.2.4 Type and extent of damage

The knowledge of the type of damage is a task that provides information the severity of damage. This is performed after the detection and localization and provides information on whether the structure can still do its job or must be replaced. Some works related to the definition of the type and the extent of damages are outlined next.

Mares and Surace [119] in 1996 presented a strategy based on genetic algorithms and residual force method (modal analysis theory) to detect, quantify and obtain the extent of damages in elastic structures. Friswell et al. [65] in 1998 used a genetic algorithm for damage detection in vibration based data in order to identify the position of one or more damages in a structure and to estimate their length. Hao and Xia [83] in 2002 used a genetic algorithm with real number encoding to identify the structural damage by minimizing the objective function, which directly compares the changes in the measurements before and after damage. They used three different criteria, namely, the frequency changes, the mode shape changes, and a combination of them. This methodology was tested in a cantilever beam and a frame.

In 2003, Mujica et al. [132] showed the use of Case Based Reasoning as tool for damage diagnosis. A wavelet transform was also used to obtain some characteristics and a Self-Organizing Map (SOM) was used as method for handling the casebase. This methodology was tested in a cantilever truss. The same year, Chang and Sun [41] proposed a novel structural condition index for locating and quantifying structure damage based on Wavelet Packet Signature (WPS). This year, Shan and King in 2003 [155] presented a methodology to locate impacts and estimate impact magnitud on smart composites using fuzzy clustering for feature selecting and adaptative neuro-fuzzy inference system for impact locating and magnitud estimating. In 2005 Mujica et al. [131] extended the methodology presented in 2003 to define the severity and the dimension of the damage. Recently in 2011, Gul and Catbas [78] presented a time series methodology to detect, locate and estimate the extent of the structural changes. The approach used ARX models which are obtained for different sensor clusters by using the free response of the structure. The approach considered also to obtain the ARX model fit ratios or the ARX coefficients as damage features.

3.2.5 Damage prognosis (DP)

Damage prognosis is the last level in SHM, which includes the quantification of the damage to determine the useful lifetime remaining for the structure and the conditions to continue operating. The publications in these kind of applications are lesser in number than those existing for damage detection. Below are some of them.

Staszewski in 2000 [162] presented a discussion focused to extraction and procedures for data pre-processing in pattern recognition procedures in order to obtain the diagnosis of location and severity of damage. In 2003, Farrar et al. [58] presented an approach for damage prognosis by integrating advanced sensing technology, data interrogation procedures for state awareness, novel model validation and uncertainty quantification techniques, and reliability-based decision-making algorithms. Later on, in 2007 Farrar and Lieven [55] presented some general concepts of Damage Prognosis some of them are: the definition of the problem, the motivation and the process of DP. Also a review of emerging technologies that will have an impact on the damage prognosis process was included.
In 2010, Zhang et al. [201] presented an approach that included the use of flexible piezo paint sensor and a probabilistic fracture mechanics based framework for on-line assessment and updating of the remaining fatigue life of steel bridges.
In 2012, Ling and Mahadevan [111] presented a Bayesian probabilistic methodology to integrate model-based fatigue prognosis with online and offline SHM data, considering various sources of uncertainty and errors. The methodology was tested in a numerical example, considering the surface cracking in a rotorcraft mast under service loading.

3.3 Structural health monitoring using statistical methods

The previous section has shown a literature review on the different levels of SHM. Although an extensive literature exists, just some of the most relevant works were cited. As was previously mentioned, the paradigm of SHM can be considered as a pattern recognition problem [59]. The review presented hereafter discusses some works that approach the subject in this way, but using statistical techniques. Special attention is paid to PCA and ICA since they are used in the methodologies proposed in this thesis.

3.3.1 Principal Component Analysis (PCA)

PCA has been extensively applied to measured structural dynamic response signals with the purpose of dimensionality reduction studies [118] [133], to distinguish between changes due to environmental and structural damage [117] [193] and for sensor validation [100], among others.

Trendafilova et al. [177] in 2000 used Proper Orthogonal Decomposition (POD) which is another way to call PCA. This was used in combination with parameter identification to identify nonlinear parameters of a structure, minimizing the difference between the bi-orthogonal decomposition of the measured and the simulated data. This methodology allowed the identification of the Coulomb friction at the end of a beam. Zang and Imregun [200] used frequency responses and ANN for detecting damages. In order to include the analysis of the frequency responses, they used PCA to reduce the data size. In 2003, Boe et al. [37] applied PCA for the diagnosis of damages using vibrational responses. With the data from piezoelectric sensor distributed in the structure it was possible to define the possible localization of the damage. Authors also declared that this methodology can be used with other kind of sensors as accelerometers. The same year, Sophian et al. [161] used PCA for feature extraction in the response obtained from the application of Eddy current in two aluminum samples. In 2004,

Nitta et al. [135] presented a two-stage-based methodology for detecting how the reduction in story stiffness of damaged building is. POD was used to estimate the modal vector of a structure in order to detect and locate damages. In the second step, a methodology for quantifying the damage was carried out by means of system identification of subsystems. Golinval et al. [75] used PCA and vibration-based signal for damage detection and localization in structures. The excitation was generated by an electro-dynamic shaker, acelerometers were used as sensors. The approach included the use of the angle between subspaces in the PCA subspace. In 2005 Yan et al. [193] [194] proposed a methodology for structural damage diagnosis which included a two step-procedure, first, a clustering of the data space into several regions was performed. Later on, PCA was applied in each region for damage detection. Galvanetto et al. in 2007 [68] and after in 2008 [67] used POD for damage detection and localization based on vibrational responses from the structures using accelerometers. The collected data were used to compare the proper orthogonal modes of the undamaged structure and those of the damaged structure.

In 2008 Mujica et al. [129] explored the use of PCA with T^2 and Q-statistics in order to detect and distinguish damages in structures. In this case, a PCA model was built for each actuator and the analysis of each model was performed in an individual form. This methodology was tested in an aircraft turbine blade using piezoelectric transducers. In the same year, Mujica et al. [133] presented another work that demonstrated the use of PCA, MPCA (Multiway PCA), PLS (Partial Least Square) and MPLS (Multiway PLS) to localization of damages in a part of a commercial aircraft wing flap. It includes also the use of Case-Based Reasoning. Xu et al. developed an enhanced sensor fault detection, diagnosis and estimation strategy for centrifugal chillers combining Wavelet analysis and PCA [192]. In 2009, Gryllias et al. [77] presented a two-step approach for crack detection in beam structures, which includes in a first step the extraction of Proper Orthogonal Modes (POMs) of a beam using Proper Orthogonal Decomposition. Later on, morphological processing using four operators (dilation, erosion, opening, closing) are applied for processing the POMs. Mujica et al. [127] included the effects of changes in the temperature to the damage detection methodology by using PCA, T^2 and Q-statistics. In 2010, Torres et al. used the Discrete Wavelet Transform (DWT) in combination with Hierarchical Non-linear Component Analysis in order to create the feature vectors from structural dynamic responses for the training of a Gaussian process for the purpose of impact identification and for acoustic emission denoising [28][26]. In 2011, Salehi et al. [149] proposed two damage detection techniques based on POD. The first approach used time responses, where POD was applied for reducing data. The second method was based on Frequency Response Functions (FRFs) where spatio-spectral FRF shape data were decomposed by means of POD. Recently, in 2012 Kullaa [95] showed an approach for damage detection and localization by modelling the sensor network as a Gaussian process and performing the generalized likelihood ratio test. In this study the discrimination between environmental, operational effects, sensor faults and structural damage was considered. PCA was used for reducing the dimensionality and using the maxima and the minima of the first principal component scores, the Extreme Value Statistics (EVS) was used to define the thresholds and define a damage. Hot et al. [86] compared two methodologies for detection of non-linearity based on time responses of a mechanical structure. In the methodologies, first, the Singular Value Decomposition of the time response matrix is calculated and later on the principal angle and the residual projection error between subspaces are calculated and compared.

3.3.2 Independient Component Analysis (ICA)

ICA is a technique also used in multivariate data analysis like PCA where the original data are redefined using statistically independent random vectors.

In 2004 Zang et al. [199] combined data extraction in time domain using ICA and neural networks. The methodology applied ICA to the time history measurements in order to calculate the mixing matrix. This matrix represented the vibration features to build a neural network model for damage detection. This methodology was tested in a numerical model of a truss structure and a bookshelf structure, where 24 acelerometers were used to gather the data. The next year, [160] presented an approach that includes the use of ICA and Support Vector Machine (SVM) to identify types and levels of structure damages. The approach applied ICA to the input data in order to calculate the independent components and use them as input data for a SVM classifier. Ren et al.[143] in 2009 used FastICA based on negentropy to extract and separate the vibration signal caused by human activity in transmission towers for SHM. Using combined empirical mode decomposition technique with the adaptative threshold method, the vibration pulses were extracted and the interference signals removed.

In 2011, Wang et al. [181] used constrained-ICA to extract desired faulty signal using some prior mechanical information as reference. The constrains were defined as pulses or square waves as reference signal from faulty states as shock sequence, inner race fault of the rolling element bearing, etc. In 2012, Loutas et al. [112] presented an approach to detect and locate damages in aerospace structures. The approach used dynamic strain measurements from four fiber bragg grating which were preprocessed using Discrete Wavelet transform to calculate the spectral density estimation and after used the Fast Fourier Transform to evaluate and, compute an average over all segments. ICA is used for the reduction of feature space and the final analysis was performed by using Support Vector Machines. The system was developed and tested on a flat stiffened composite panel. Damage was simulated by slightly varying the mass of the panel in different zones of the structure by adding lumped masses.

3.3.3 Other approaches

In 1998, Farrar et al. [54] showed the results of applying different methodologies such as: damage index method, mode shape curvature method, change in flexibility method, change in uniform load surface curvature and change in stiffness method, to the Bridge I-40 from Rio Grande in Albuquerque. In all the methods, the identification of a damage using data from the structure with and without damage is performed. They showed that all studied methods are successfully locating the most severe damage but does not if a minor damage is presented. They also concluded that the damage index provides better results when all the tests are included.

Worden et al. [189] in 2000, performed a study of a statistical method for detecting defects based on the Mahalonobis distance. In this methodology, signal deviations from normal conditions were used to detect damages using outlier analysis in order to indicate the deviation from the norm. The method was applied in four case studies: a simulation, two pseudo-experimental and one experimental. In 2001 and later in 2002, Sohn et al. [158], [157] applied two pattern recognition techniques based on time series analysis to data obtained from

two different structural conditions of a fast patrol boat. The first technique was based on an analysis of two-stage series that combines a predictive model autoregressive (AR) and other auto-regressive with exogenous input (ARX). The second technique used an analysis of outliers by means of the Mahalanobis distance measure. Both techniques allowed to distinguish the data obtained from the different structural conditions. In 2003, Lei et al. [109] used time series analysis of vibration signals in order to consider the influence of the variability of excitation and the orders of the ARX model prediction on the originally extracted damage-detection feature. To determine the existence of damage, the residual error was obtained by comparison of the signals from the structure under test with the structure without damage. The applicability of the modified approach was investigated by using different acceleration responses generated with different combinations of finite element structural models. Iwasaki et al. in 2004 [92] proposed a diagnostic method for the damage that does not require data from the damaged structure. This method used system identification and statistical similarity test of the identified system using an F-test. This methodology was tested in a beam of composite material. Woo and Sohn [187] in 20006 used EVS (extreme values statistics) for damage detection in structures. This detection is the comparison of data from a structure under test with the healthy structure. To perform the detection, the tails of the distributions were analyzed to identify irregularities. In 2007, Park et al. [139] presented a modified autoregressive model with exogenous inputs (ARX) in frequency domain constructed from the measured impedance data to diagnose structural damage with statistical confidence levels. Also a review of the methods developed in impedance-based SHM were included. The authors presented a study to demonstrate how this experimental techniques can be used to detect structural damage in real time. Methods of signal processing and compression of data associated with the impedance method were showed. Moreover, Fassois and Sakellariou [61] performed a review of the principles and methods of time series analysis for detection, identification and estimation of damages. Similarly, they present new methods based on time series, these methodologies are tested on 3 stages: a panel plane, a skeleton at a plane and, a simulated nonlinear structure. In 2008, Wang et al. [182] used an AR model based in vibrational responses. The coefficients of these AR models were extracted to make a set of multivariate data known as vibration response data characteristics, and then Hotelling's T^2 control chart was applied to monitor these characteristics. The methodology was demonstrated by numerically simulated acceleration time histories based on a progressively damaged reinforced concrete (RC) frame, either with or without addressing the autocorrelation in the characteristics data. Later on, in 2009 [60] they showed again the benefits of using statistical time series for detecting damages in a time-varying arm, ie an arm that can change its length.
Azarbayejani et al. [30] in 2008 and 2009 [29] presented a probabilistic approach in order to identify the optimal number of sensors to localize damages. This work involved the use of a neural network to establish the probability distribution, and therefore, to identify the optimal localization of sensors to damage detection.

Mujica et al. [128] in 2009 applied Multiway Partial Least Square (MPLS) as a regression tool to estimate the location of impacts on an aircraft wing. In this work, 574 experiments were collected hitting the wing at the surface and receiving signals from nine sensors. The same year, Bornn et al. [105] proposed to model the vibration data obtained from sensors using a nonlinear time series model by means of support vector machines (SVM), and therefore, to identify the different sensors that are more influenced by structural damage. In the same year,

Leao et al. [107] compared different techniques to monitor the health state of aircraft flap and slat systems. They applied T^2 and Ranger U^2 statistics based on measurements of motor command current and operational conditions.

Another approaches include the use of Bayesian models. For instance, in 2010, Lombaert et al. [125] used Bayesian Finite Element (FE) model updating for damage identification of a full-scale seven-story reinforced concrete building which was tested using a shake table. The same year, Papadimitriou et al. [138] used a Bayesian model class selection and updating framework for damage identification and quantification. Flynn and Todd [63] presented an approach that include a Bayesian experimental design. It approach included five steps: evaluate risk and cost, choose feature extraction process, calculate feature characteristics as a function of design parameters, derive a detector and calculate detector performance. Bernal[35] examined the importance in changes that statistical noise may have on the ability of the use of Kalman filter as a damage detector.

Doebling et al. [49] in 2000 presented an algorithm to estimate the statistical distribution of certain modal parameters determined on the basis of random errors associated with estimates of the average frequency response function. In this paper, the modal parameters were assumed to be random variables and the objective was to estimate the statistical distribution. The algorithm used a classical approach in order to estimate the error in the average frequency response function using the coherence function averaged over a set of samples measured. A Monte Carlo simulation approach was used to propagate errors of the estimated spectral function trough the process of identification of modal parameter. A Bootstrap estimation of the modal parameters was used in all the individual samples to verify the Monte Carlo algorithm. In 2009, Adewuyani et al. [21] presented an algorithm to damage identification vibration based in civil structures. This algorithm used the regression analysis of peak values of the magnitudes of frequency response function (FRF) of target sensors relative to the reference wherein the statistical features were used for data reliability assessment and damage localization. Strain gauges and long gauge fiber Bragg grattings (FBG) are the sensors used in a flexible structure.

Chapter 4

CASE STUDIES

The methodologies developed and presented in this thesis have been subjected to different experimental tests using simplified structures and structures in real scale. In particular, eight structures were tested: three aluminum plates, two composite plates and three real parts of aircraft structures. More descriptions about the physical features, excitations signal and damages applied are included in the following sections.

4.1 Aluminium plate with reversible damages

This structure corresponds to the most simple case studied. It is an aluminum plate with dimensions $(250mm \times 250mm \times 2mm)$ as can be seen in Figure 4.1. The plate was instrumented with four PZT transducers bonded on the surface. The transducers dimensions are: diameter $26mm$ and thickness $0.4mm$.

The excitation signal to the actuators was generated using a chassis PXI 1033 from National Instruments, by means of a generator NI PXI-5412. The data acquisition was performed by a NI PXI-5114 digitizer card inserted in the chassis. More details about this equipment are included in the appendix section. Damage on the tested plate was simulated by adding masses at different positions on the surface. The aim of this form of artificial damage is to introduce reversible changes in the mechanical impedance in the structures along the wave propagation paths [64]. Figure 4.2 shows the damage description and the position of each damage.

As excitation input, a BURST signal (Figure 4.3) is applied. To determine the carrier central frequency for the actuation signal in the structure, a frequency sweep was performed and the spectral analysis of each signal was explored. As result of this analysis a BURST signal with 50 KHz and 3 peaks was defined. Before applying the signal to the structure, it was amplified to 50 V using a wideband power amplifier. The collection of the data was performed in different phases, in each phase, one PZT transducer was selected as actuator, the excitation signal was applied to this PZT transducer and the vibrational response in different positions were collected by the other piezoelectrics.

For the analysis, 750 experiments were performed and recorded: 150 with the undamaged structure and 100 per damage. All data were averaged to obtain one signal for each 10 experiments in order to eliminate the possible noise in the data.

Figure 4.1: Aluminium plate.

Figure 4.2: Damage description and location.

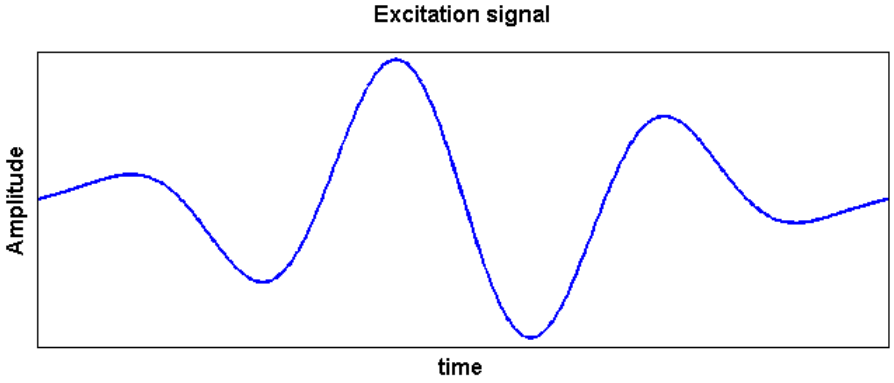

Figure 4.3: Excitation signal.

4.2 Aluminium plate with real (non reversible) damage

This specimen corresponds to an aluminium plate (Figure 4.4a) with the same features and dimensions as the previous structure. Equally to the previous case, this plate was instrumented with four PZT transducers attached on the surface. The data acquisition was performed using the chassis PXI 1033 from National Instruments applying a BURST signal of 3 peaks and 50KHz as carrier frequency. As in the previous case, the transducers dimensions were diameter $26mm$ and thickness $0.4mm$.

In contrast with the previous case, a real damage was made between the PZT transducers 2 and 4 as shown in Figure 4.4b. In total, 300 experiments were performed and recorded: 100 using the undamaged structure, and 200 using the structure with different size of the damage (increasing the depth).

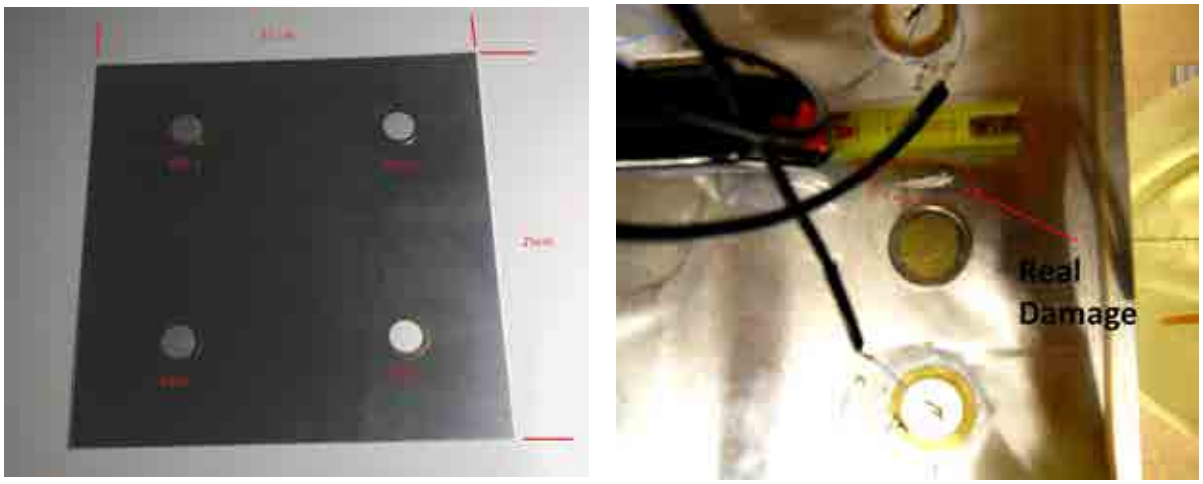

(a) (b)

Figure 4.4: Aluminum plate and damage description.

4.3 Composite plate 1

This specimen corresponds to a CFRP plate and is one of the structures tested in the Siegen University. Figure 4.5a shows this plate which is made of 4 equal layers and stacking of [0 90 90 0] with dimensions: $200mm \times 250mm$ and a thickness of approximately $1.7mm$. Nominal material parameters of the unidirectional (UD) layers are $E_1 = 122GPa$, $E_2 = 10GPa$, $v_{12} = 0.33$, $v_{13} = 0.3$, $v_{23} = 0.34$, $G12 = G13 = 7.4GPa$ and $G_{23} = 5.4GPa$. The density is about $1700kg/m^3$.

Nine PZT transducers PIC-151 from PI Ceramics were attached to the surface of the structure with equidistant spacing. The piezo transducers have a diameter of $10mm$ and a thickness of $0.5mm$. The excitation signal to the actuators was generated using the arbitrary signal generation capability of a Handyscope HS3 (a combined signal generator and oscilloscope

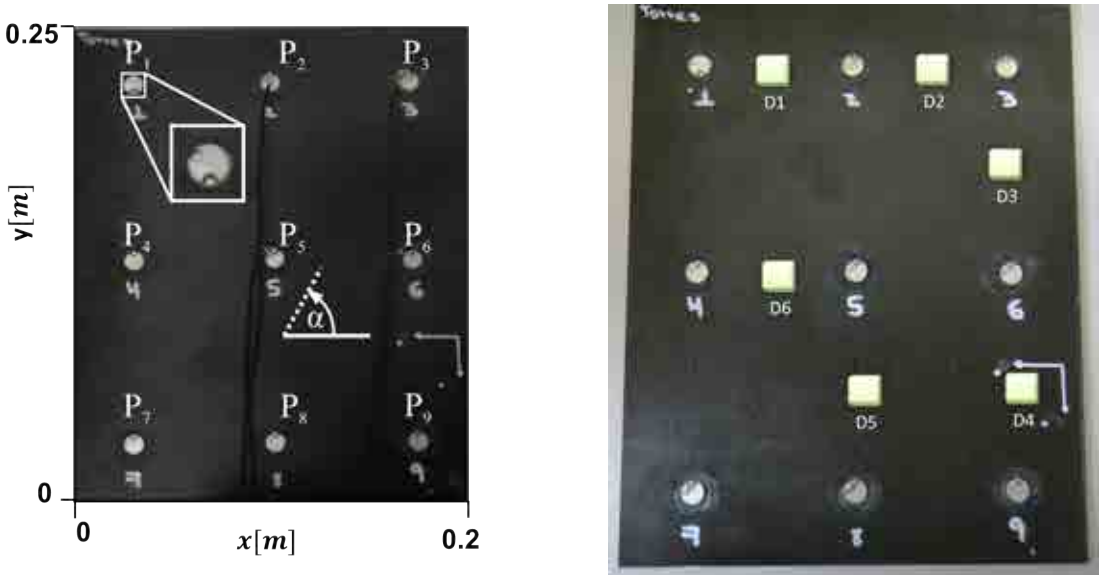

(a) (b)

Figure 4.5: CFRP plate and damages positions.

Figure 4.6: Damage 3 in the CRFP Composite Plate.

instrument manufactured by TiePie Engineering, The Netherlands). The excitation voltage signal was a 12V Hanning windowed cosine train signal with 5 cycles and 200 experiments were recorded per sensor-actuator configuration. The carrier frequency was found to be 30KHZ. The data acquisition is performed by some HS4-HandyScopes. To ensure a good signal to noise ratio each signal was averaged 100 times. For this experiment, the transducers were connected directly to the inputs of the oscilloscope. Damage on the tested composite plate was simulated by adding masses at different positions and a total of seven structural states were studied: six damages and the healthy structure. Figure 4.5b outlines the positions for the simulated damage on the multilayered composite structure and Figure 4.6 shows one of these damages.

4.4 Composite plate 2

This structure was also tested in the Siegen University and corresponds to a plate made of six equal layers with a total thickness of 3mm made of TEPEX dynalite 102-RG600(x)/47 % Roving Glass - PA 6 consolidated composite from Bond Laminates GmbH. The thickness per layer is 0.5mm. The properties of the material were $V_{Fiber} = 47\%$, $E_1 = 22.4GPa$, $E_2 = 21.5GPa$, $v_{12} = 0.17$, $v_{13} = 0.17$, $v_{23} = 0.3$ and $G_{12} = G_{13} = 4.9GPa$. The density was about 1800 kg/m^3. As in the previous case, nine PZT transducers PIC-151 were bonded to the surface and the inspection was performed by using the Handyscopes HS3 and HS4. The time histories were digitized at a sampling frequency of 50 MHz and averaged 100 times to ensure a good signal to noise ratio. The carrier frequency was found to be 30KHZ. Damage on the multilayered composite plate was simulated by placing magnets with different masses at random orientations on both faces of the structure as artificial damage. Figure 4.7 outlines the positions for the simulated damage on the structure.

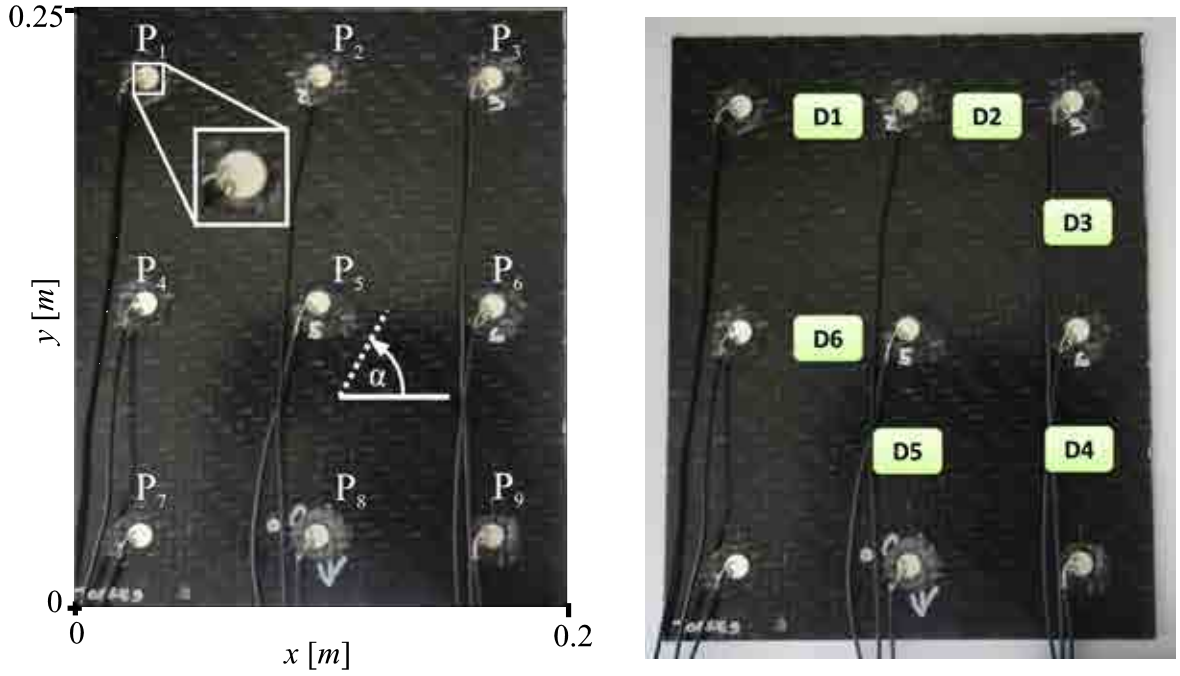

(a) (b)

Figure 4.7: Multilayered composite plate.

4.5 Aircraft turbine blade

This specimen corresponds to an aircraft turbine blade which was tested in the “Universidad Politécnica de Madrid”. An important feature to highlight from this structure is that it has an irregular form and includes a stringer in both faces. This blade was instrumented with seven piezoelectric transducers attached on the surface: three of them were distributed in one face and the others on the other face. The transducers dimensions are diameter $26mm$ and thickness $0.4mm$. Dimensions and physical shape of this blade are depicted in figure 4.8.

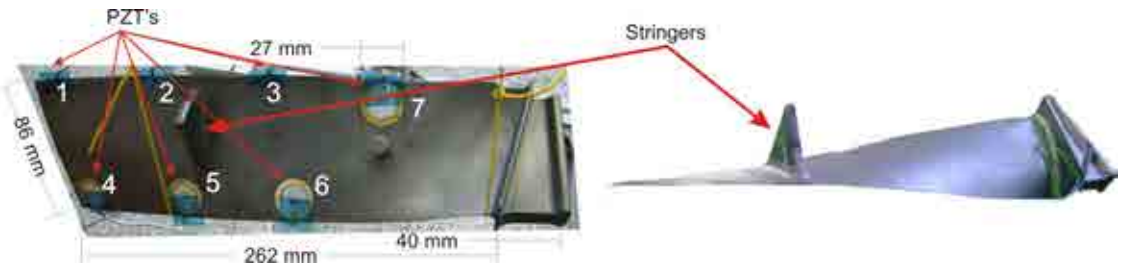

Figure 4.8: Aircraft turbine blade.

To assess the structure, a ScanGenie® from Acellent technologies was used. As excitation signal, a BURST signal with 250 KHz and 3 peaks was applied. Ten different structural states were studied: the healthy structure and nine damages which were simulated adding two masses in different locations as is shown in Figure 4.9. A total of 140 experiments were performed and recorded: 50 with the undamaged structure, and 10 per damage. The dynamical response saved by each experiment is the result of the average of ten repetitions. This was done to ensure a good signal to noise ratio.

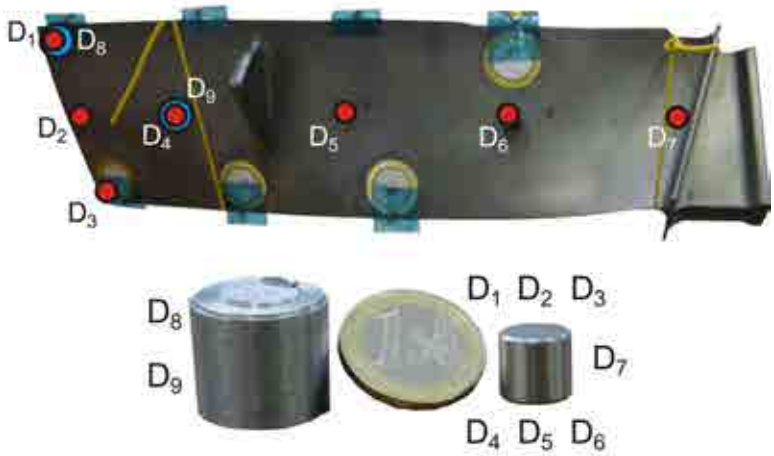

Figure 4.9: Damage distribution on the aircraft turbine blade.

4.6 Aircraft wing skeleton

This structure corresponds to an aircraft wing skeleton and is one of the structures tested in the "Universidad Politécnica de Madrid". This is divided in small sections by means of stringers and ribs as is shown in Figure 4.10. For testing the approaches, two sections of this structure were used. Dimensions of each section and damage description are depicted in Figure 4.11. These sections were instrumented with 6 PZT transducers, two in the upper section, two in the lower section and two in the rib. The transducers dimensions are diameter 26 mm and thickness 0.4 mm.

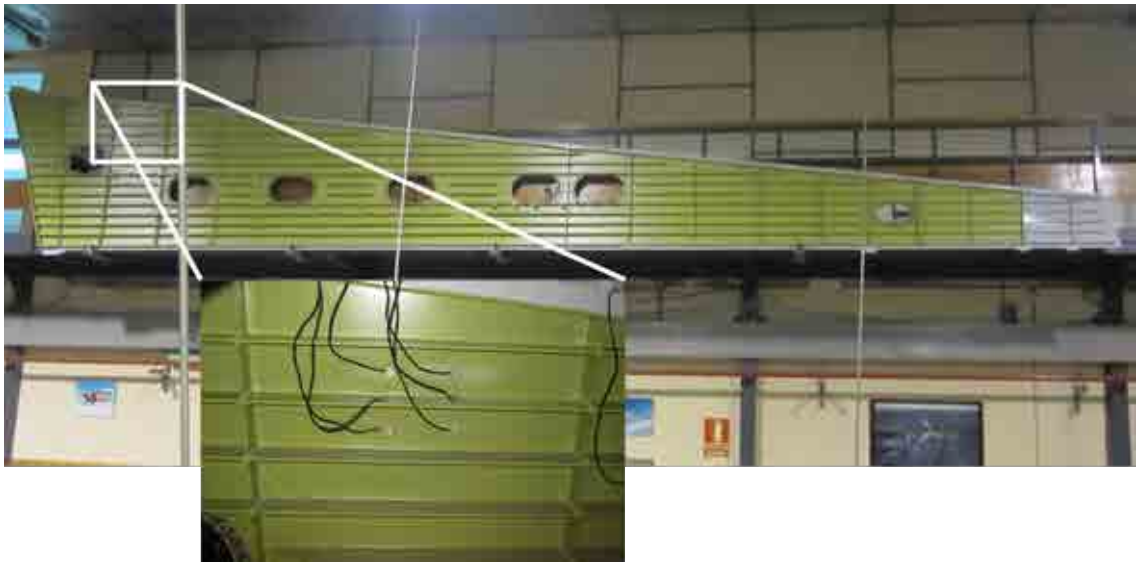

Figure 4.10: Sections tested with the PZT location.

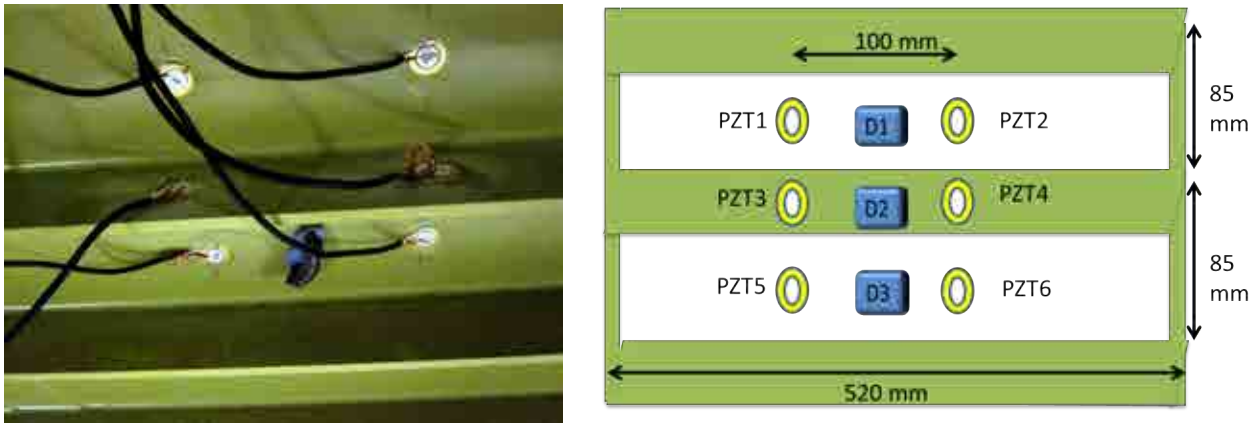

(a) (b)

Figure 4.11: Damage description.

As excitation input, a BURST signal with 205 KHz as central frequency and nine peaks was used. Four different states of the structure were analyzed: the healthy structure and the structure with three different damages. Damages were simulated by adding a mass at three different positions (Figure 4.11), two of them on the skin and the other on the stringer, 100 experiments were performed and recorded: 25 with the undamaged structure and 25 per damage. To ensure a good signal to noise ratio each signal was averaged 10 times. To apply and collect the signals to the PZT transducers, a chassis PXI 1033 from National Instruments ® was used. Due to the complexity and the size of this structure, a wideband power amplifier model 7602M of Krohn-Hite corporation is used to amplify the signal applied to the actuators.

4.7 Aircraft fuselage

This structure corresponds to an aircraft fuselage from an Airbus A320 and was one of the structures tested in the Siegen University during the research visit. The structure includes a curved plate, four vertical stringers and seven horizontal ribs. The fuselage was instrumented with nine broadband piezoceramics PIC-255 from PI Ceramics bonded on the curved plate surface with the purpose of transmitting and receiving ultrasonic guided waveforms. The transducers dimensions were diameter 10mm and thickness 0.25mm. The transducers configuration is illustrated in Figure 4.12. The length, width and thickness of the fuselage are 2000mm, 1250mm and 2mm, respectively.

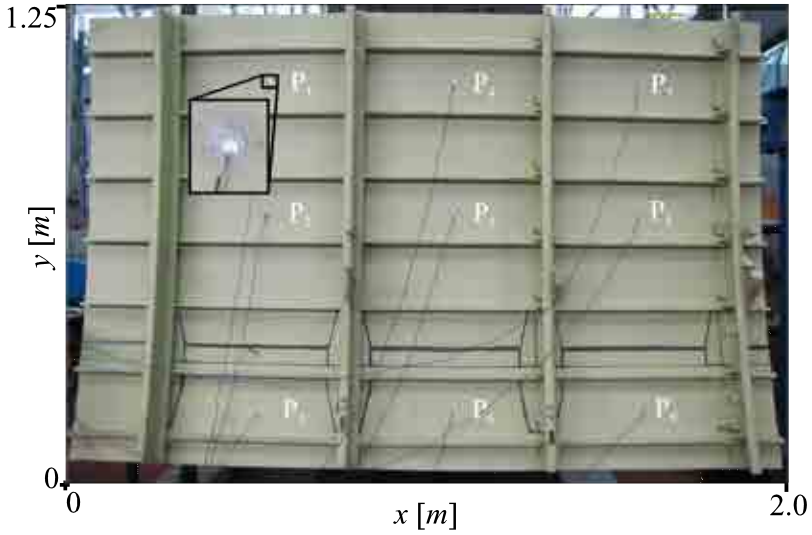

Figure 4.12: Airbus A320 Fuselage.

Figure 4.13: Damage distribution in the Airbus A320 Fuselage.

(a) (b)

Figure 4.14: Damage 1 and 2 in the aircraft fuselage.

The excitation of the structure and the data acquisition were performed using the Handyscope HS3 and HS4. To ensure a good signal to noise ratio, each signal was averaged 100 times. Due to the complexity and the size of this structure, as in the previous structure, a wideband power amplifier model 7602M of Krohn-Hite corporation was used to amplify the signal generated at the HS3. A gain of ten times the input amplitude was selected. Damage on the tested fuselage was simulated by adding masses at different positions on the surface of the curved plate. Figure 4.13 shows the positions for the simulated damage on the fuselage structure and the Figure 4.14 shows two of these damages.

4.8 Aluminium plate with reversible damages and temperature variations

(a) (b)

Figure 4.15: Damages in the aluminum plate.

This structure corresponds to an aluminum plate with dimensions $200mm \times 200mm$ instrumented with 5 PZT transducers (PIC-151). This structure was one of the structures

tested in the Siegen University in collaboration with the PhD student Maribel Anaya during the research visit. Damages in the structure were simulated by adding masses at four different positions on the surface as is shown in Figure 4.15.

To assess the structure, the Handyscopes HS3 and HS4 without pre-amplification were used. As excitation, a BURST signal of 50KHz as central frequency was used and each collected experiment was averaged 100 times to ensure a good signal to noise ratio.

This structure was subjected to temperature changes. To perform these experiments, the structure was introduced in a oven with controlled temperature and data from the structure under six different temperatures (24, 30, 35, 40, 45 and 50 °C) for each structural state were collected. To avoid the contact between the metallic surfaces and eliminate the noise in the experiments, some plastic elements are used. For each temperature, 100 experiments were collected for each state.

Chapter 5

DAMAGE DETECTION SYSTEM

5.1 Problem statement

One of the most important tasks in Structural Health Monitoring (SHM) corresponds to the damage detection. This is the first step of the process discussed in [148]. In this task, the existence of damage should be determined, the aim is to know if there is damage in the structure.

In the literature it can be found several potentially useful techniques for damage detection, and their applicability to a particular situation depends on the size of the critical damages that are admissible in the structure. Almost all of these techniques follow the same general procedure: the structure is excited using actuators and the dynamical response is sensed at different locations throughout the structure. Any damage will change this vibrational response. The state of the structure is diagnosed by means of the processing of these data. Several studies have shown that the detection of changes in a structure depends on the distance from the damage to the actuator as well as the configuration of the sensor network. This chapter is concerned with the practical application of a methodology for the problem of detection of damages in structures by using statistical data driven models built from structural dynamic responses when the structure is know to be healthy. In the following sections, a detailed description of the methodology is presented. The methodology is the basis of this thesis and it can be adapted and extended to localize and classify damages as will be presented in the next chapters.

5.2 Damage detection methodology

5.2.1 Overview

The damage detection methodology proposed in this thesis involves the use of a multiactuator piezoelectric system (distributed piezoelectric active network), Principal Component Analysis (PCA) and some damage indices. In general terms, the practical application of this approach is performed in two stages:

1. **Baseline modeling**: In this stage, experiments of the structure are performed when is well known that the structure is undamaged. Data gathered by sensors are organized and

preprocessed to obtain the statistical data driven baseline models based on PCA. Scores and indices obtained in this stage are also stored as the baseline indicators.

2. **Data projections onto the models**: In this stage, the structure to study is subject to the same experiments performed to the healthy one. Data are organized, preprocessed and projected onto the models obtained in the previous stage. Consequently, scores and indices are calculated and compared with the obtained ones using the healthy structure.

Details about the multiactuator piezoelectric system and the way of performing the experiments are presented in the next sections. Although the theoretical background about PCA was introduced in Section 2.3, the procedure for: (i) organizing the data gathered by experiments, (ii) building the baseline PCA model and, (iii) projecting the data from new experiments, are described also in the following sections.

5.2.2 Experimental setup and data acquisition

The structure to test is instrumented with several PZT transducers bounded on the surface. It is isolated in order to remove the environmental noise and the boundary conditions. To perform the excitation and collect the vibrational responses from the structure, several actuator phases are used. In every actuator phase, a single PZT transducer is used as actuator and the others as sensors that receive the wave propagated across the structure at different points. Typically, a BURST signal with a frequency defined for each structure is used as signal excitation. This frequency is chosen once a sweep frequency response test is performed. In some structures, depending on its complexity, this signal should be amplified by using a wideband power amplifier. To remove the noise in the signals, one experiment consists of repetitions which are averaged. Several structural states are studied for each structure. In general, these states contain the healthy structure and the different damages.

5.2.3 Preprocessing

The dynamic responses collected from each actuator phase are stored by the data acquisition system into a matrix with dimensions $(I \times K)$, where I represents the number of experiments and K the number of sampling times. Denoting J as the number of PZT transducers that are receiving the dynamical responses for each experiment, J matrices with the information from each sensor by each actuator phase are finally stored. Therefore, the whole set of the data collected in each actuator phase can be organized in a 3D matrix $(I \times K \times J)$ or in a 2D unfolded matrix $(I \times JK)$ where data from each sensor are located besides the other sensors as can be seen in Figure 5.1. This is a very common practice in multivariate statistical procedures for monitoring the progress of batch processes [186], [136].

As a preliminary step to implement the PCA methodology, the pre-processing of the data collected in each phase should be performed. For this kind of data sets (unfolded matrix), several studies of scaling have been presented in the literature: continuous scaling (CS), group scaling (GS) and auto-scaling (AS) [184]. According to these studies, GS is selected for this

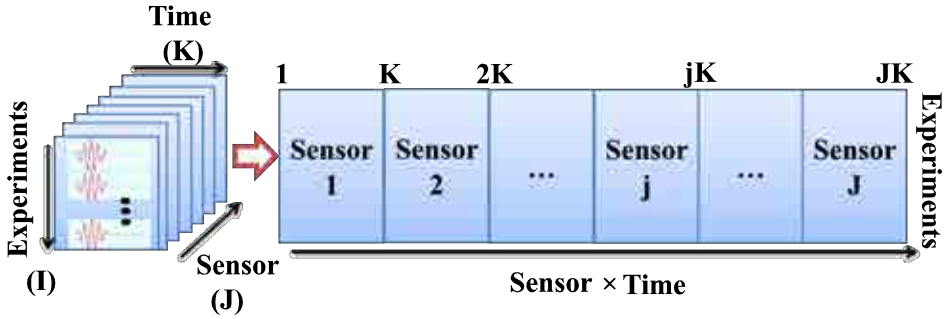

Figure 5.1: Unfolding the collected data in 3D to bi-dimensional matrix (I×JK).

work because it considers changes between sensors and does not process them independently. Figure 5.2 shows the unfolded matrix of the actuator phase 1, where the data from the j^{th} sensor is highlighted to show how the normalization is applied. Using this normalization, each data point is scaled according to equation (5.2) using the mean of all measurements of the sensor at the same time (equation 5.1) and the standard deviation of all measurements of the sensor (equation 5.3).

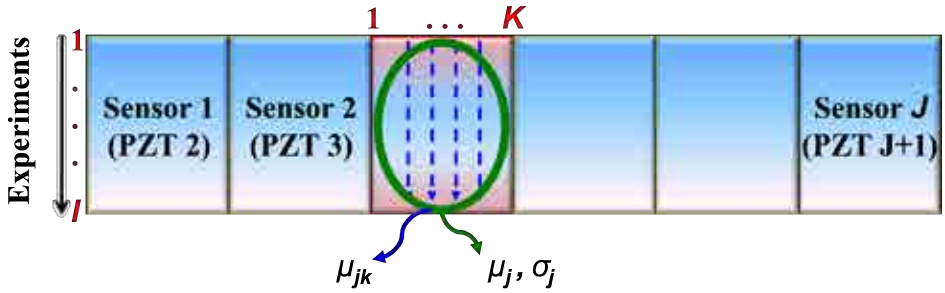

Figure 5.2: Group scaling pre-processing.

$$\mu_{jk} = \frac{\sum_{i}^{I} x_{ijk}}{I} \tag{5.1}$$

$$\mu_j = \frac{1}{IK} \sum_{i=1}^{I} \sum_{k=1}^{K} x_{ijk} \tag{5.2}$$

$$\sigma_j^2 = \frac{\sum_{i}^{I} \sum_{k}^{K} (x_{ijk} - \mu_j^2)}{IK} \tag{5.3}$$

$$\overline{x}_{ijk} = \frac{X_{ijk} - \mu_{jk}}{\sigma_j} \tag{5.4}$$

where x_{ijk} is the k^{th} sample of the j^{th} sensor in the i^{th} experiment, μ_{jk} is the mean of the all k^{th} samples of the j^{th} sensor, μ_j is the mean of all measurements of the j^{th} sensor, σ_j is the

standard deviation of all measurements of the j^{th} sensor, and $\overline{x}_{ijk}$ is the scaled sample (equation 5.4). Once the normalization is applied, the mean trajectories by sensor are removed and all sensors are made to have equal variance.

5.2.4 Baseline model building and calculation of damage indices using PCA

In a first stage, A PCA baseline model is built for each actuator phase (PZT1 as actuator, PZT2 as actuator, and so on) using the signals recorded by sensors during the experiments with the undamaged structure. The scheme showed in Figure 5.3 summarizes the procedure. PCA baseline modelling essentially consists of calculating the matrix **P** for each phase as was explained in the theoretical background chapter (Equations 2.7 - 2.11).

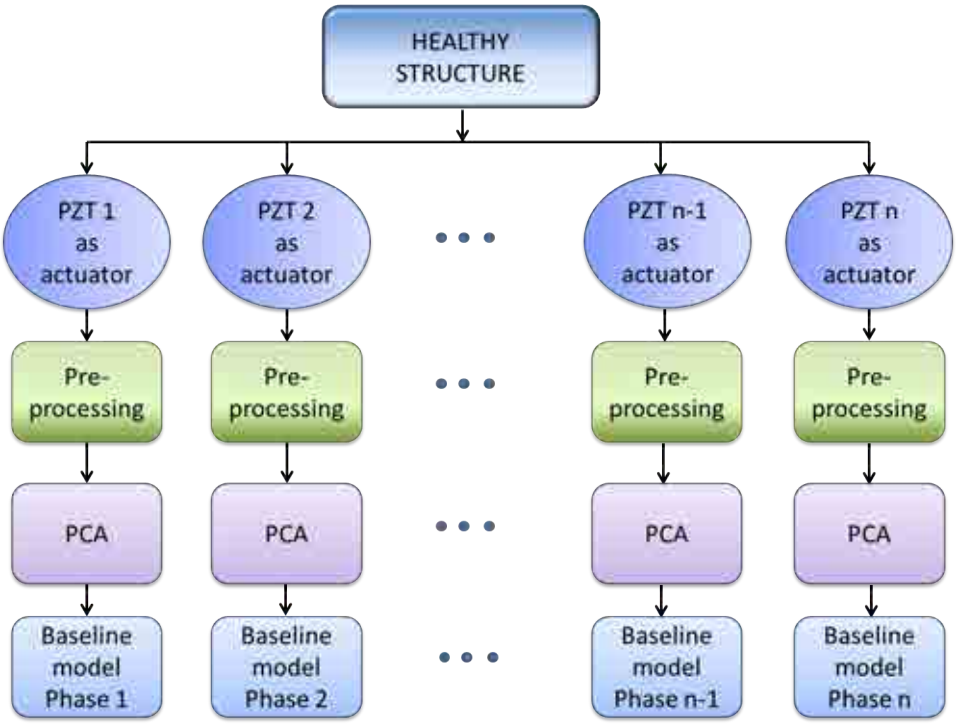

Figure 5.3: Baseline definition methodology.

In a second stage, experiments are performed using the structure in the different possible states or scenarios (undamaged and different damages). Figure 5.4 illustrates the procedure. These signals are pre-processed and organized according to the PCA modeling procedure. Afterward, they are projected on the corresponding PCA model ($\mathbf{T} = \mathbf{XP}$). A selected number of the first principal components (scores-**T**) are obtained. In addition, some damage indices are calculated by each baseline PCA model using the equations (2.13 - 2.16) introduced in the theoretical background chapter. In this work, each PCA model is created using a percentage of the whole dataset collected using the undamaged structure. Signals from the remaining data, besides the data from the structure in different states are used in a second stage.

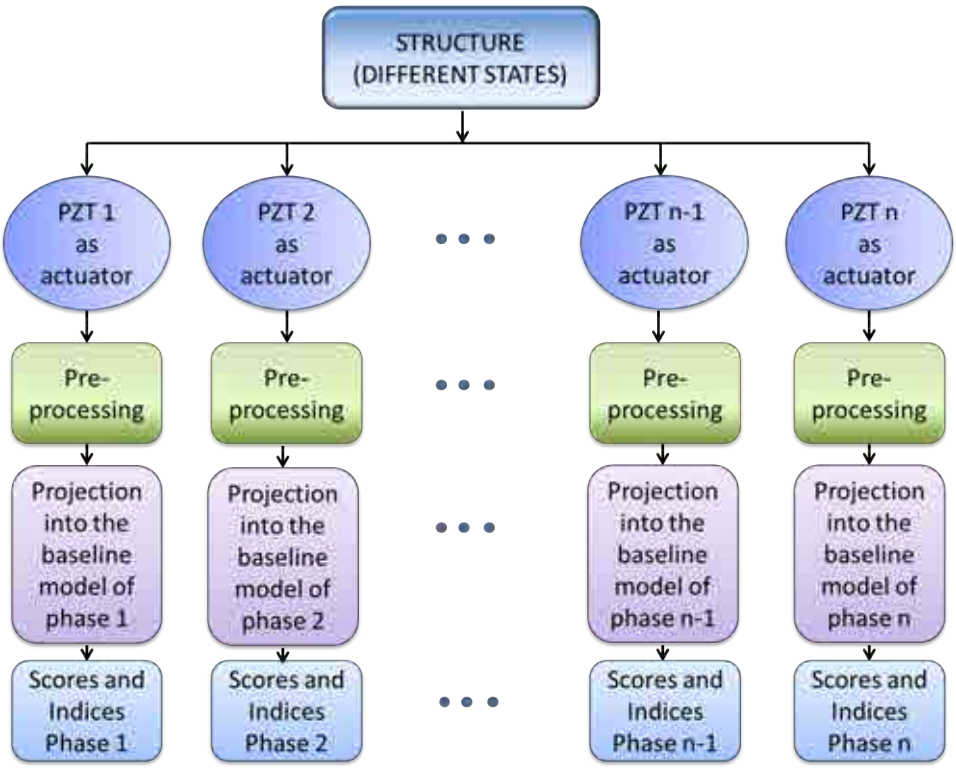

Figure 5.4: Data projection into the PCA models.

5.3 Generalization of the methodology

Let us remark that the damage detection methodology can be implemented using any Multivariate Statistical Method (MSM) in which it is possible to obtain a representation by components and damage indices. Considering just one actuator phase, the general methodology is depicted in Figure 5.5.

In this sense, a statistical method known as Independent Component Analysis (ICA) is also used instead of PCA. As was explained in the theoretical background chapter, this method allows to re-express the data in a new space by calculating the new components that are mutually independent, uncorrelated but not necessary orthonormal. Additionally, in other works [175], [173], [174] the author together with partners from the Siegen University showed the use of this methodology as preliminary step for the classification of damages using Hierarchical Non-linear PCA. These results are useful to demonstrate that is possible to generalize the methodology.

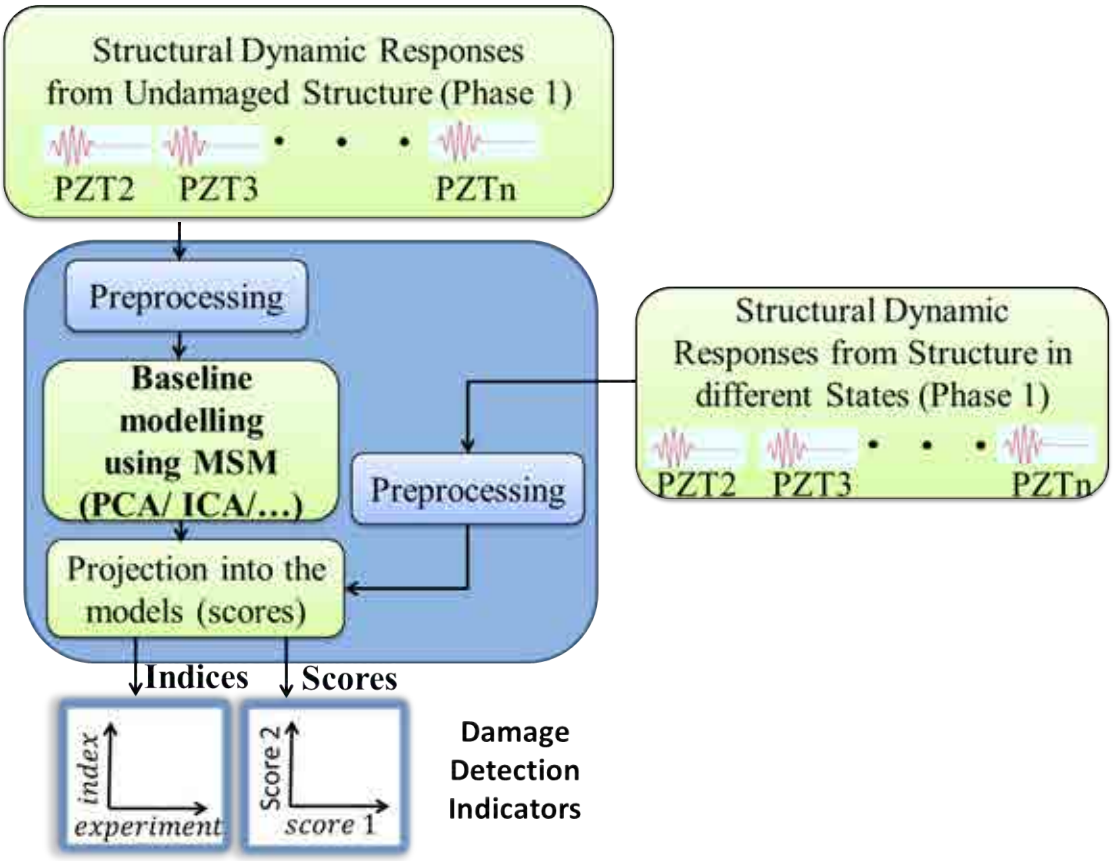

Figure 5.5: Generalization of the methodology for damage detection considering just one actuator phase.

5.4 Experimental results

5.4.1 By using PCA baseline models

The validation of the damage detection methodology using PCA models is carried out by using data from experiments performed to two different specimens: an aircraft turbine blade and an aircraft wing skeleton. As is mentioned in sections 4.5 and 4.6 where the structures are described, the aircraft turbine blade was instrumented with seven PZT transducers, therefore seven actuator phases were accomplished. Besides, nine defects were simulated. On the other hand, the wing skeleton was instrumented with six PZT transducers (6 actuator phases) and three defects were simulated.

Distribution of variance

Once the baseline PCA models were built by using experiments from the healthy structure, an analysis of the variance captured by each Principal Component (PC) was achieved. This analysis is important in order to ensure that enough variance is retained in the model, which allows performing an optimal reduction. The distribution of the retained variance in four of the actuator phases of each structure is depicted in Figure 5.6 and 5.7. Just the components with a

significant variance value are shown. The components with the highest variance represent the most important pattern in the data with the largest quantity of information. Figures 5.6 shows that, using the aircraft turbine blade, the first two components represent more than 80% of the cumulative variance in each model. Similar results are obtained in the other phases.

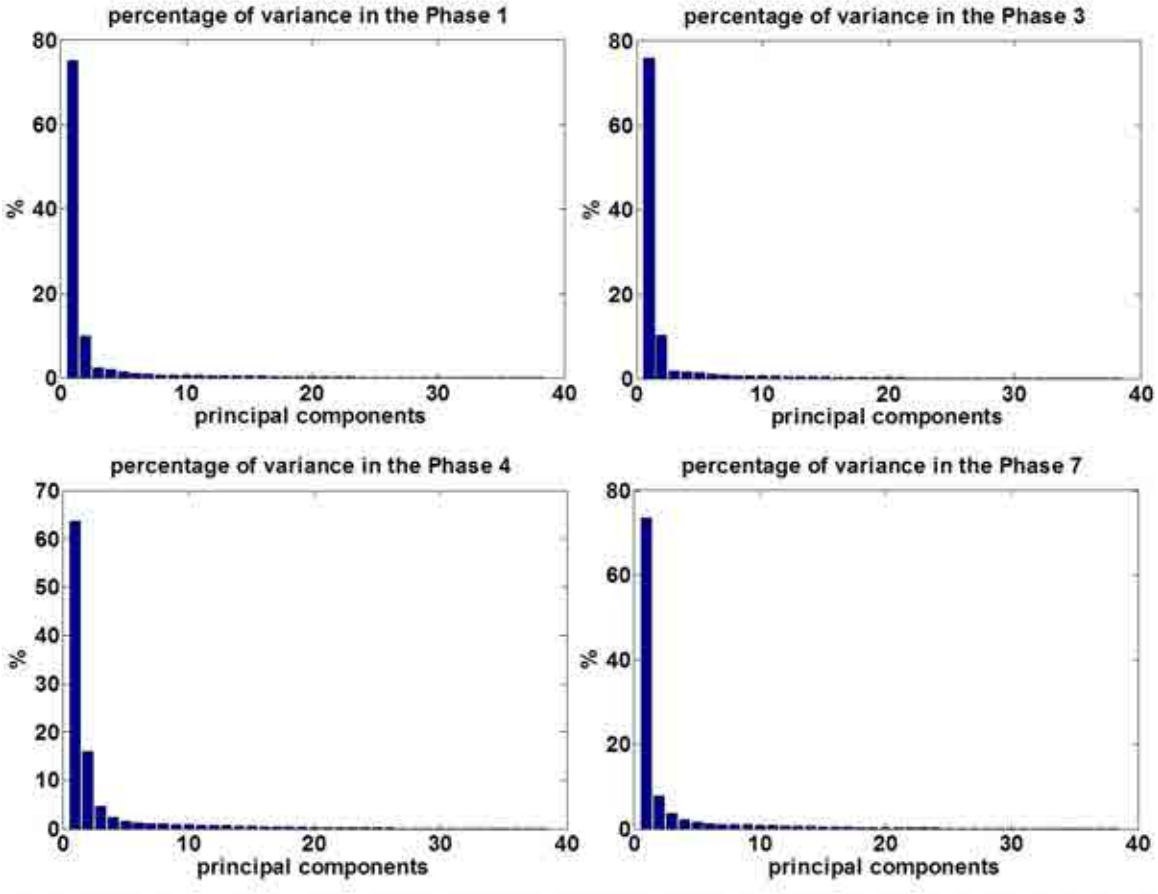

Figure 5.6: Distribution of the variance in phase 1, 3, 4 and 7 in the aircraft turbine blade.

On the other hand, from Figure 5.7, it can be seen that the percentage of the variance of each component in the aircraft wing skeleton is lesser than the obtained in the previous structure. Although the two first components are the most significant, these just contain 37 % of the cumulative variance. This difference can be explained by the differences between the structures.

In order to define a standard criteria for the comparison and for maintaining simplicity in the analysis and the visualization tasks, just two scores are used in both cases in order to show how this choice affects the results of each structure for each of the proposed approaches.

A previous work [124] showed the advantages and disadvantages in the use of the scores plots for detecting damages. This chapter aims to show how the results in these plots can be different in some cases, thus requiring additional analysis tools such as damages indices for performing a good detection and classification task.

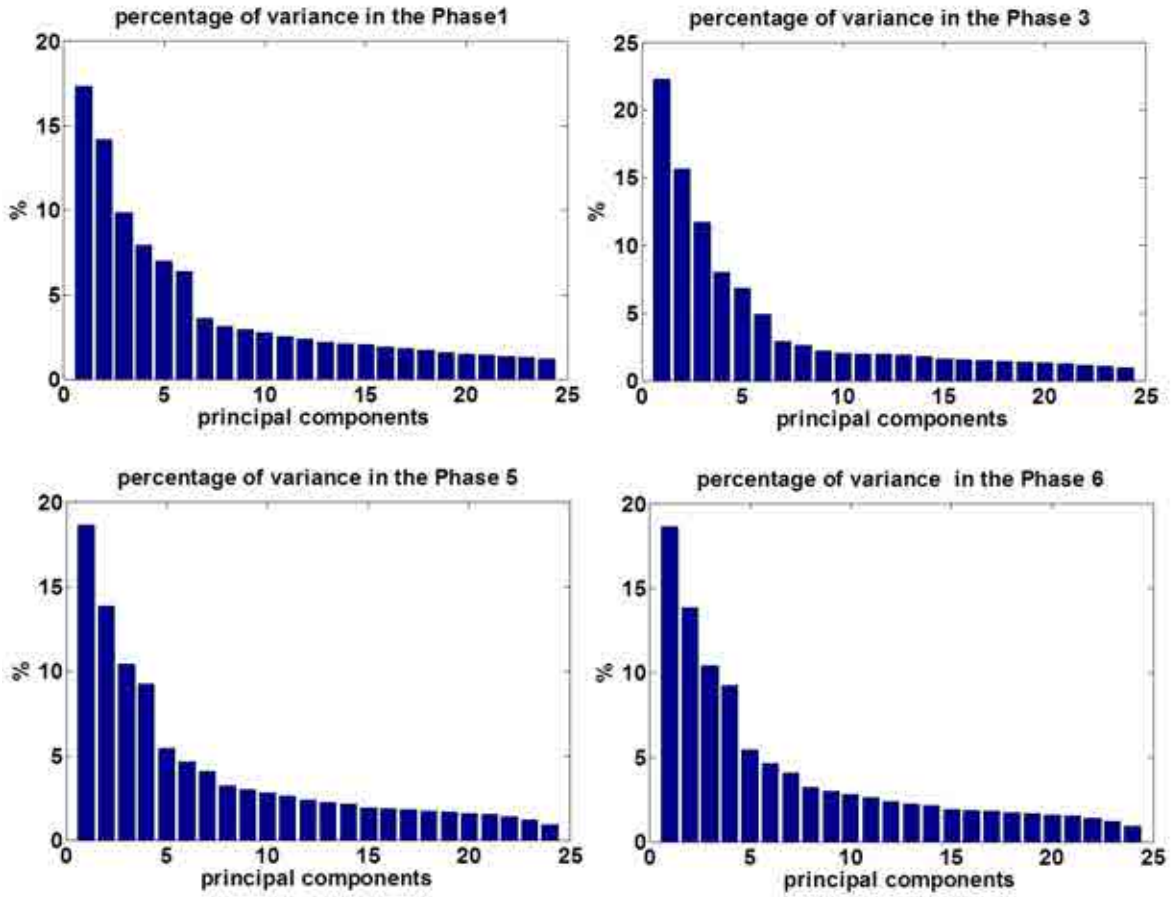

Figure 5.7: Distribution of the variance in phase 1, 3, 5 and 6 in the aircraft wing skeleton.

PCA score plots

The projections of each experiment onto the principal components subspace are called scores. Plotting two scores in a scatter plot allows to visualize the structure of the original data, and is known as score plots.

Figures 5.8 and 5.9 show the score plots of the first and second principal components of different actuator phases of the aircraft turbine blade and aircraft wing skeleton respectively. As was previously mentioned in Section 5.2.2, each actuator phase corresponds to the experiments performed when just one PZT transducer is defined as actuator and the rest are used as sensors. Since the state or condition of the specimen (undamaged, damage 1, damage 2, etc.) is known in each experiment, each projection is labeled in order to identify each group data. Different shapes and colors represent the different conditions of the specimens.

As can be seen from Figure 5.8 corresponding to the aircraft turbine blade, all the damages can be clearly distinguished from the undamaged structure state (green plus sign), similar results are obtained in the other phases not showed. This separation can be used to confirm changes in the structure and can be defined as an abnormal situation. This means that it is possi-

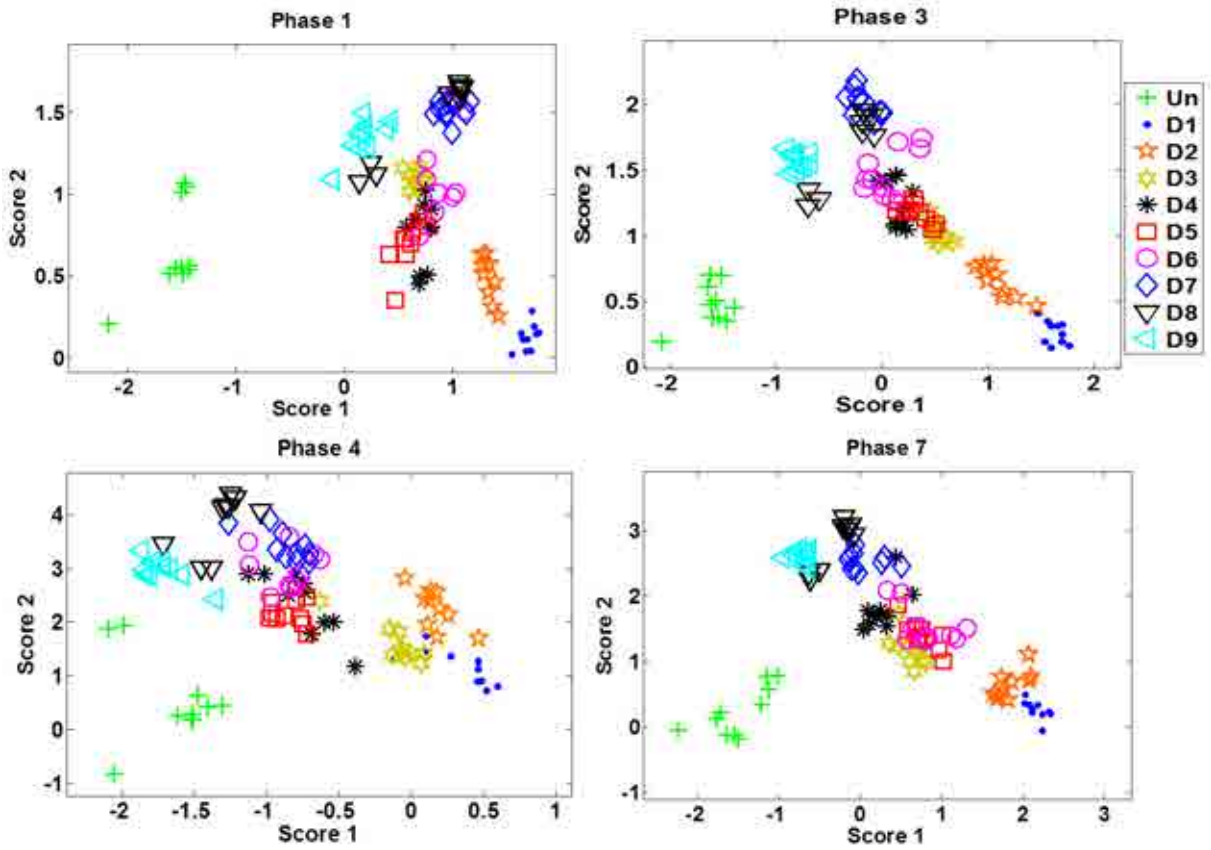

Figure 5.8: Score 1 vs. score 2 in the aircraft turbine blade in the phases 1, 3, 4 and 7.

ble to detect the presence of damages. Besides, it is possible to distinguish some data sets which are in some cases near between them, which means that the vibrational responses are similar. This result is interesting because showing these plots can be used for damage classification in a further analysis using, for instance, some additional pattern recognition technique [172],[124].

On the other hand, from Figure 5.9 it can be seen that in the aircraft wing skeleton is also possible to identify the dataset gathered from the damaged structure. However, in contrast to the turbine blade, this separation is not clear in all phases (phases 1 and 3). In this context it is possible to admit that this result could be related to the complexity of the structure. This result implies that it is necessary to use another type of measurement or statistic to obtain a better discrimination of the presence of damage in any structure for each one of the phases. As a solution to this problem, in this thesis, it is proposed the use of the damage detection plots by means of the use of different indexes. The following subsections show the results obtained by using the different indexes explained in Section 2.4.

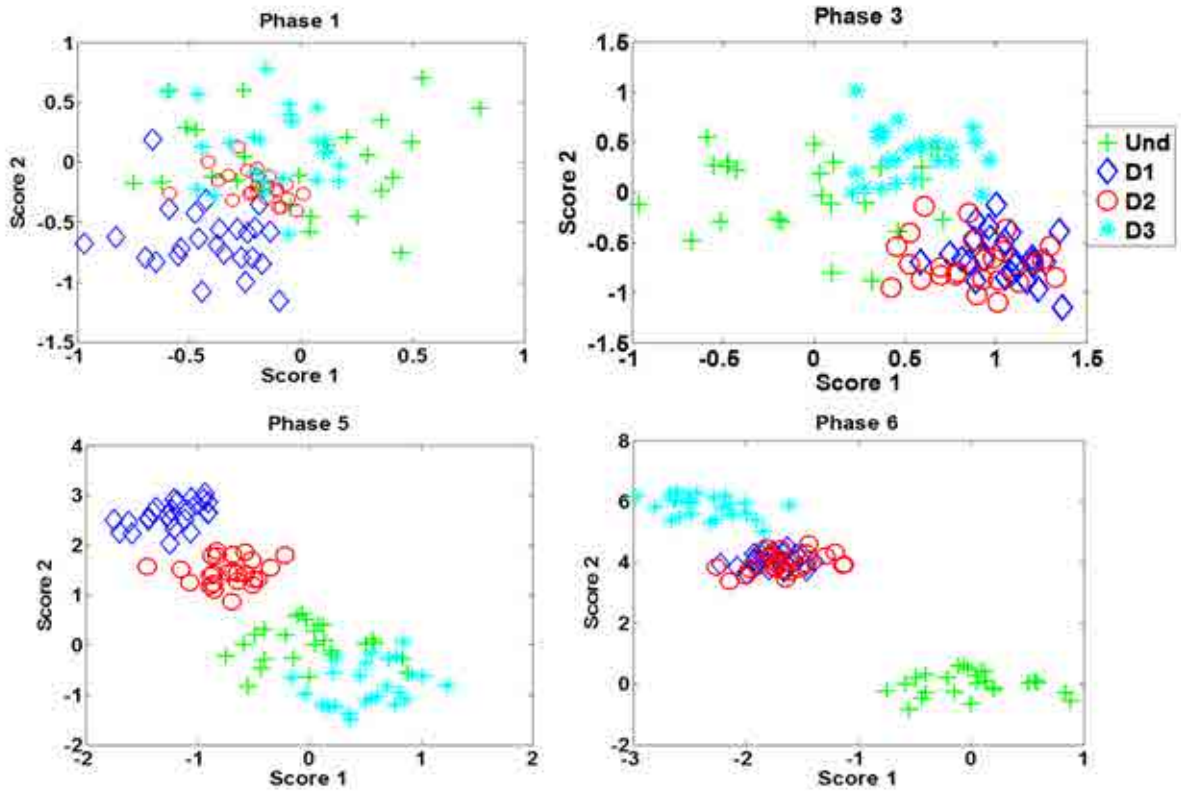

Figure 5.9: Score 1 vs. score 2 in the aircraft wing skeleton in the phases 1, 3, 5 and 6.

Damage index plots

As was mentioned in Section 2.4, there exist in the literature several statistical measurements that can explain the behavior of the projected data into the model. If the original data and the baseline data differ, it should be reflected in the score and/or these indices.

T^2 Index

From Figure 5.10, it can be seen the T^2 index by each experiment using the aircraft turbine blade in four actuator phases. The results show that each actuator phase depict different ways to visualize all the datasets with the information of the damages. In all these actuator phases, the damages 1, 2 and 3 have values of T^2 Index similar to the undamaged state and therefore can not be considered as damages. From the evaluation of the phases 1 and 4, it is possible to define that the damage 4 has similar value to the undamaged state, but in difference with these phases it is possible to identify a higher separation in the phases 3 and 7. The rest of the damages are well separated from the undamaged state. Considering the aircraft wing skeleton, Figure 5.11 shows the plots of the T^2 Index by each experiment. As it is disclosed, damage 1 is clearly separated from the undamaged state in all the phases, additionally, all the damages are well identified by the phases 1 and 3. In difference with the phases 1 and 3, phases 5 and 6 show that damages 2 and 3 have similar value of T^2 Index as the undamaged state.

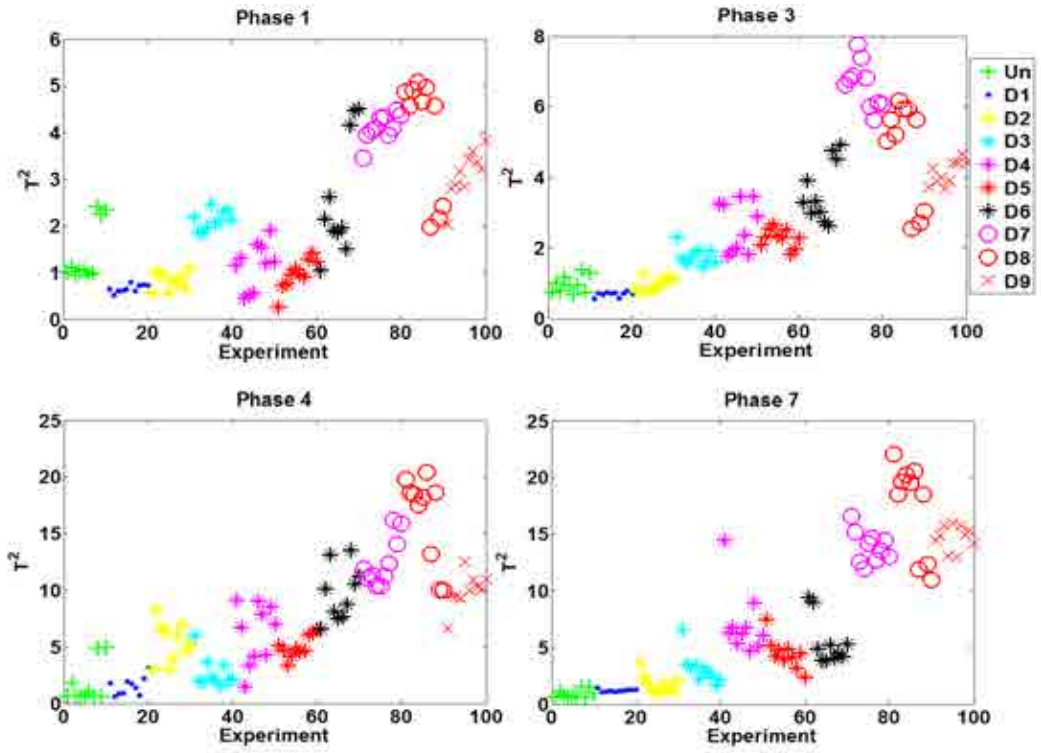

Figure 5.10: T^2-index in the aircraft turbine blade.

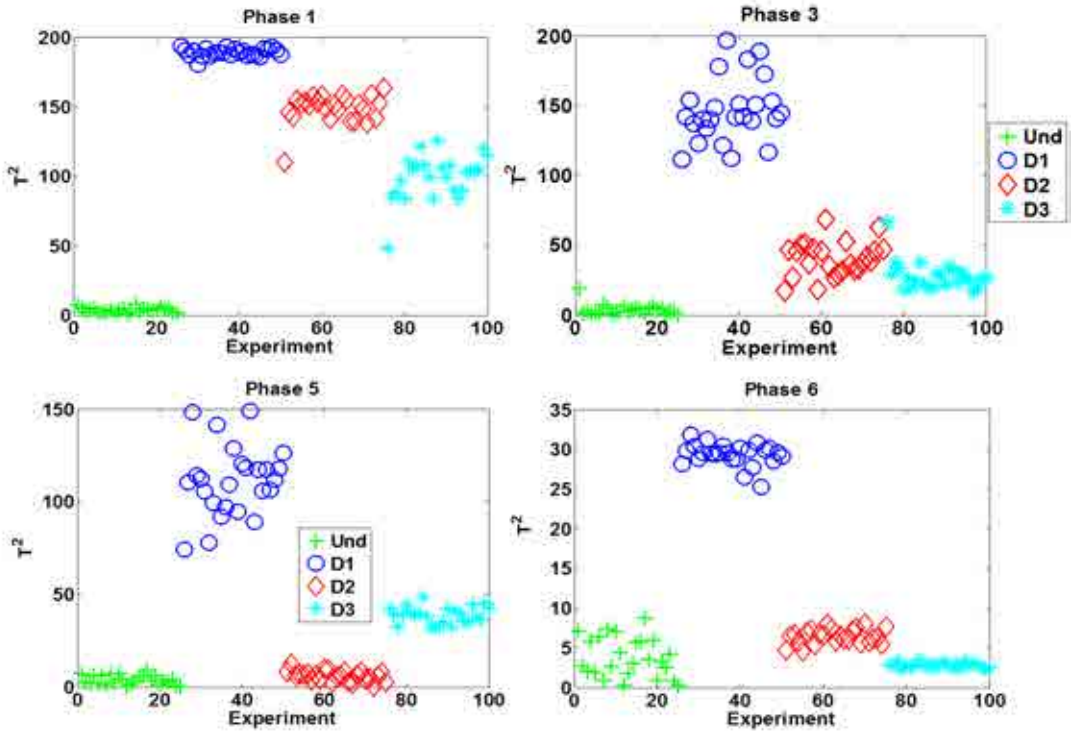

Figure 5.11: T^2-index in the aircraft wing skeleton.

Q Index

From Figure 5.12, it can be seen the Q index by each experiment using the aircraft turbine blade in the actuator phases number 1, 3, 4 and 7. In difference with the T^2 index, the phase 1 allows to identify the damage 1. Additionally in all the cases, the damage 3 is well separated from the undamaged state. The rest of the damages are not well identified.

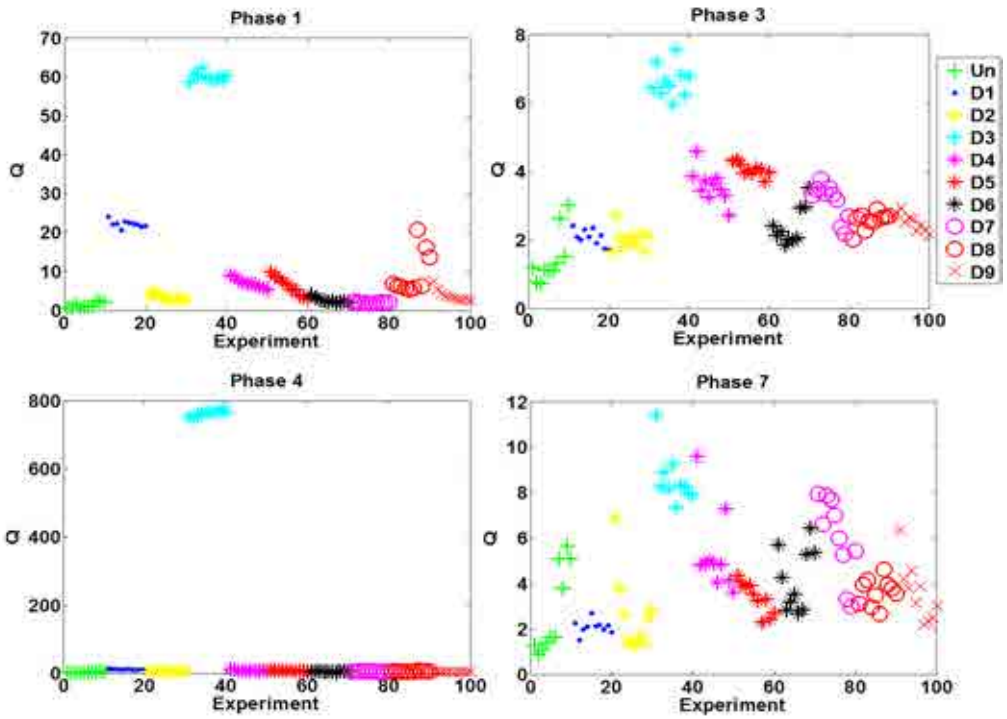

Figure 5.12: Q-index in the aircraft turbine blade.

Figure 5.13 shows the results in the use of the Q Index with the aircraft wing skeleton. The results in this structure show that in all the phases, the three damages are clearly separated from the undamaged state and, additionally, these states are easily distinguishable between them.

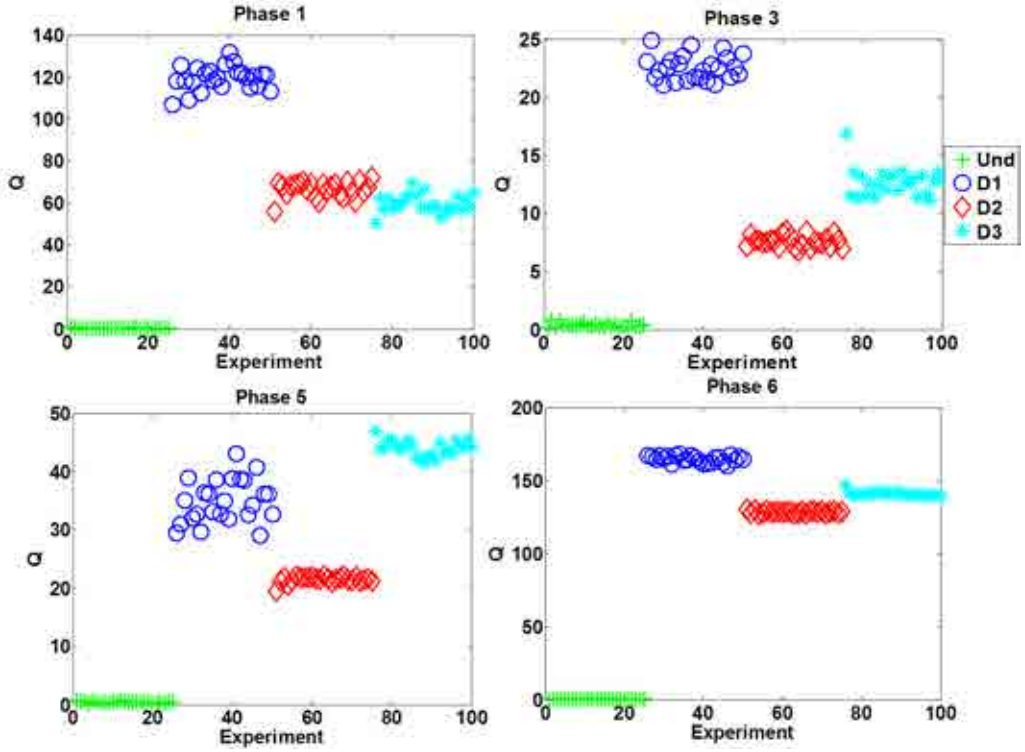

Figure 5.13: Q-index in the aircraft wing skeleton.

I^2 Index

From Figure 5.14, it can be seen the I^2 index allows to identify the damage 1 in the aircraft turbine blade. Additionally, some experiments of the damages 3, 4, 5 and 8 allow to define these states as damages. One important feature to highlight in comparison with the Q-index is that in this plot just significant differences are visible. In this way, values near to the healthy state are defined as zero.

Figure 5.15 shows the results in the aircraft wing skeleton with the I^2 Index by each experiment. Similar to the results obtained with the Q index, all the damages are clearly separated from the undamaged state. This result confirm the big differences between each state and the data from the healthy structure.

Combined Index (ϕ)

Figure 5.16 shows the results of the ϕ index in the aircraft turbine blade equally in four actuation phases. These results show how the damage 3 is clearly identified in every actuation phase. Additionally, the rest of the damages need to be identified by the analysis of the different phases.

Applying this index to the aircraft wing skeleton, the results show in Figure 5.17 are obtained. In this case, at the same manner as with the Q and I^2 indices, all the damages are clearly separated from the undamaged state.

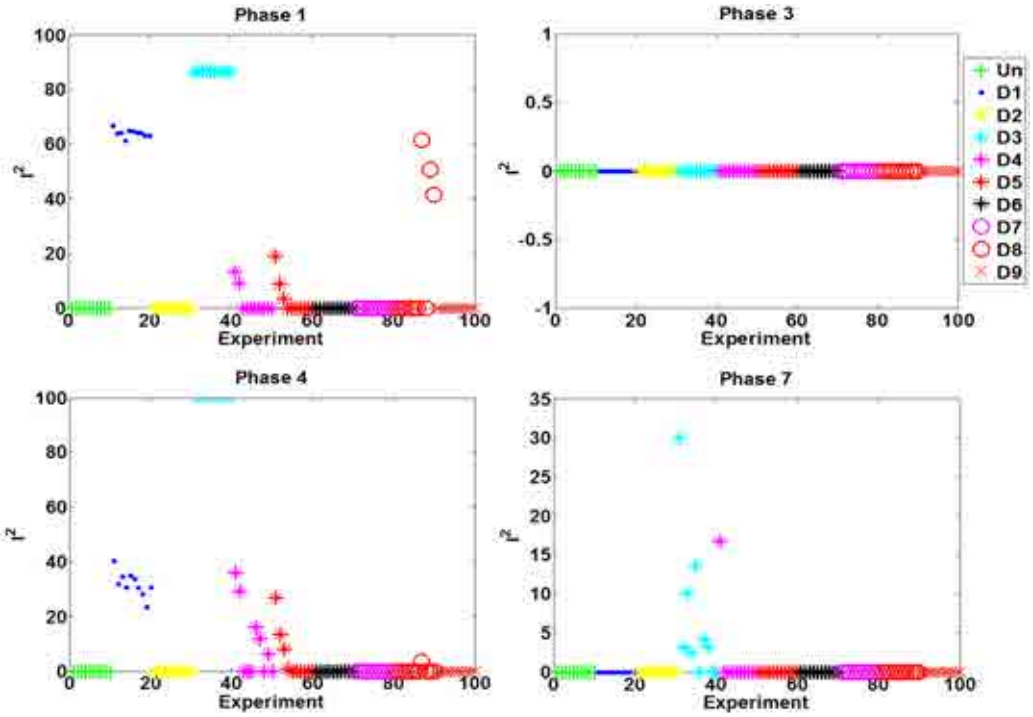

Figure 5.14: I^2-index in the aircraft turbine blade.

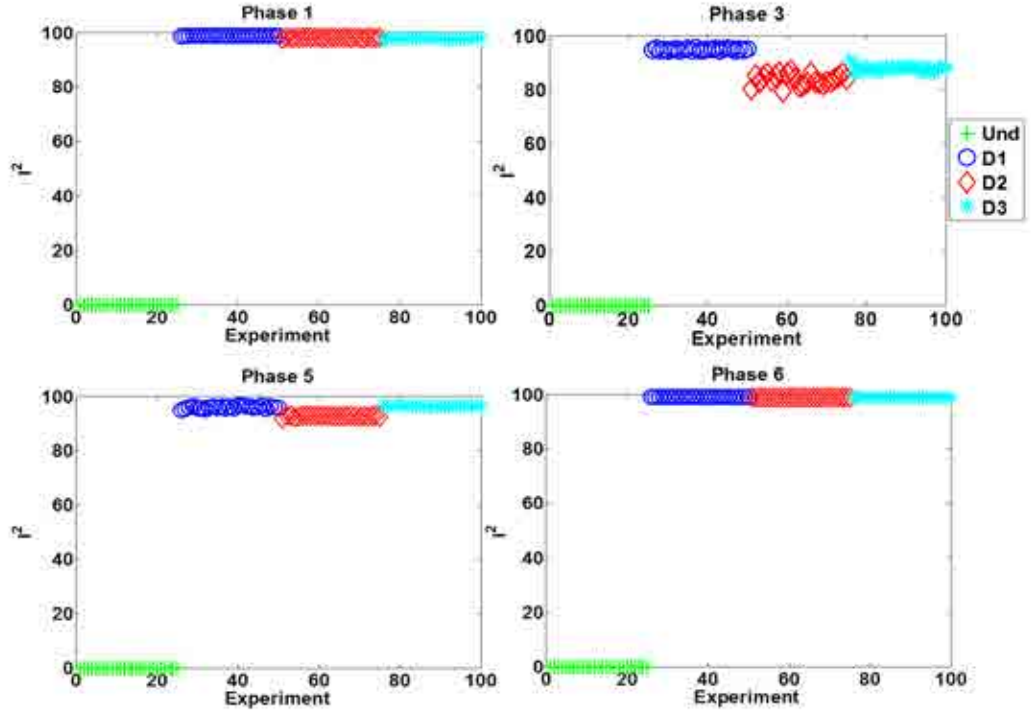

Figure 5.15: I^2-index in the aircraft wing skeleton.

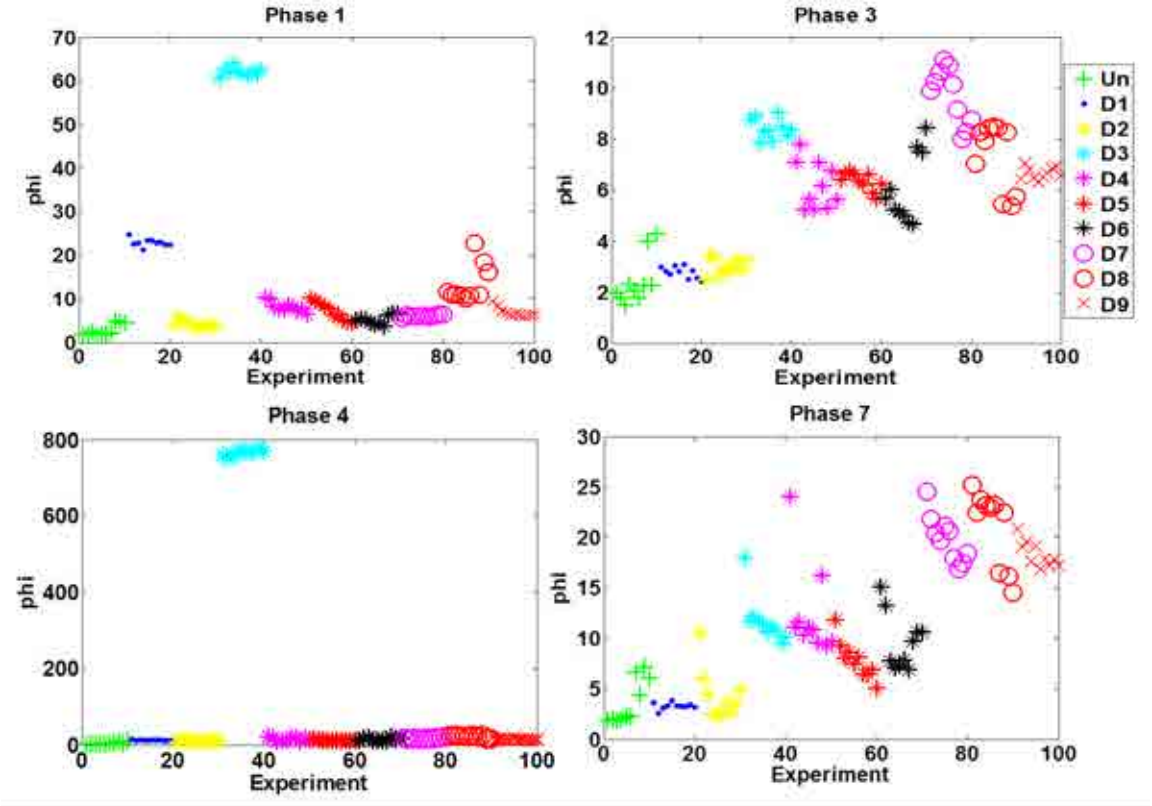

Figure 5.16: ϕ-index in the aircraft turbine blade.

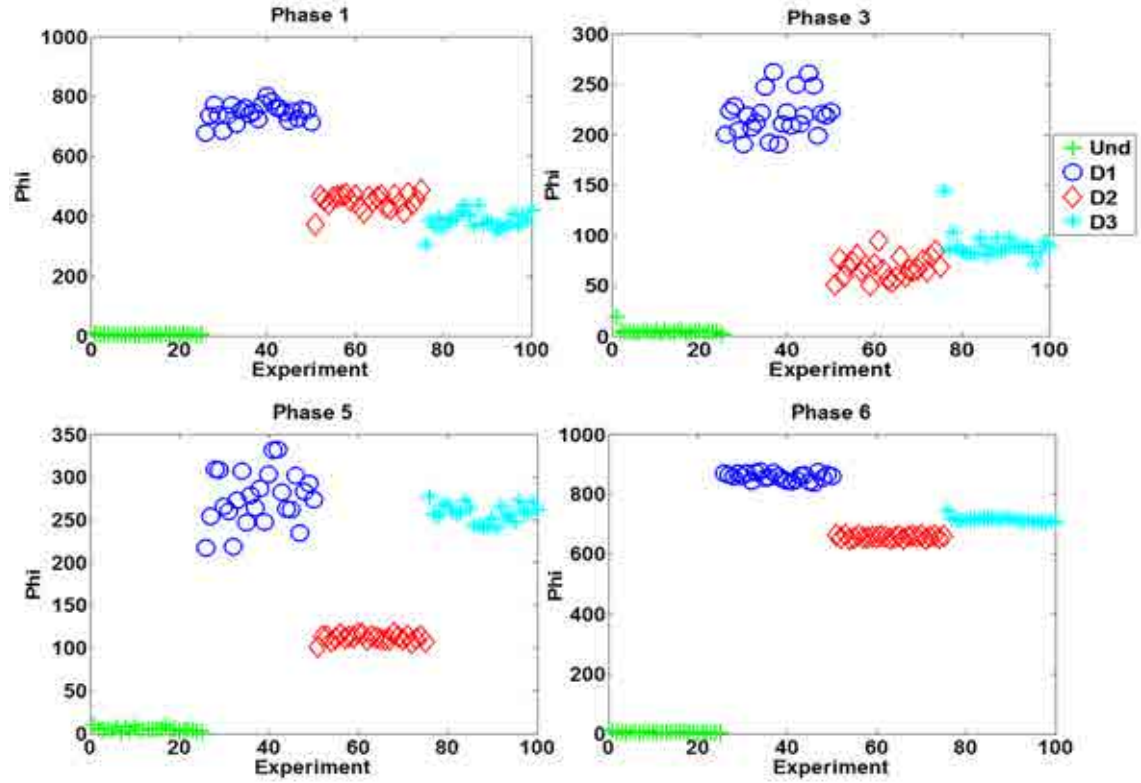

Figure 5.17: ϕ-index in the aircraft wing skeleton.

5.4.2 By using ICA baseline models

To validate the damage detection methodology using ICA models, the experiments performed to the aircraft wing skeleton were used. This set of experiments is the same previously used in Section 1.4.1.

ICA score plots

To perform the analysis, at the same manner as in the PCA case, the components are calculated using the data from the undamaged structure by each actuator phase. The new data with the information from the structure in different states are projected into each ICA model and two of these projections are plotted by each phase. Since it is necessary to perform a reduction and it is not possible with ICA, to determine which component is most relevant in the analysis, PCA is used to apply this reduction as was explained in the theoretical background (Chapter 2).

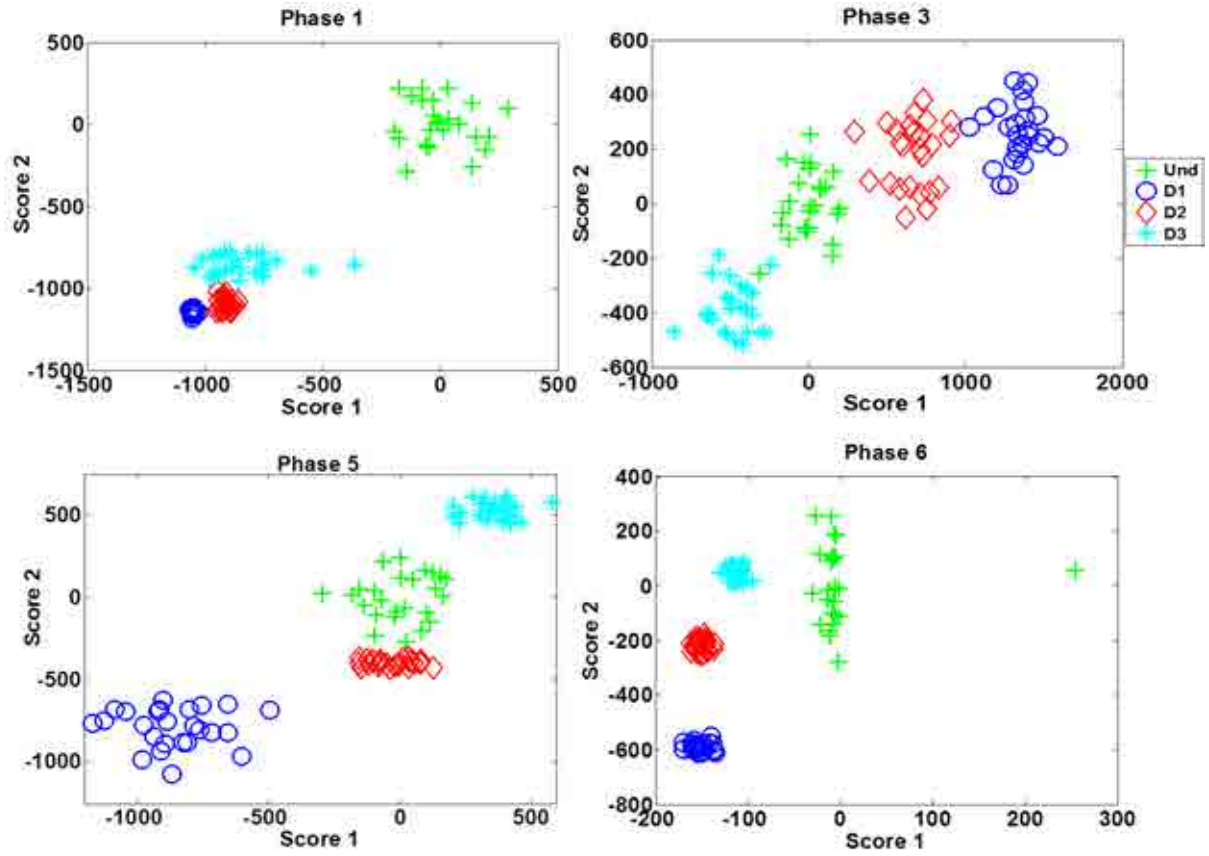

Figure 5.18: ICA score plots in the aircraft wing skeleton.

In the results, it is expected that experiments using the structure without changes appear grouped in the plot. Since the state of the structures in each experiment is known, each projection is labeled in order to identify each grouped data. It can be seen from Figure 5.18, which shows the score plots of four phases (1, 3, 5 and 6), that damages are clearly separated from the healthy structure. Also, it is possible to observe that scales obtained in the phases are

different. This is because some phases are more sensitive to the ICA model. In other words, the location of the damage in reference to the location of the PZT transducers and its severity is important.

The results obtained confirm that it is possible to use the methodology changing PCA as pattern recognizer by other multivariate statistical method with excellent results for detecting damages. Comparing the results of the score plots obtained with PCA and ICA, it is possible to observe that using ICA the results are better. These results can be observed comparing the different phases; in comparison, ICA needs several algorithm runs in order to achieve optimal results. However, if the results are based on a one-shoot basis run, the results by ICA can significantly change but in most of the cases it is possible to detect the damages. This is because with PCA it is possible to ensure that these components contain the most relevant information with maximal variance, while with ICA is not possible to define which components are more relevant directly from the algorithm if a previous reduction is not performed with PCA.

Although, there is one damage in the stringer which is detected by the sensors attached in the same stringer, this is also detected by using both methodologies for other phases as in the phase 1. This means that the combined analysis of the sensors (using all phases) is a very useful tool because allows to consider the dynamic responses in the whole sensor network.

5.5 Discussion

The performance of the methodologies presented for damage detection using PCA as pattern recognition tool to build the baseline model, in which the projection to the principal components (scores) and four statistic measurements (T^2, Q, ϕ and I^2) are selected as damage indicators has been tested using an aircraft wing skeleton and an aircraft turbine blade. The results have revealed that the approaches have potential for real applications and can be used in a combined way to evaluate the state of a structure.

Some important elements can be highlighted from the results in this chapter:

- The results showed that there are differences between the data from the undamaged structure and the different damages, and these differences can be used to define the presence of damages in the structures. Similarly, the presented plots allowed in most cases to separate and distinguish damages between them.

- Comparing the results from the two specimens, it was shown that the score plots with PCA are not very useful when the variance contained in the selected scores is not significant. In these cases, the use of a combined analysis with the damage indexes plots can be used for detecting damages with better results.

- It was shown that the score plots obtained by PCA or ICA in the aircraft wing skeleton allowed detecting the damages, exhibiting in most cases a clear distinction between the

data from undamaged structure and the other three damage states. The results can change depending on the phase to being analyzed but in all cases it is possible to distinguish the presence of damage. In addition, it was shown some differences between the results using both methodologies, for instance the definition of the number of Components or the possibility of defining different data set by identifying the kind of damage due to the separation that is possible to see in some of the phases. An important difference between PCA and ICA is related to the number of components used in each methodology. In the PCA case this number can be determined by the variance criteria, but in the ICA case it does not exist a criterion for determining how many components represent the dynamic of the data. In spite of this, it was shown that the use of a previous reduction with ICA to obtain just two components allowed to define the presence of damages. Of course, if this reduction is not performed, it is necessary to evaluate all the combinations to determine which components show better results. One way to improve the results with ICA could be using another tool that includes all the Independent Components by each phase or performing data fusion including the components from all phases.

In addition, it is also possible to distinguish some data sets which can be used for damage classification in a further analysis using, for instance, some additional pattern recognition technique.

In general it is possible to conclude that, in all the cases, the evaluation of all the phases allow to define the presence of a damage in the structure. This full analysis is a necessary step, because as it was shown in the results, each phase defines the states in a different manner. In this way the results presented in this chapter motivate the need of a more robust tool to perform a combined analysis of the phases and to simplify the final analysis.

Finally, it is necessary to highlight that the methodology will be used and extended in the Chapters 6 and 7 to localize and classify damages.

Chapter 6

DAMAGE LOCALIZATION SYSTEM

6.1 Damage Localization

The damage localization task is the second step in the SHM levels as was mentioned before. This task allows to locate the damage in the structure based on the measurements obtained by a sensor network from the structure under test. Some clear advantages can be obtained from its application, for instance, the simplification of the inspection and reparation of the damaged component, specially in large and complex structures by using automated inspection and data driven approaches.

6.2 Damage Localization Methodology

To localize damages, the damage detection methodology presented in the previous chapter is extended using several methods to analyze the contribution of each sensor to each damage index. The theoretical background of these methods was also introduced in Chapter 3. Figure 6.1 shows the flow diagram of the general methodology for damage localization. When the structure needs to be analyzed, experiments are performed and the gathered data are projected onto the PCA model. Finally, scores and damage indices are calculated according to the previous chapter; Q-index, T^2-index, ϕ-index and I^2-index can be considered as good features to detect the damage. Selecting one of these indices (probably that which present a high value), the contribution of each sensor to this index is calculated by each actuator phase. It is expected that the damage is located between the actuator and the most influenced sensor. Therefore, in each actuator phase, a region of the structure is selected as the region where the damage is located. Considering all phases (data fusion), a general diagnosis could be performed by intersecting all the regions. These data fusion is desirable because provides some positive elements to the methodology such as: higher signal-to-noise-ratio, robustness and reliability, better information regarding independent features, more complete picture of the monitored system, improved resolution, increased hypothesis discrimination and reduced measurement times [164].

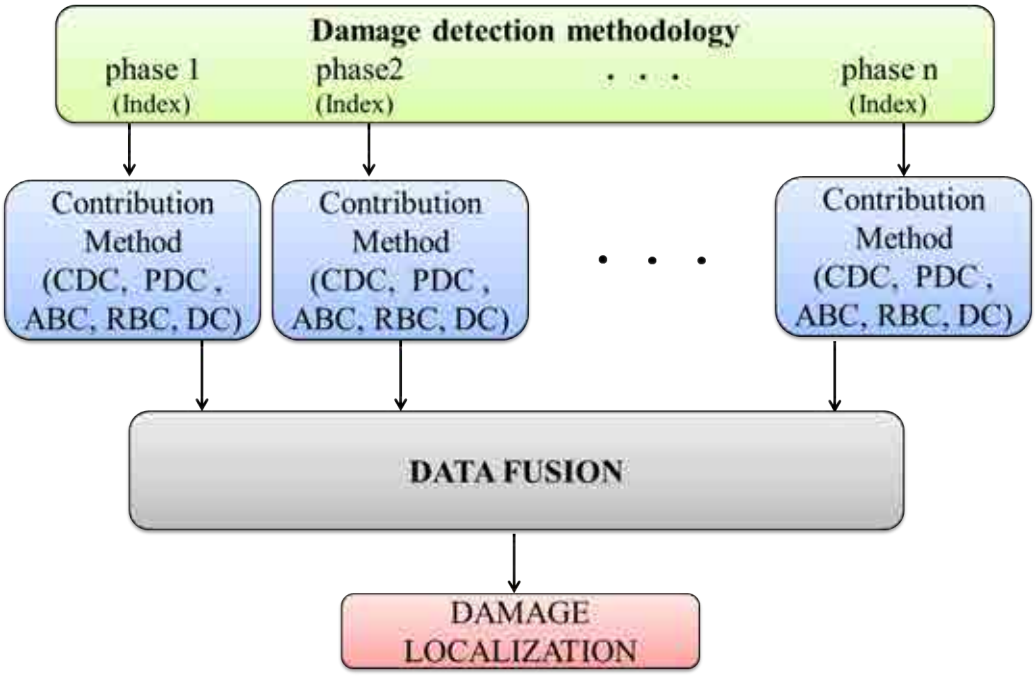

Figure 6.1: Damage Localization Methodology.

6.3 Experimental Results

To validate the damage localization methodology, two specimens were used. The aircraft turbine blade and the aluminum plate which are instrumented with several piezoelectric transducers as was described in the Sections 4.5 and 4.2 respectively. The results are set out in the following sections.

6.3.1 Aircraft turbine blade

In this structure two damages were selected to be localized using the different methods of contribution analysis to each index. Firstly, an extensive interpretation of the results using Complete Decomposition Contribution (CDC) is presented by each damage index. Finally, a comparison between the different methods is performed.

Using complete decomposition contribution to Q- index

This section shows the results concerning to the localization of the damage 3 in the aircraft turbine blade using CDC analysis (Section 2.4.1) to the Q-index (Section 2.4). From Figure 4.9 it can be seen that the damage 3 is located over the PZT4.

Each plot in the Figure 6.2 depicts the contribution of each sensor (PZT 1 to 7) to the Q-index in each actuator phase. Analyzing these plots it is possible to observe the following: during the actuator phase 1 (PZT1 as actuator), the contribution of PZT1 is equal to zero (PZT1 does not contribute to the Q-index). On the contrary, the highest contribution is obtained by the PZT4. Therefore, the analysis suggests that the damage is probably located between PZT1 and

PZT4. A similar situation is found in phases 2, 3, 5, where the highest contribution is presented in the PZT4. On the other hand, in phase 6 it can be seen that the highest contributions are achieved by PZT4 and PZT5. This result implies that the damage could be located between the PZT6 and PZT4, but equally it is probably that this damage is placed between PZT6 and PZT5. Besides, in phase 4 the highest contributions are given by PZT2 and PZT5. Furthermore, in phase 7 the highest contribution is presented in PZT2 followed by the contribution of the PZT5.

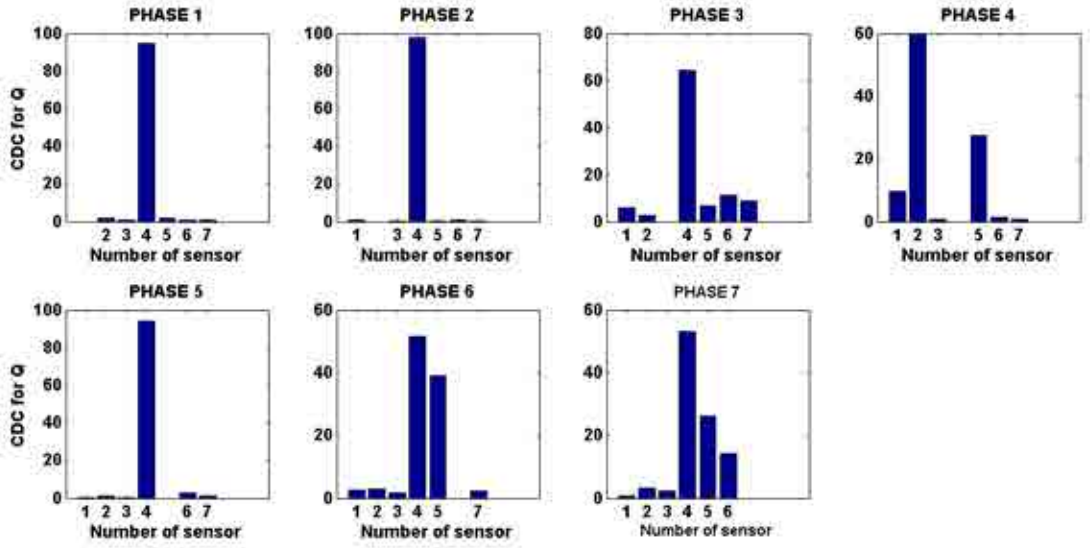

Figure 6.2: Contributions of each PZT transducer to the Q-index.

Although the analysis of the other damages is not included in this thesis, the obtained results are similar to the previous one.

Using complete decomposition contribution to T^2 - index

In this section, results concerning to the localization also of the damage 3 are presented, using CDC but to the T^2-index. Figure 6.3 shows the contribution of each sensor to T^2-index. In the same way as the previous index, the PZT corresponding to the one used as actuator in each actuator phase is null. In all the phases, it can be seen that some contributions are negative. Negative contributions do not have any physical sense and therefore, they are not considered in the analysis. Phases 1, 2, 3, 5 and 7 show that the highest contribution is given by the PZT4, which means that the damage is probably located between the actuator in the each actuator phase and the PZT4. In contrast, the phase 6 shows the highest contribution in the PZT7.

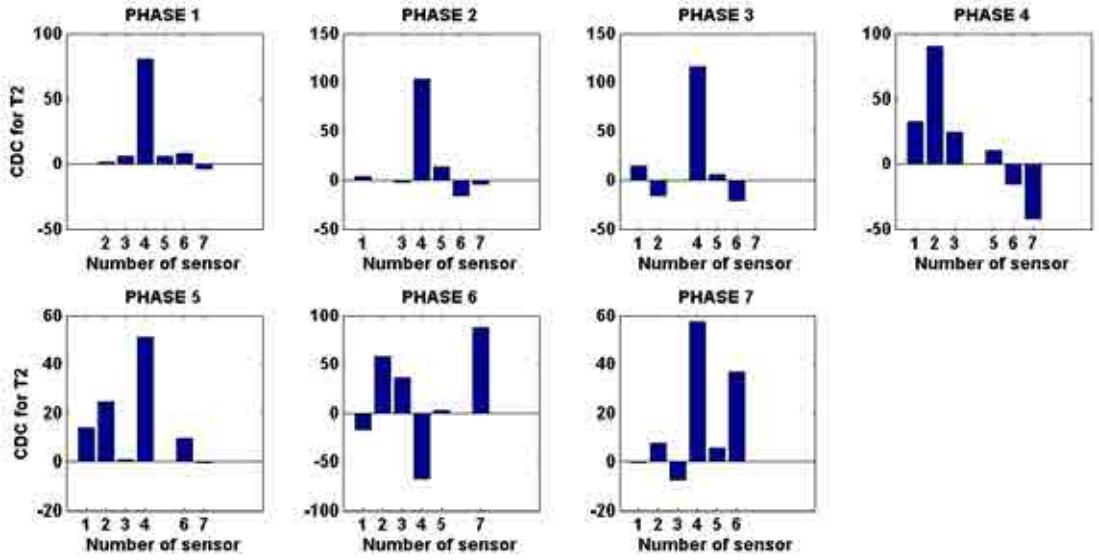

Figure 6.3: Contributions of each PZT to T^2-index.

Using complete decomposition contribution to ϕ- index

Keeping the same analysis but using ϕ-index, it can be seen that similarly to the case where T^2-index is used, there are some negative contributions (Figure 6.4), which are discarded.

In Figure 6.4, phases 1, 2, 3, 5 and 7 show that the highest contribution is given by the PZT4. Again, the phase 4 shows the highest contribution in the PZT2. In difference, phase 6 shows highest contribution in the PZT5 followed by the PZT7.

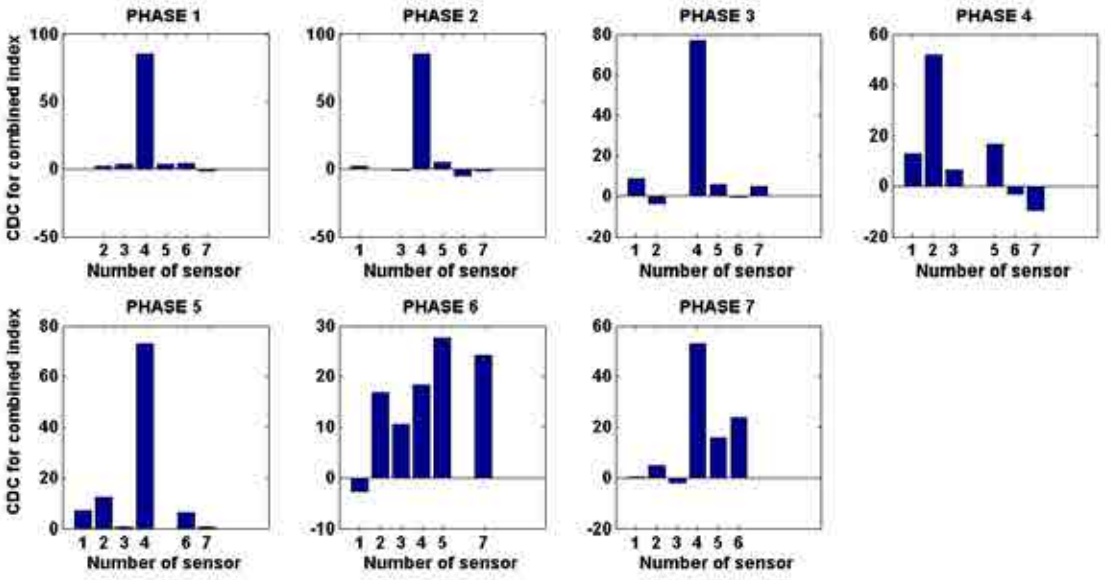

Figure 6.4: Contributions of each PZT to ϕ-index.

Using complete decomposition contribution to I^2- index

Finally, analyzing the contributions to the I^2-index (Figure 6.5), results show that phases 1, 2, 6 and 7 has the highest contribution in the PZT 4. In the same way as the previous cases, the phase 4 shows that the highest contribution is given by the PZT2. Additionally, from the results in the phase 5, it is found that the highest contribution is obtained by the PZT2. In difference with the results obtained with the previous indices, the phase 3 shows that any PZT transducer contributes to I^2- index, which means that there is no significant contributions in this phase and there is no relevant information to consider from this phase.

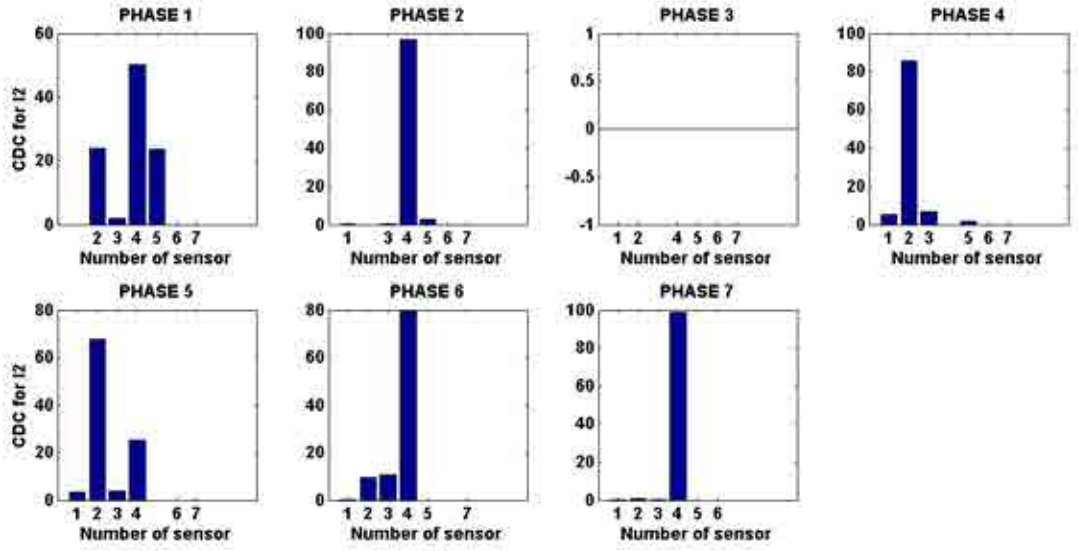

Figure 6.5: Contributions of each PZT to I^2-index.

Comparison between the contribution methods

In order to compare the results obtained by the different contribution analysis methods (CDC, PDC, RBC, ABC, DC), two indices and one specific damage are used. Specifically in this study, the ϕ and I^2 indices are used to localize the damage 1. From Figure 4.9 it can be seen that the damage is located over the PZT 1. Figures 6.6 to 6.12 show the comparison between the five methods of contribution of each sensor to the corresponding index by each actuator phase. In the plots, the methods are numbered as follows: method 1 corresponds to the CDC method, method 2 to corresponds to PDC, 3 to RBC, 4 to ABC and 5 to DC. Sensors in the figures are the corresponding PZT transducers. Additionally it is necessary to keep in mind that the actuator in each phase is removed, this means that for instance in the actuator phase 1 the first PZT transducer corresponds to the PZT2, sensor 2 corresponds to the PZT3, and so on.

In general terms, the results show that all methods allow to locate the damage. In addition, the contributions in most cases have similar results, although it may be noted that in some cases the methods PDC, RBC, ABC and DC provide major contributions compared with the CDC method.

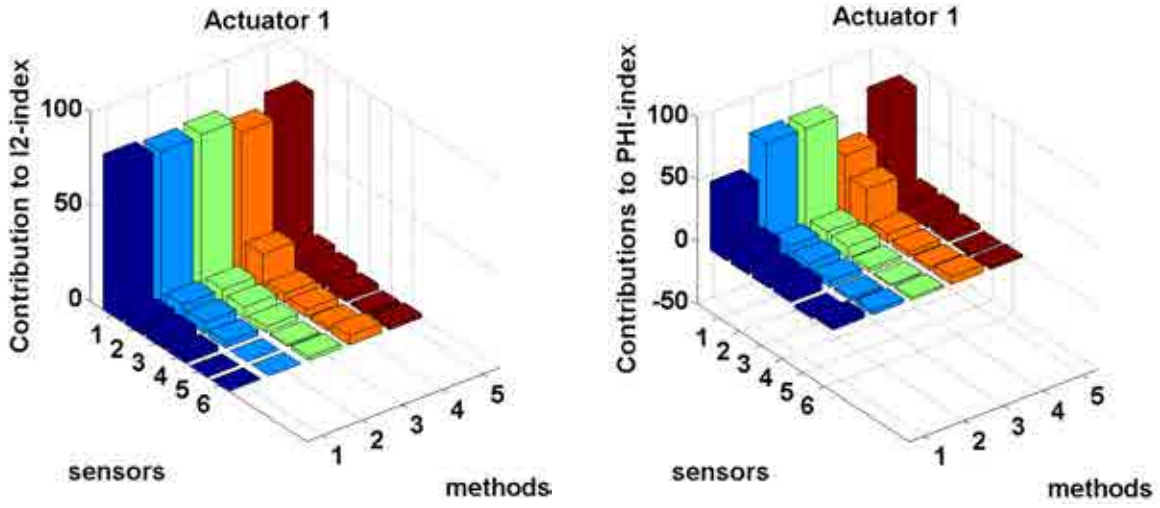

(a) (b)

Figure 6.6: Comparison between methods of contribution using PZT 1 as actuator to (a)I^2-index and (b)ϕ-index.

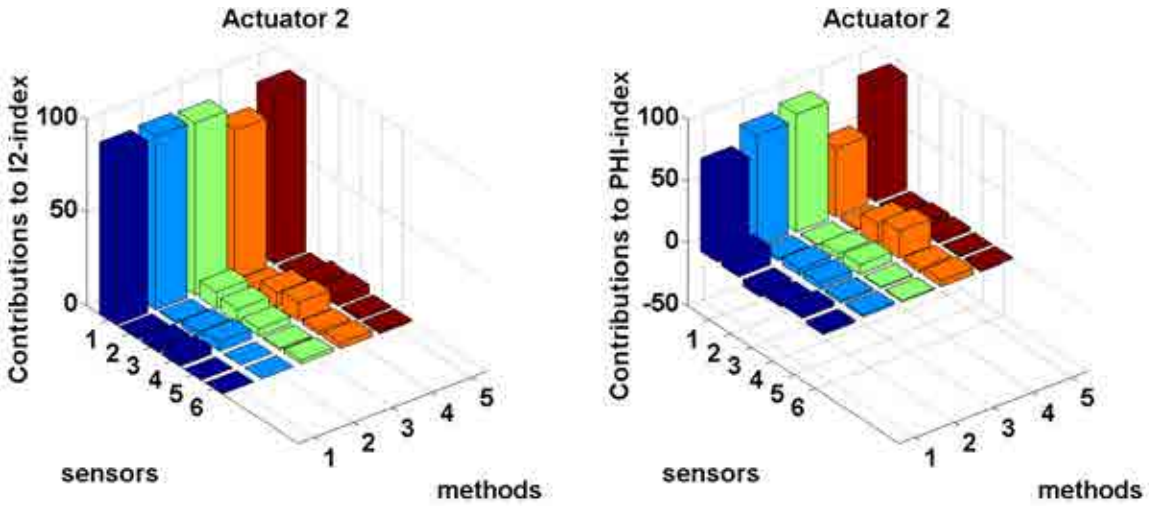

(a) (b)

Figure 6.7: Comparison between methods of contribution using PZT 2 as actuator to (a)I^2-index and (b)ϕ-index.

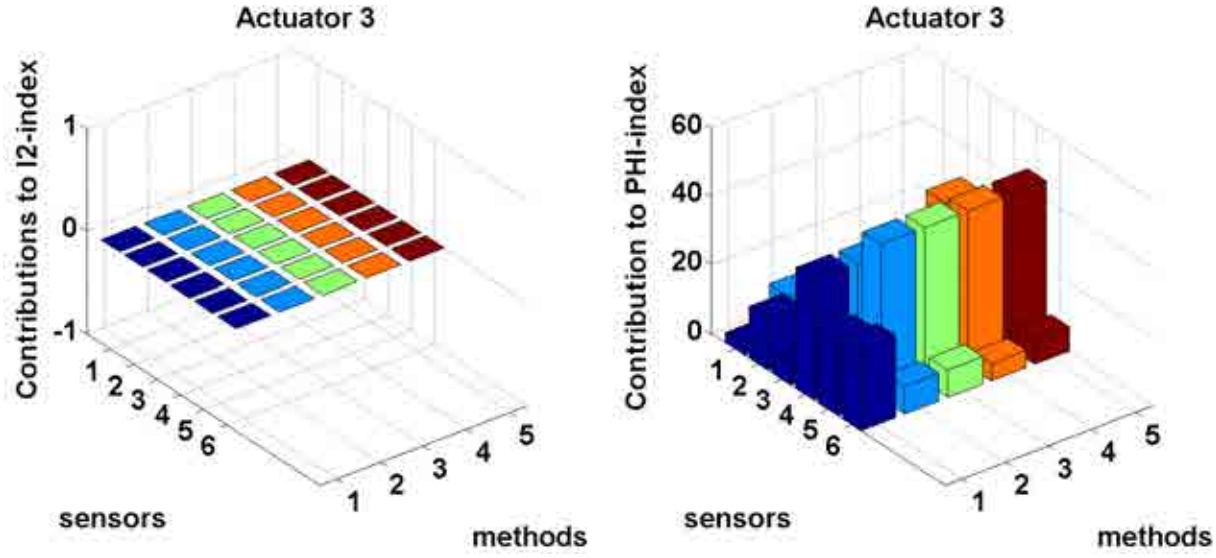

(a) (b)

Figure 6.8: Comparison between methods of contribution using PZT 3 as actuator to (a)I^2-index and (b)ϕ-index.

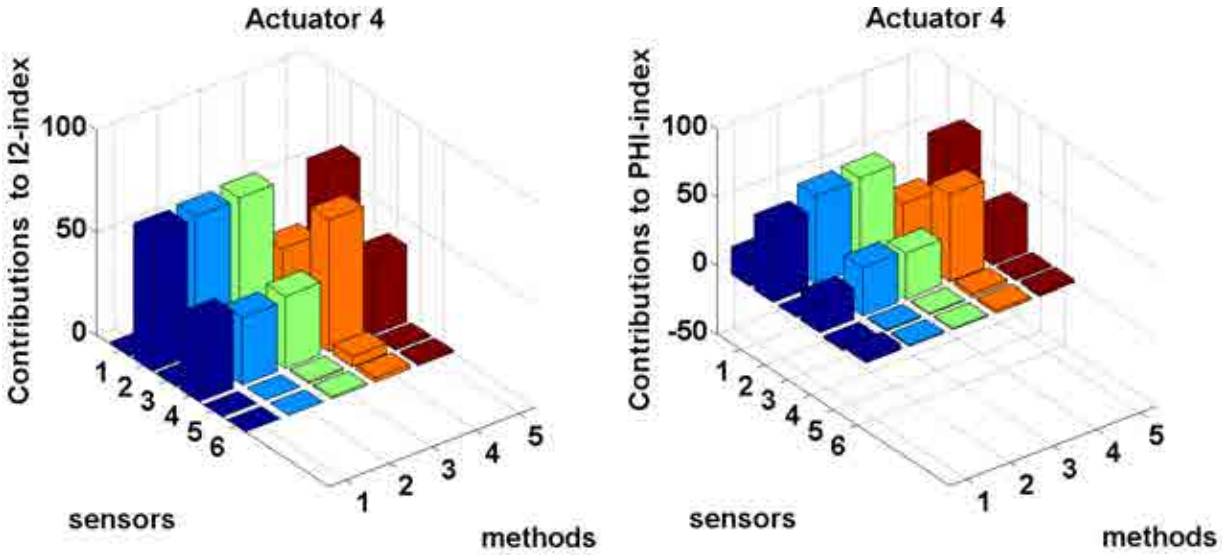

(a) (b)

Figure 6.9: Comparison between methods of contribution using PZT 4 as actuator to (a)I^2-index and (b)ϕ-index.

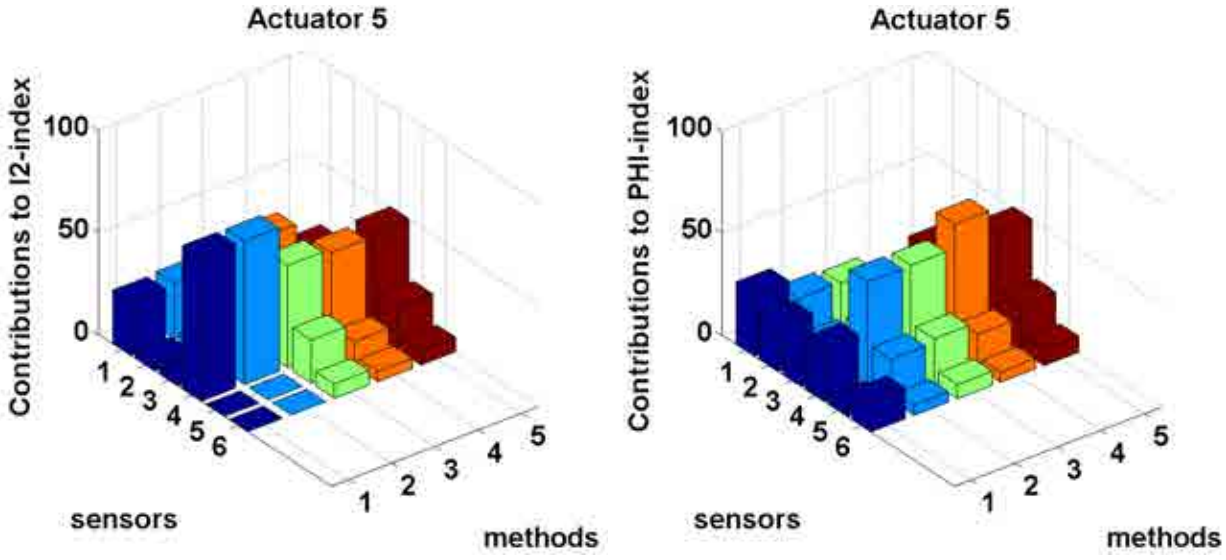

(a) (b)

Figure 6.10: Comparison between methods of contribution using PZT 5 as actuator to (a)I^2-index and (b)ϕ-index.

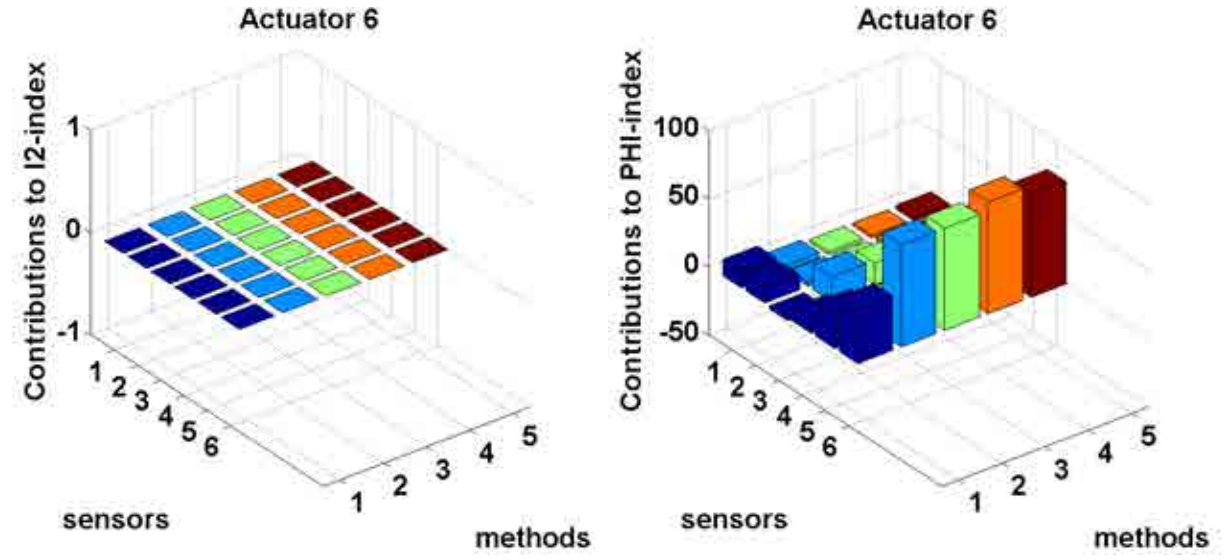

(a) (b)

Figure 6.11: Comparison between methods of contribution using PZT 6 as actuator to (a)I^2-index and (b)ϕ-index.

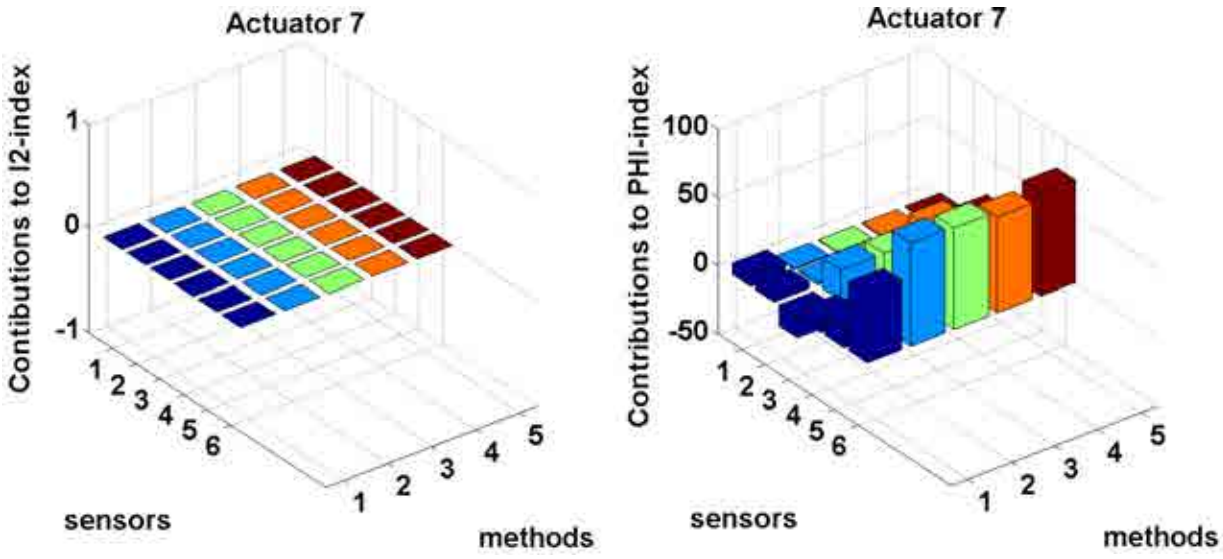

(a) (b)

Figure 6.12: Comparison between methods of contribution using PZT 7 as actuator to (a)I^2-index and (b)ϕ-index.

Negative contributions such as those obtained to ϕ index in Figures 6.6, 6.9 and 6.12 have no physical sense as was previously explained. Therefore, they are not included in the final analysis. Another result to remark from the figures in the case of the I^2-index is that the phase 7 have contributions equal to zero in all the sensors since in this case are far from the damage and there is a stringer on the way between the actuator and the sensors.

Data fusion

The data fusion corresponds to the way that all the information obtained from the different actuator phases is used to define a final combined diagnostic. As was previously explained, the application of data fusion gives to the methodology some advantages and simplifies the final diagnostic for the user.

In order to show the final diagnostic (considering contributions at all phases) it is necessary to specify areas in the structure that consider paths between actuator and sensors. The contribution of each sensor in each phase defines the weight of the path (region between actuator and sensor). Finally, the sum of all the weighted regions establishes the region where the damage is located. In a general way, the region or area can be defined as the intersection of the different areas found by each actuator phase. As one example of this data fusion, Figure 6.13 depicts the process for the damage 3, previously presented using CDC method. First, in the actuator phase 1 the highest contribution is given by the PZT4, while also the sensors 2,3 and 5 give contribution values. In this manner in the plot each path is depicted between the actuator and the sensor with different color tone according to its value. This procedure is applied in all cases for the actuation phases. Finally, in the lower part of the figure, the localization of the damage is depicted as result of the combination of all the actuation phases.

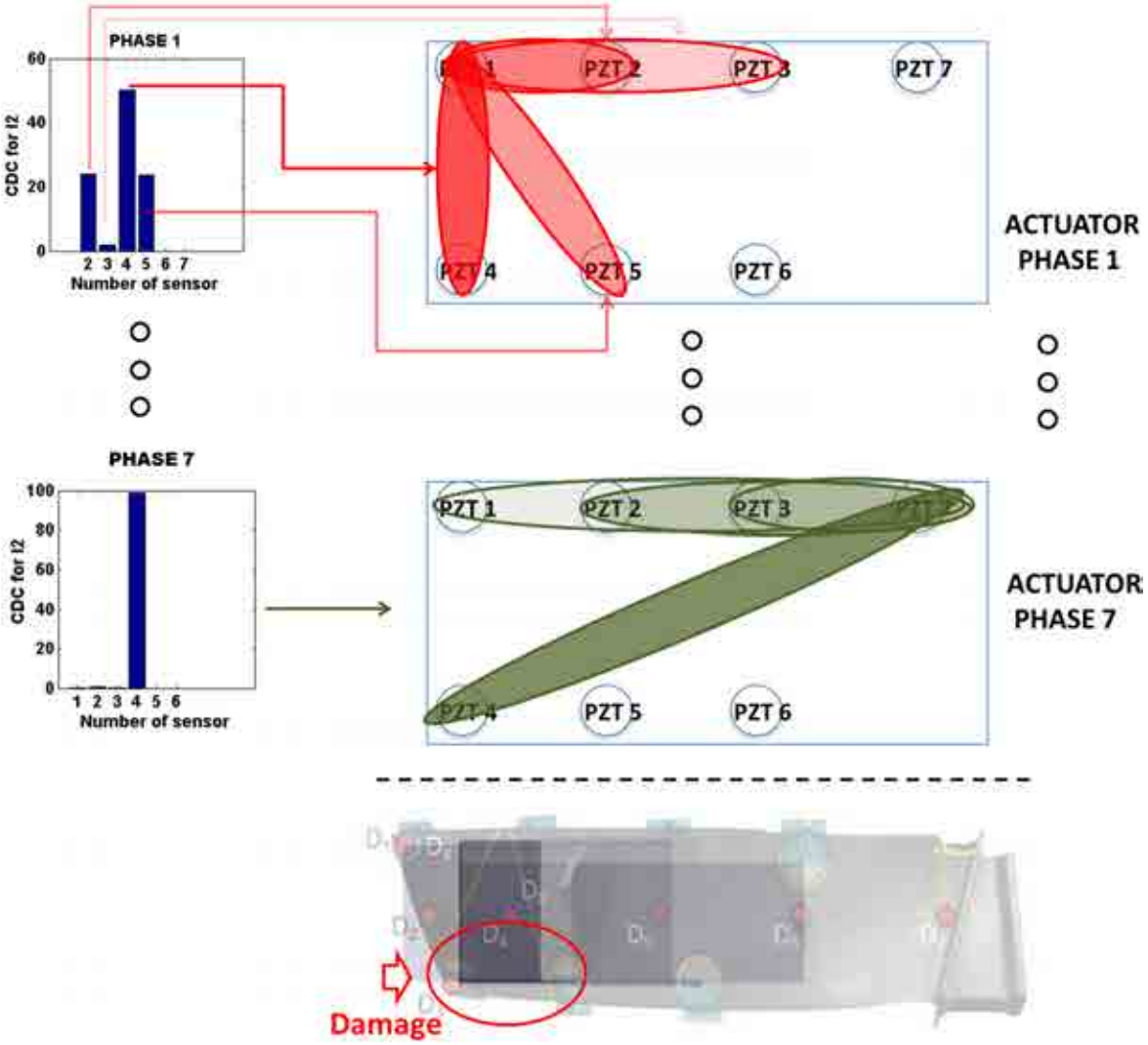

Figure 6.13: Data fusion in the damage localization methodology.

From Figure 6.14 it can be seen the software application developed in Matlab ®. Here, the image of the structure is loaded, and the position of every PZT is manually defined (using the mouse). The algorithm find paths between sensors and define all the region with the corresponding weight.

After defining the method of contribution analysis and the index, the software shows the damage of the structure and indicates the region of the localization of the damage. For instance, the final diagnostic of the structure with damage 3 by using CDC to Q-index is presented in Figure 6.15 (the higher the value of the color, the more probability of the localization of the damage). As it is expected, the damage is located near to PZT4.

Figure 6.14: Interface for damage localization.

Figure 6.15: Localization of the damage 3 using CDC to Q-index.

As additional example, Figure 6.16 presents the final localization of the damage 1 using Q-index and CDC.

Figure 6.16: Damage localization for damage 1 using CDC to Q-index.

6.3.2 Aluminum plate

All the five methods for contribution analysis and Q and T^2 indices are used to localize damages in the aluminum plate with non reversible damages. This structure and the damages were previously described in Section 4.2. The real damage corresponds to one hole located between PZT 2 and PZT 4 with different depths. Figure 6.17 shows the more probability of the localization of damage 1 using DC, CDC, PDC, ABC and RBC to the Q-index with the higher value of the color. As it is expected, the damage is located between PZT2 and PZT4.

Figure 6.18 shows the contributions obtained for each path between the different PZT transducers for the five methods. As shown, in each method, the path between PZT 2- PZT 4 contains the highest values of contribution, this is because the damage is located in this path. With all the methods it is possible to locate the damage with different values, the lowest contribution being found with CDC method. Additionally, it is possible to see that in all the methods, the difference between the contributions of the path 2-4 and the rest is significantly greater, except for CDC method where the values are similar.

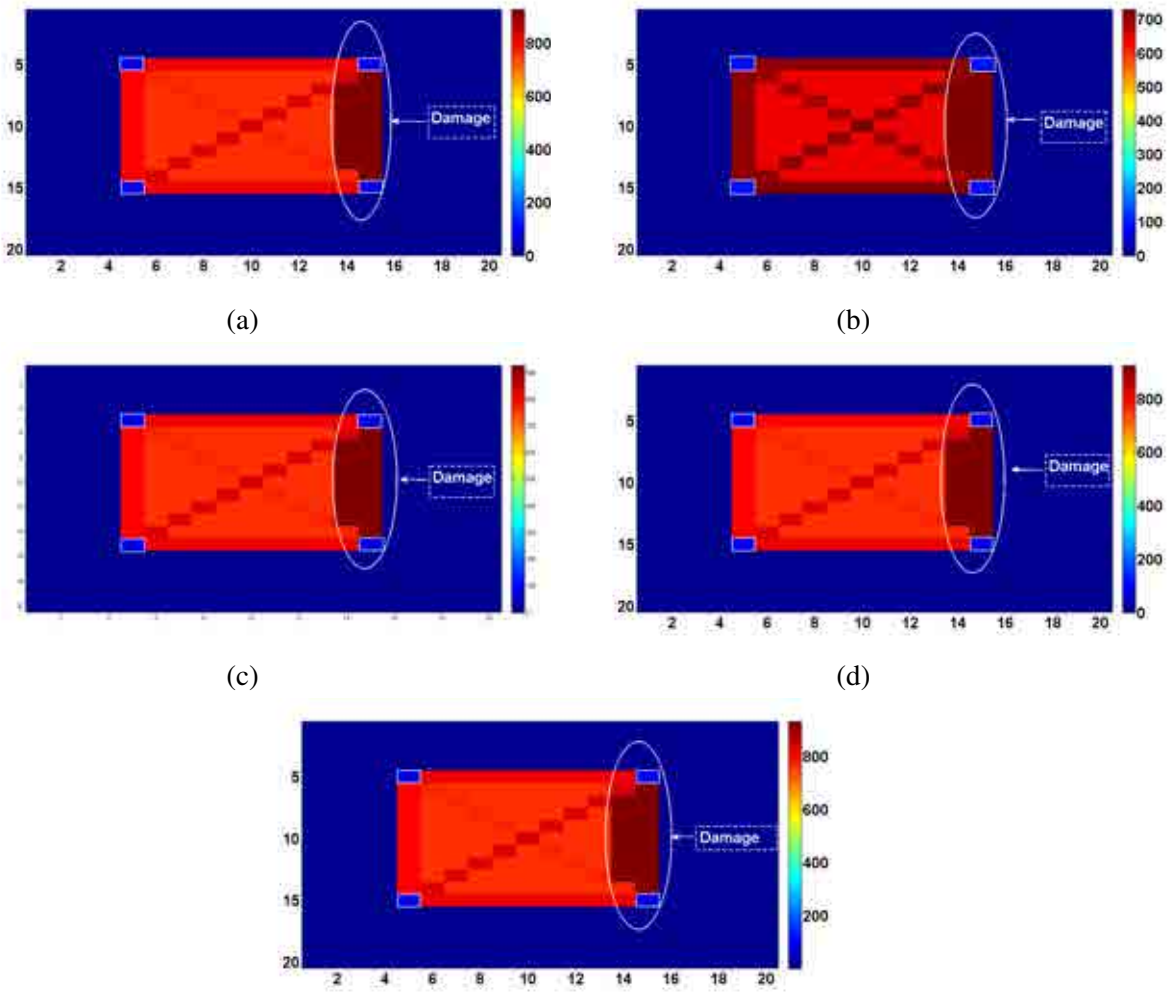

Figure 6.17: Damage localization with Q-index for the damage 1 using (a) DC, (b) CDC, (c) PDC, (d) ABC, (e) RBC.

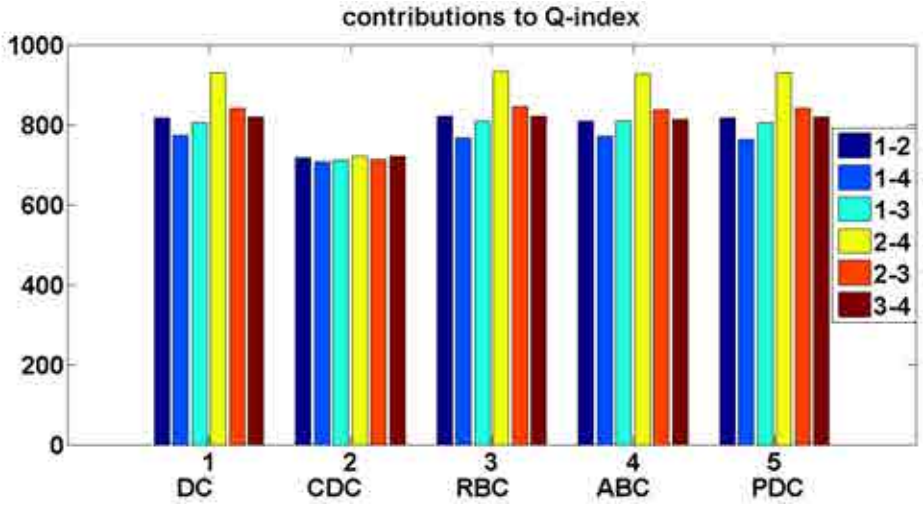

Figure 6.18: Comparison between the methods using Q-index.

Changing Q-index by T^2 index, the same five contribution methods are applied to locate the damage 2. This damage is similar to the damage 1 (same position) but different depth. Results are shown in Figure 6.19 with the higher the value of the color, the more probability of the localization of the damage. As it is expected, the damage is located between PZT2 and PZT4.

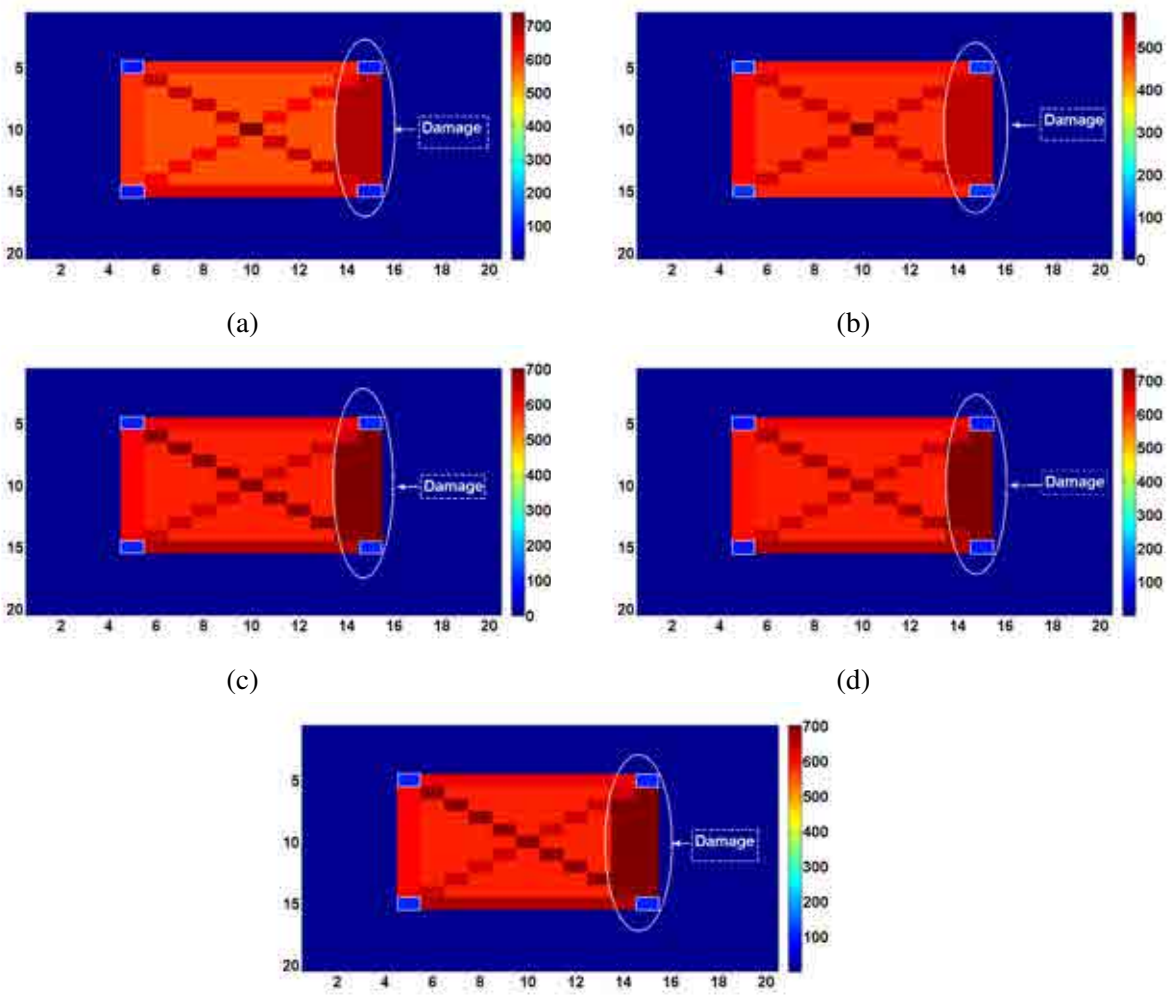

Figure 6.19: Damage localization with T^2-index for the damage 2 using (a) DC, (b) CDC, (c) PDC, (d) ABC, (e) RBC.

Figure 6.20 shows the contributions obtained for each path for the five methods. As the previous results (using Q-index), in each method, the path between PZT 2- PZT 4 contains the highest values of contribution, it happens because the damage is locate in this path. In this case, comparing with the previous results obtained with Q-index, more differences exist between the different paths using CDC method.

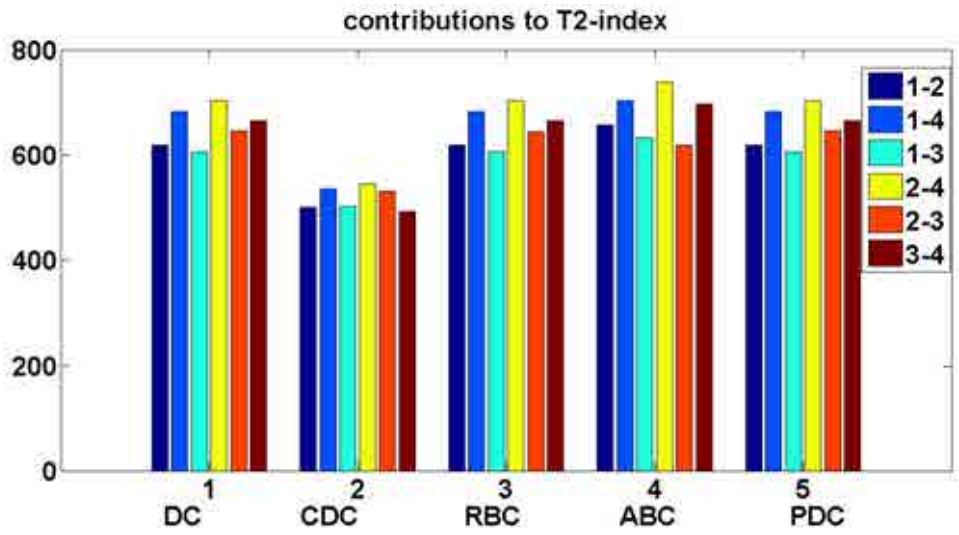

Figure 6.20: Comparison between the methods using $T^2 - index$.

6.4 Discussion

A new methodology for localization of damages has been developed. This approach combines the use of data from a multiactuator piezoelectric system, which is attached to the structure and data driven approaches to study: (i) the dynamic response of the structure at different exciting and receiving points; (ii) the variation of these dynamical responses compared with a baseline when some damage is present in the structure by using PCA and some statistical measures that can be used as damage indices; and (iii) the influence of every sensor in the indices, so that this contribution can be used to localize the origin of the change in the vibrational response (damage).

It was shown that it is possible to extent the damage detection methodology for localizing damages using contribution methods and data fusion. Its use allows to define the region which contain the damage by finding the highest value area. For this purpose, the sum of the contributions obtained for each sensor to each index in each actuator phase is calculated. This result is important because it allows to integrate the results obtained from all the actuator phases in the sensor network to provide robustness and reliability to the damage localization task.

The five presented methods allowed to localize the damages in both structures. Results showed that in some cases there are less contributions when the CDC method is used. Of course, the results vary for each actuator and the best results were obtained in the piezoelectric transducers closest to the excitation signal.

Although, as shown in the results, the damage was not properly detected in all the phases with each index, the use of data fusion allowed to compensate the final result by considering all the results obtained from the other phases. To improve the results in a future work, it is necessary to evaluate in depth elements such as data fusion and the final representation.

Similarly, a study of the parameters in the excitation signal and the acquired signals such as frequency, amplitude and length should be performed, since, if a very large length signal is selected, the influence of all possible wave reflections (due to edges or defects) can appear and change the results in the localization.

Chapter 7

DAMAGE CLASSIFICATION SYSTEM

7.1 Damage classification

Damage classification is an important issue within Structural Health Monitoring going beyond the purely damage detection. Among the big quantity of damages that can be presented in the normal service of a structure it can be found [50] [56]:

- Gradual (e.g. fatigue, corrosion, aging).
- Sudden and predictable (e.g. aircraft landings, planned explosions in confinement vessels).
- Sudden and unpredictable (e.g. foreign-object-impact, earthquake, wind).

At the same time, these different kinds of damages can be also classified depending of its severity in three big groups:

- Light damage: This corresponds to the initial stage of a damage, which can be relatively easily-repairable and is not dangerous for the normal operation of the structure.
- Moderate damage: In comparison with the previous one, this damage requires major repairs and need to be evaluated more carefully in order to define if the structure can operate in normal conditions.
- Severe damage: This type of damage unlike previous damages requires big reparations or the replacement of the structure.

In this thesis most of the damages in the structures are simulated (adding masses at different positions) mainly because most of these structures were provided for testing with reversible damages during research visits of the author to different laboratories.

7.2 Methodology for damage classification

7.2.1 General approach

In this chapter the damage detection methodology presented in Chapter 5 is extended in order to classify damages in structures using data fusion of the results obtained by each actuator

phase, considering a specific structure and several possible damage scenarios. The structure can be experimentally tested by means of an active multiactuator system as was explained in Chapter 5. The methodology is implemented in two different stages, which are referred to as: 1) baseline pattern building (training and validation); and 2) diagnosis (testing). The scheme presented in Figure 7.1 summarizes the general approach. Within the baseline pattern building stage, the methodology for damage detection explained in Chapter 5 is used to calculate the scores and damage indices by each actuator phase. Afterwards, data fusion is applied to combine the results from all the actuator phases and obtain a pattern with the information of the classification using all the structural states. In the diagnosis step, new data from the structure which is blindly tested are collected and entered into the Self Organizing Map (SOM) obtained in the previous step in order to be classified.

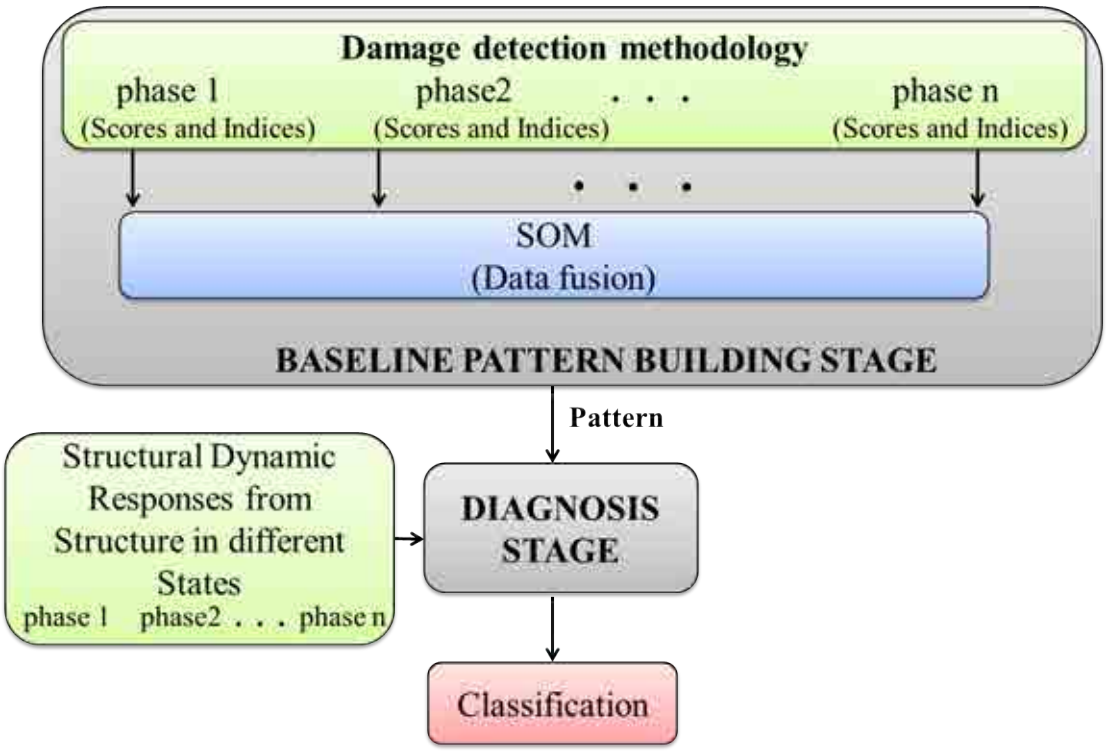

Figure 7.1: Methodology for damage classification.

Baseline pattern building

In this stage, the methodology for damage detection is extended to build the baseline pattern for damage classification. The additional task consists of merging all the data obtained from different actuator phases and propose just a single pattern that will be used in the following stage: diagnosis.

The structure to build the baseline pattern should be considered as undamaged. Several experimental actuator phases are performed. For each actuator phase, a single actuator is excited and the time history responses of the whole set of sensors are recorded, organized and prepro-

cessed as was explained in the Section 5.2.3. After, these data are used to build a PCA reference model. This is repeated for each single actuator.

The structure is tested under different known damage states (damage scenarios). For each state, the previous experimental actuator phases are performed, in the same way as the data were collected. These data are organized and normalized following the steps defined for the damage detection methodology. Results obtained for each phase: the projections of the data onto the reference PCA models; and the damage indices will be used for damage classification.

The results obtained for each phase are combined and contrasted using a Self Organizing Map (SOM). A SOM is chosen since its characteristics can provide a good support for the classification and graphical representation, grouping input data with similar features in clusters. One important characteristic of this kind of ANN is that it does not need previous knowledge about the state of the structure (healthy or with some damage) to obtain the final clustering (unsupervised algorithm). As a result, the SOM produces an organized map by grouping in clusters data with similar characteristics. It is relevant to remark that until now the information about the structural state has not previously used. The result is a map that includes the number of experiments grouped together in each output neuron or cluster (Figure 7.2). In order to validate the effectiveness of classification and to obtain the final baseline pattern, the known information from the states of the structure at each experiment is used to label each cluster. According to the experiments (or states), these are organized in each output neuron as is depicted in Figure 7.3. More details about the representation will be explained in the next sections.

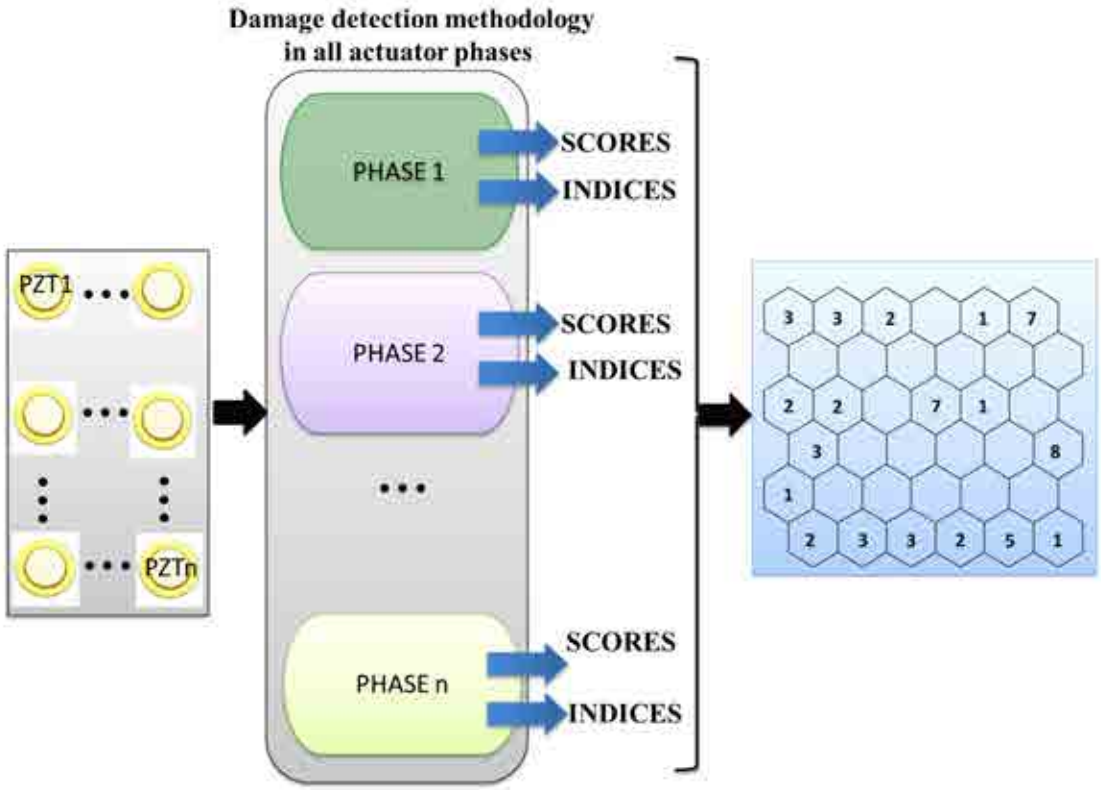

Figure 7.2: SOM training.

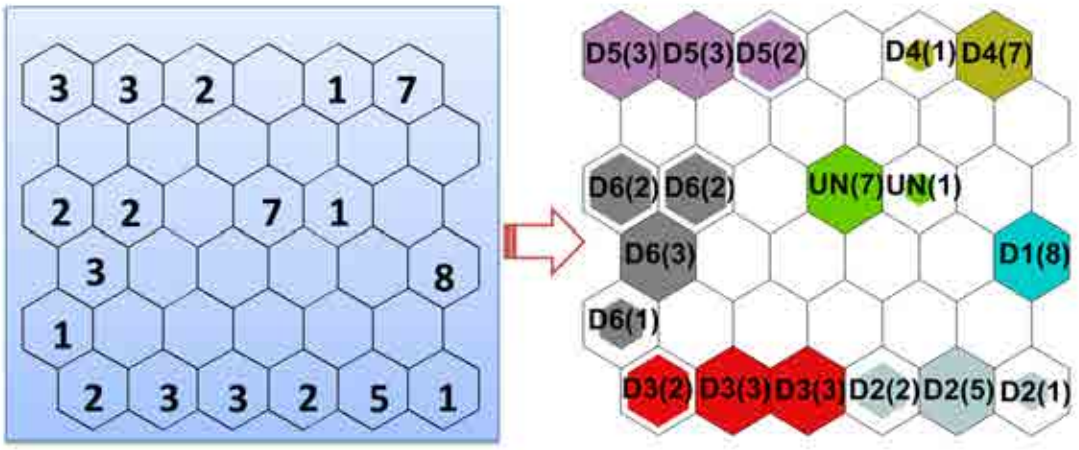

Figure 7.3: Final baseline damage pattern.

Classification and diagnosis

Once the baseline pattern building has been finished, the known damaged states under consideration are used a posteriori to validate the effectiveness of the classification and to obtain the final baseline pattern.

In the diagnosis stage, any structure is blindly tested. The different phases are performed for each single actuator as in the baseline pattern building. The results are entered into the trained SOM and the new pattern is obtained. Comparison with the baseline pattern allows the damage detection and classification.

7.2.2 Discrete Wavelet Transform as feature extraction

From the previous analysis it is possible to define the basic parameters for performing a good classification. Of course, some of these parameters as the normalization and the number of scores need to be evaluated for each structure.

Since the methodology should be able to apply to any structure instrumented with an active piezoelectric system with any number of sensors, it is necessary to bear in mind that a big sensor network requires a large computational cost. Considering that, in some cases, the computational cost is a critical parameter, it is suggested the inclusion of an extra tool for reducing data. To do that, the DWT is selected in order to obtain the coefficients for representing the time-frequency information of the recorded signals providing a more robust methodology with less computational cost.

This approach includes a similar idea to the previous approach but making use of the DWT to obtain approximations and detail coefficients (see Figure 7.4) allowing the analysis of fast and slow changing features at different frequency scales. The two-channel subband coding scheme is applied to the recorded structural dynamic responses in order to produce a signal re-

construction to the level in which the signal could be properly reconstructed from the calculated coefficients with the minimum loss of information. Determining the optimal basis function, i.e. mother wavelet, for signal decomposition is also a very important step in wavelet analysis since it guarantees an accurate decomposition of the original signal into the different frequency bands.

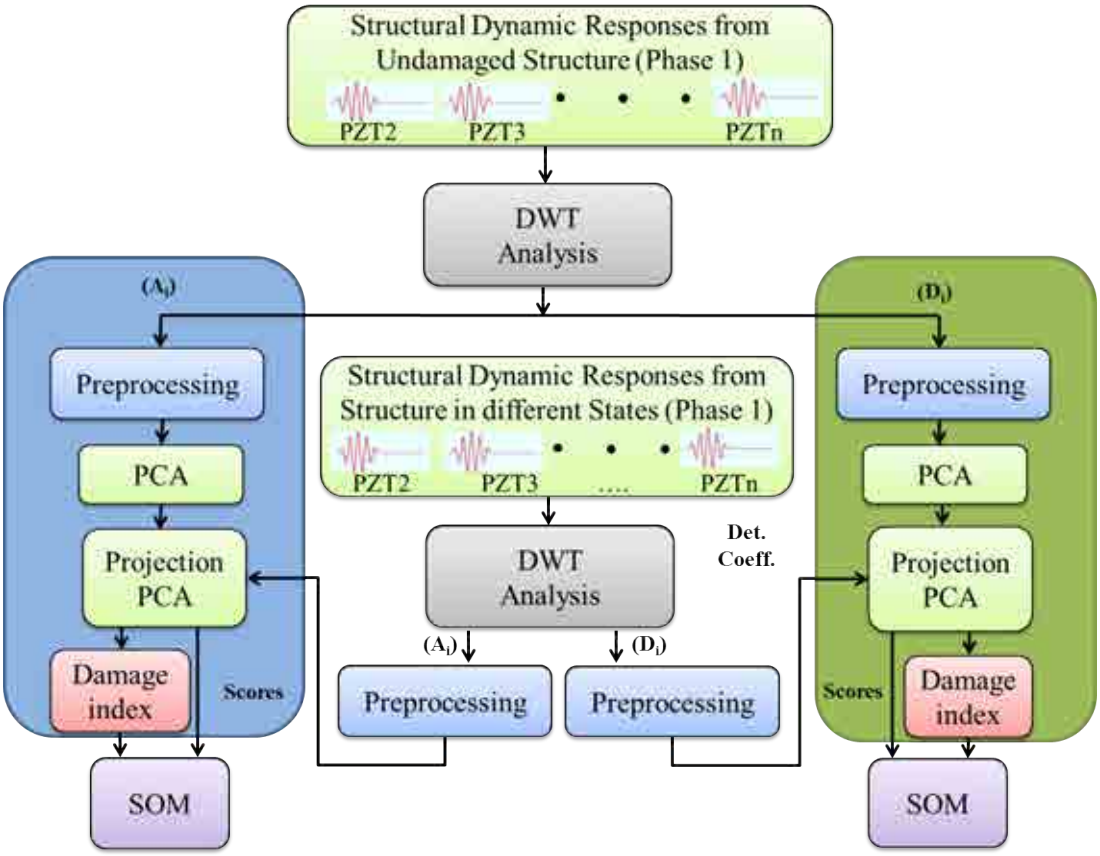

Figure 7.4: Damage detection and classification including the DWT within the Phase 1.

The use of the DWT is justified by two important points. Firstly, this modification to the methodology presents advantages such as the reduction in the computational cost in comparison with the original methodology. This is given by the fact that the size of the matrix that has to be processed is considerably reduced since a small amount of compressed parameters are used. On the other hand, the extracted wavelet coefficients give a compact representation that shows the energy distribution of the structural dynamics not only in time but also in frequency.

After implementing the use of the DWT for preprocessing the data, the steps to follow are the same as those just explained in the previous section.

7.3 Experimental results

The results in the validation of the methodology are organized in 5 subsections. The first two subsections include the results in the training and diagnosis stages and its main objective is

to define the configuration parameters and the definition of the pattern for the classification. These results are obtained by using data from the aluminum plate defined in Section 4.1. After, the results of the behavior of the DWT in the methodology are shown using data from the aircraft fuselage and the CRFP plate. These structures were described in Sections 4.6 and 4.3 respectively. Later on, PCA is replaced by ICA in order to demonstrate the generalization of the methodology using a multilayered composite plate. Also a comparison between the results using PCA and ICA are discussed using the same specimen. Finally, to evaluate the behavior of the methodology under temperature changes, an aluminum plate subjected to six temperatures is used. The SOM Toolbox of Matlab [180] is used for the implementations.

7.3.1 Configurating the baseline pattern

To define the optimal set of parameters to configure the data fusion tool, several SOM's were trained and validated. To determine the cluster size, a study was previously performed. Larger map sizes present more detailed patterns. On the contrary, smaller map sizes present more general patterns. Maps smaller than 4×4 show many overlapped clusters, big SOMs generate too many empty clusters that add uncertainty to the classification of the damage. In this structures, optimal results are obtained using a map of 6×6 clusters. Additional to the map size, the map lattice and shape must be specified. The SOM lattice gives the local topology of the map, i.e. the connectivity of the map units. The lattice can be either rectangular or hexagonal in the SOM toolbox. For the present study, hexagonal lattice is used. Different shapes such as sheet, cylinder or toroid can be chosen. For ease, a flat sheet shape is considered here. Additionally, a Gaussian neighborhood function is used.

On the other hand, this study also analyzes in depth how the classification results are affected by three issues: (i) the method used to normalize the input data; (ii) the number of scores used in the input vector; and, (iii) the specific damage detection indices, which a priori are T^2-statistic and Q-statistic. Six possible normalizations are implemented in the toolbox to preprocess the input data: $range$, var, log, $logistic$, $histD$, $histC$ [180]. According to [180] the normalization type var, performs a linear transformation which scales the value such that their variance is equal to one. Normalization type $range$ scales the variable values between [0,1] using also a linear transformation. Log normalization makes a logarithmic transformation of the input variables. The $logistic$ normalization is more or less linear in the middle range and has a smooth nonlinearity at both ends, which ensures that all values (even in the future) are within the range [0,1]. Normalization type $histD$ is a discrete histogram equalization. It sorts the values and replaces each value by its ordinal number. Finally, it scales the values such that they are between [0,1]. Normalization type $histC$ is a continuous histogram equalization. The value range is divided into a number of bins and the values are linearly transformed in each bin. All the normalizations were implemented using, as input vector, eight scores and both damage indices (T^2- and Q-statistic) by each actuator phase. After validating the resulting maps (labeling the cluster), it can be seen that the maps with least amount of clusters with different state of the structure (overlapped clusters) are these such are normalized using $histC$, $histD$ and var normalization. These maps are depicted in Figure 7.5, each cluster (or output neuron) of the SOM is represented by a hexagon. The color of the cluster shows the kind of damage (Undamaged, Damage 1, D2, D3, etc), and the portion of the cluster shows the portion of the

damage among the total of the experiments grouped in the cluster. Besides, the damage and the number of experiments of this damage are shown (i.e. D3(2) means that 2 experiments with the damage 3 are grouped in the cluster).

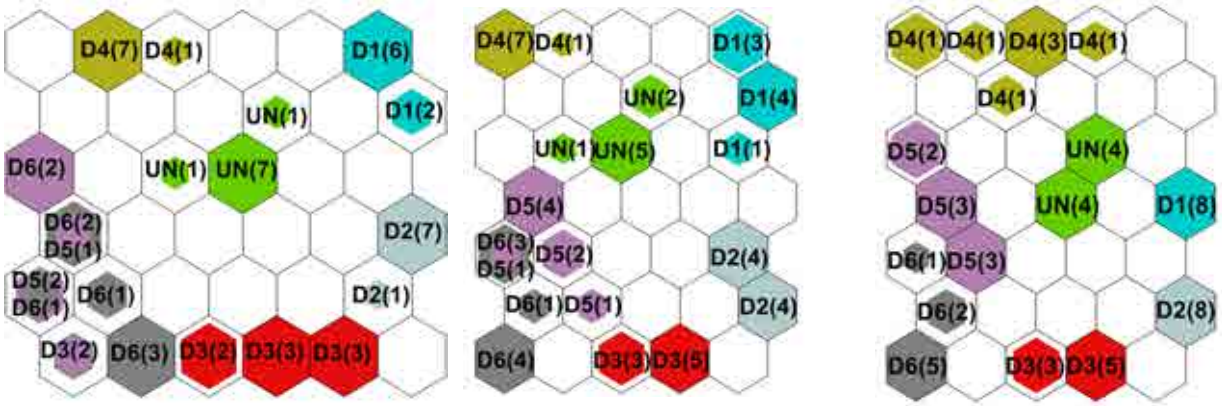

(a) (b) (c)

Figure 7.5: Classification of damages using eight scores, both damage indices (T^2 and Q-statistic) and normalization type (a) $histC$, (b) $histD$, (c) var.

Since T^2-statistic is a measure calculated from the scores, including this damage index together with the scores in the input vector to the SOM could be redundant. To analyze the influence of T^2-statistic into the SOM, three maps were trained and validated using eight scores and only Q-statistic as damage index by each actuator phase. These maps have a configuration similar to that presented in Figure 7.5. After validating (see Figure 7.6) and comparing with the maps from Figure 7.5, it can be seen that T^2-statistic does not influence so much in the results, but does increase the number of elements in the input vector as actuator phases (PZT transducers) has the system.

The size of the input vector is also a parameter to consider when a SOM is being trained. To

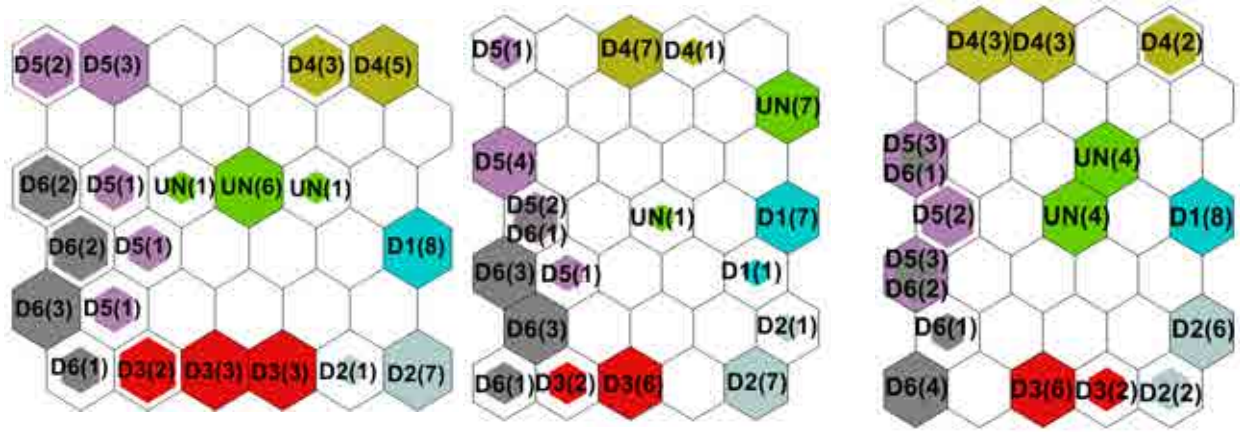

(a) (b) (c)

Figure 7.6: Classification of damages using eight scores, Q-statistic and normalization type (a)$histC$, (b)$histD$, (c)var.

study the number of scores to be used, several maps were trained and validated. The number of scores was varied between 2 and 10 and the normalization methods were those chosen in the previous analysis ($histC$, $histD$ and var). In general, results show that the more scores are used, the better classification, although not big differences are found. On the other hand, time consuming is also greater. To see this disparity, the resulting maps after using 2, 7 and 8 scores are depicted in Figures 7.7, 7.8 and 7.9.

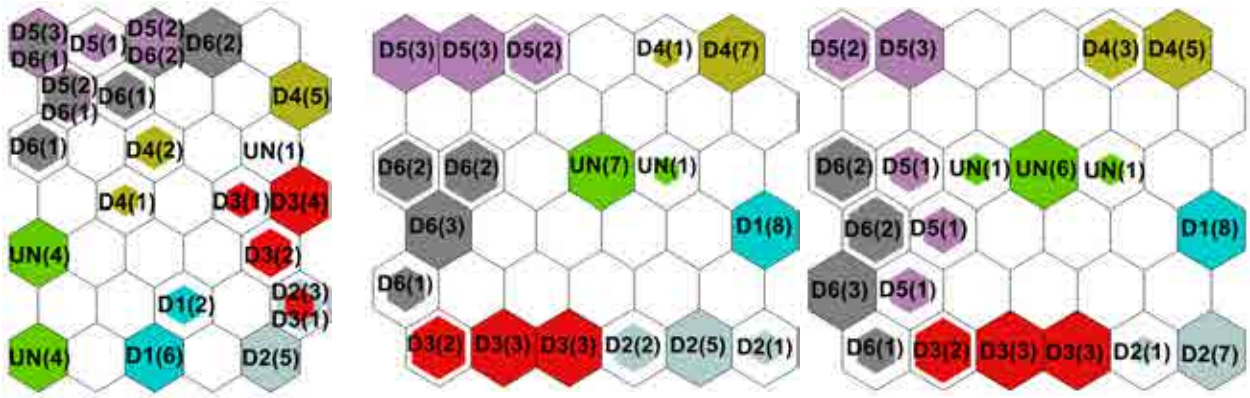

(a) (b) (c)

Figure 7.7: Classification of damages using Q-statistic, normalization type $histC$ and (a) 2 scores, (b) 7 scores, (c) 8 scores.

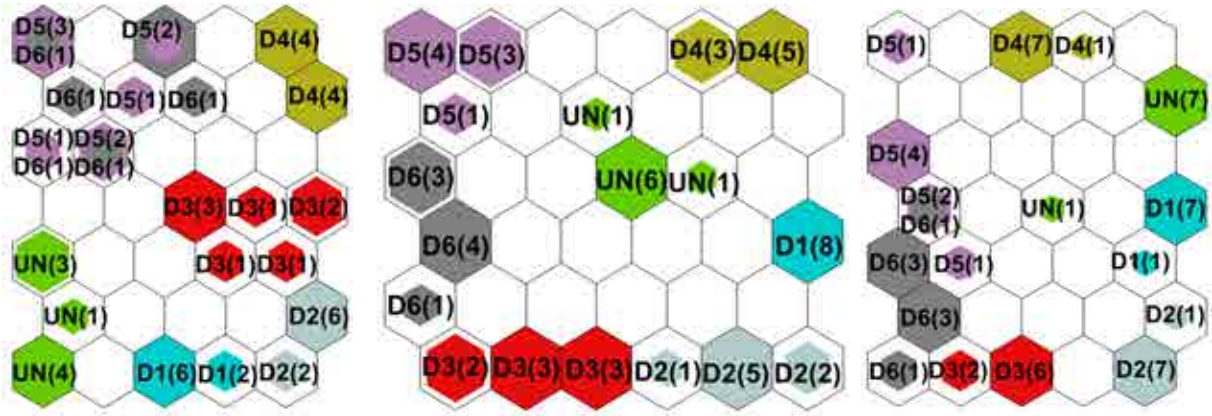

(a) (b) (c)

Figure 7.8: Classification of damages using Q-statistic, normalization type $histD$ and (a) 2 scores, (b) 7 scores, (c) 8 scores.

From these figures, it may be observed that, using 7 and 8 scores and any normalization, maps have less overlapped clusters than using just 2 scores. Moreover, comparing the normalization methods, $histC$ is the one that classifies better the damages.

Summarizing, there are certain important results to highlight here. First, it is possible to use a reduced number of inputs in the SOM to obtain a good classification of the different structure states. Furthermore, it is demonstrated that it is not necessary to include the T^2-statistic index.

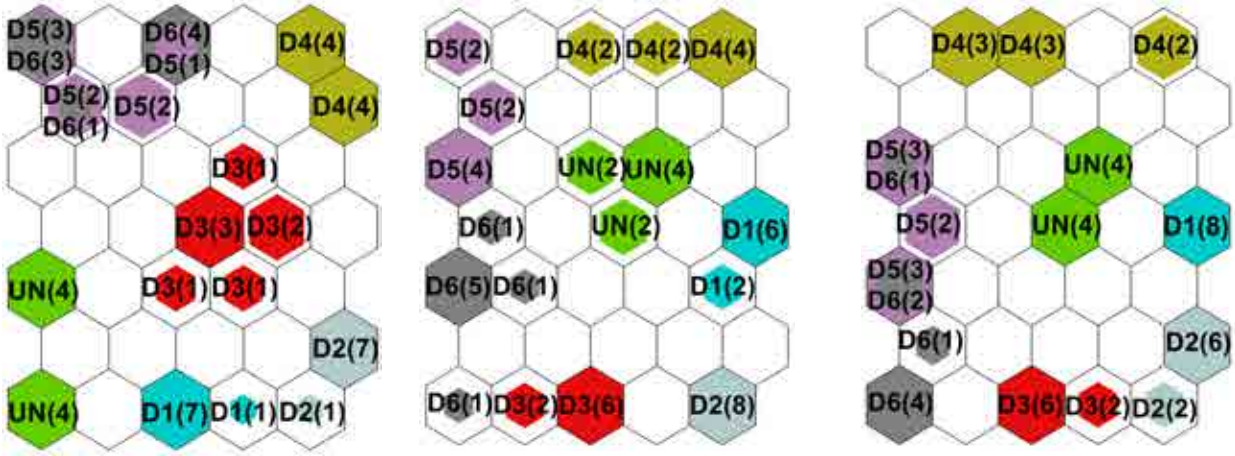

(a) (b) (c)

Figure 7.9: Classification of damages using Q-statistic, normalization type var and (a) 2 scores, (b) 7 scores, (c) 8 scores.

Another important result is concerned to the relationship between the normalization method and the inputs in the SOM, since, as shown the results there are differences between the results with each normalization.

7.3.2 Using the baseline pattern for diagnosis

From the results obtained in the training and validation stage, a 6×6 map that uses $histC$ method for normalization and, 7 scores and T^2-statistic as input vector (Figure 7.7b) was selected as the baseline pattern to be used in future diagnosis of structures. To assess the effectiveness of such diagnosis, two new experiments for each state of the structure were performed, which were not included in the training and validation stages. For each experiment, the data matrix is projected into the reference PCA model for each actuator phase. The first seven scores and Q-statistic from each model are the inputs to the baseline pattern SOM. Each experiment activates one cluster of this SOM. Since the baseline is labeled, it is possible to identify which damage has occurred if such damage was included in the training/validation stage. Figure 7.10 shows the clusters activated by each experiment. The direct visual comparison with Figure 7.7b (baseline) clearly shows that each state of the structure is satisfactorily identified.

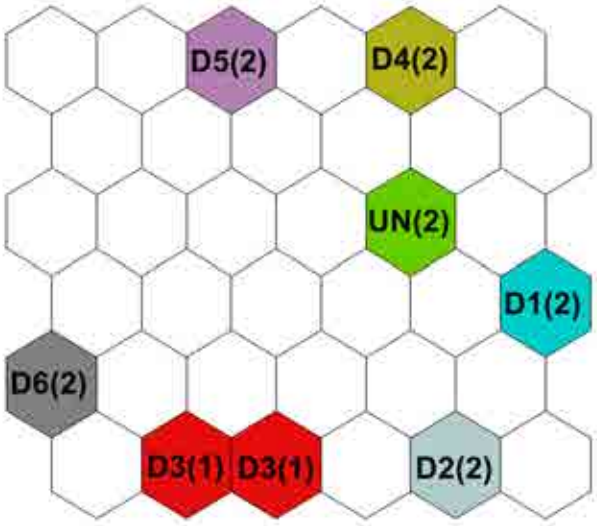

Figure 7.10: Tested map using $histC$ normalization, 7 scores and Q-index.

7.3.3 Analysis and discussion of the results using DWT

To test the benefits of using the DWT in the methodology, two structures are used: an aircraft fuselage and a CFRP plate, which correspond to the structures explained in Sections 4.7 and 4.3 respectively. In both structures, six reversible damages were inspected.

The two-channel subband coding scheme was applied to the recorded structural dynamic responses in order to produce a signal reconstruction to the level in which the signal could be properly reconstructed from the calculated coefficients with the minimum loss of information. The family of Daubechies wavelets ('db8') was chosen for this study. The optimum number of level decompositions was determined based on a minimum-entropy decomposition algorithm [45]. By using the minimum entropy criterion, the optimal basis that minimizes the number of significant coefficients in the signal representation was selected. Once the optimal decomposition level is found, the approximation and details coefficients are calculated at different levels. In this manner, the contributions of these coefficients can be studied in greater detail for the purpose of robust damage detection and classification. In this way, the best encoding scheme of the original signal showing robust features can be analyzed.

First, a preliminary analysis similar to the one explained in Section 5.4.1 about variances retained in the components was performed in order to define the optimal number of principal components required for building the PCA model. Figure 7.11 shows a plot of the cumulative variance in one of the actuator phases, in particular in the phase 8 in the aircraft fuselage, where only the first 46 components are shown to allow a better visualization. It can be seen that this number of components comprises more than 95% of the total variance. Besides using the three first components, around 80% of the variance is included into the model. This previous analysis is important in order to ensure that enough variance is retained in the model that allows performing an optimal reduction.

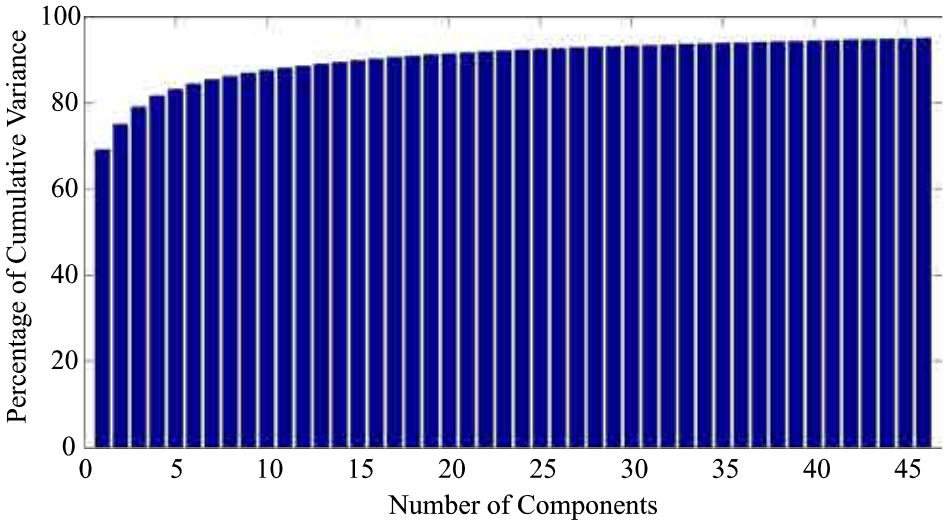

Figure 7.11: Percentage of cumulative variance in the actuator phase 8 in the aircraft fuselage.

Finally, three components were selected as a good representation of the input data. To illustrate the application of the discrete wavelet transform for feature extraction, a series of experiments were carried out in order to generate different signals at different levels from the approximation and detail coefficients which could then be investigated using the proposed methodologies. The objective of this investigation is to examine the suitability of coefficients from the different levels of decomposition as robust features for the detection and classification of damage. The full decomposition of each signal by the wavelet transform is carried out and all the components up to the ninth level were calculated and analysed in order to find the dominant energy levels. As previously mentioned, for the case under study, the family of Daubechies wavelets 'db8' was selected with the index number referring to the number of coefficients. The number of vanishing moments for each wavelet is equal to half the number of coefficients, so 'db8' has 4 vanishing moments. A vanishing moment confines the ability of the wavelet to represent polynomial behaviour in a signal. Figure 7.12 shows the level wavelet decomposition of a structural dynamic response signal for the fuselage from the levels number four to nine. Each signal at each level represents a specific frequency range, and the frequency range increases with increasing the wavelet levels. Regarding the different details decomposition it can be observed that identifiable waveforms emerge as the level number of decomposition is increased. Approximation level nine was found to be the more appropriate level for signal reconstruction from the approximation coefficients.

To evaluate the influence of the number of principal components and to validate the selection of three scores and $Q - statistics$ as inputs to the SOM using direct signals and signals pre-processed by DWT, a preliminary study by training different SOMs was performed. This study included the review of the results in the U-matrix by changing the number of scores. The U-matrix is another representation of the Self-Organizing Map which allow to visualize the distances between neurons by means of colors between adjacent neurons, in this way, dark colors show large distances which is the same as big differences between the data in the neurons. The results showed that 3 scores and $Q - statistic$ by each actuator phase are enough for a good representation in the SOM. Figures 7.13(a) and 7.13(b) show two of these results

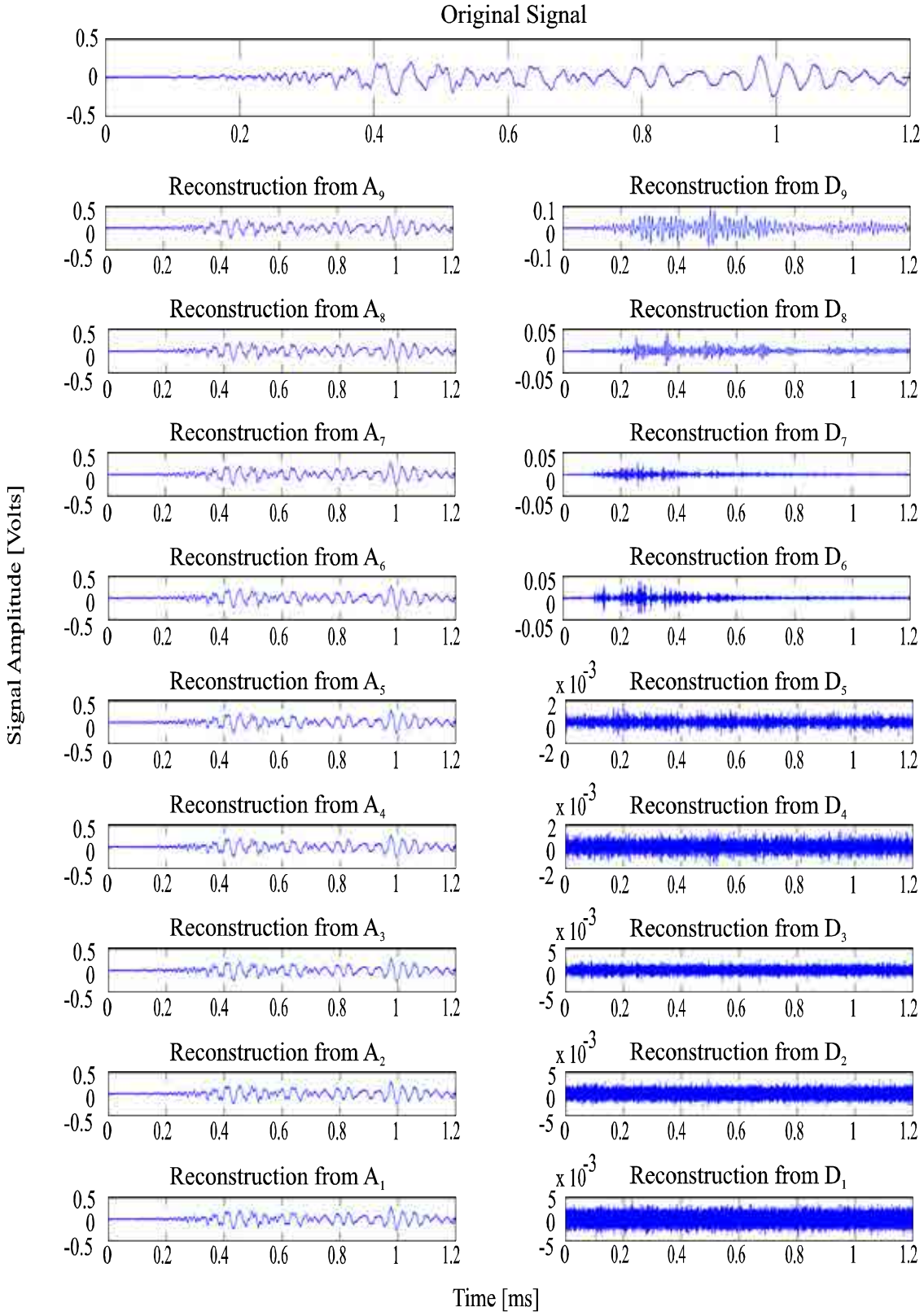

Figure 7.12: Wavelet decomposition.

using the approximation coefficients obtained from the DWT applied to the data collected directly from the aircraft fuselage using 3 and 199 principal scores respectively and including the $Q - statistic$. As it is shown, in this case the use of 3 scores and the $Q - statistic$ allows a good classification by separating the regions of each state into the map. Even when the regions are not labelled, it is possible to observe that the map is divided in seven regions. Further details and discussion are given in the next section. In computational terms, this reduction implies to work with smaller matrices by reducing the PCA models. As a result of the previous analysis, a four dimension vector is selected as input to the SOM by each actuator phase (3 scores and $Q - statistic$); this means that the inputs to the SOM are 200 vectors (number of experiments) where each vector has 4 elements (3 Scores and $Q - statistic$) $\times$ (number of actuators).

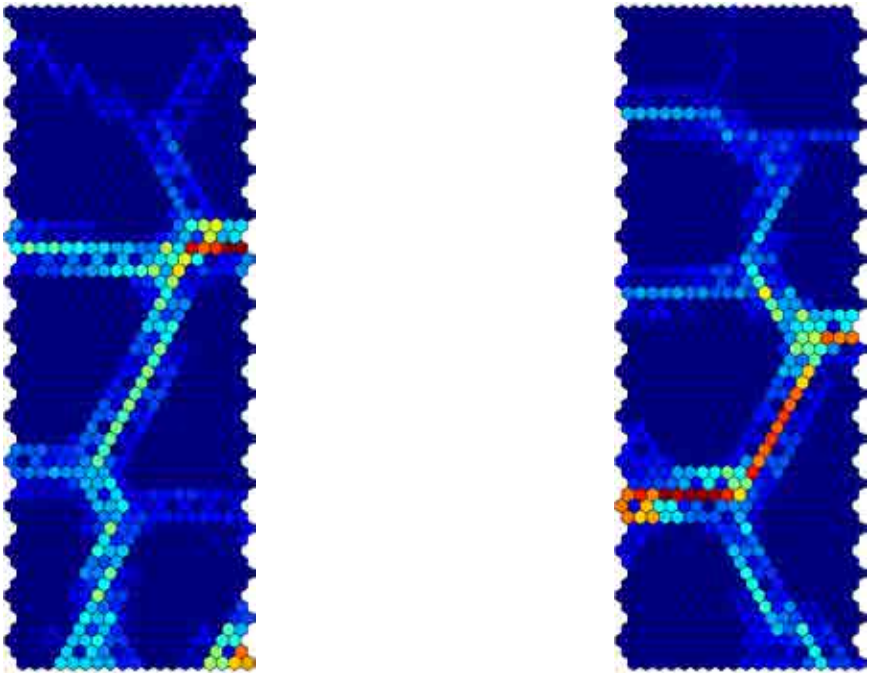

Figure 7.13: Cluster maps varying the number of scores in the aircraft fuselage with the direct signals.

To find the optimal map size, a control run is repeated by changing the map size. In order to accomplish the selection of the optimal map size, two quantitative measures of mapping quality known as the average quantization error (QE) and topographic error (TE) were analyzed. The QE is the average distance between each data vector and the BMU. The TE gives the percentage of the data vectors for which the first BMU and the second BMU are not neighbouring units. Lower QE and TE values indicate better mapping quality. As a result of the analysis, a map size of 30×10 is defined. Additional to the map size, the map lattice and shape must be specified. The SOM lattice gives the local topology of the map, i.e. the connectivity of the map units. The lattice can be either rectangular or hexagonal in the SOM toolbox. For the present study a hexagonal lattice is used. Different shapes such as sheet, cylinder or toroid can be chosen. For ease, a flat sheet shape is considered here. Additionally, a Gaussian neighbourhood function is used. Figures 7.14 and 7.16 show the results obtained by means of the cluster map in the aircraft fuselage and CFRP plate respectively. In addition, the U-matrix is used to show the

results in the classification in both structures (Figures 7.15 and 7.17). The cluster map can be used as a tool to show the different data set grouped with similar characteristics showing the clustering tendency. In each figure, each output neuron of the SOM is represented by a hexagon and the colors in the map represent the clustered areas, it means, each state of the structure (Undamaged, D1, D2, D3,. . .). The size of the portion with color in each output neuron shows the quantity among the total of the experiments grouped in each specific output neuron. In the U-matrix, it is also shown the clustered groups and, additionally it is useful to show the sparser regions between the clusters. More details on the results for these two structures are given below.

Aircraft Fuselage

Figures 7.14 and 7.15 depict the results obtained with the aircraft fuselage case. The former shows the clusters map using: the direct signal, the approximation coefficients and the detail coefficients. In a similar manner, the latter shows the U-matrix using the direct signal, the approximation coefficients and the detail coefficients. As it is possible to observe by means of the separations between the groups in the cluster maps, the best classification is obtained from the direct signals and the approximation coefficients. In this case, seven clusters seem to have been well identified. The approximation coefficients can be then used for classification with similar results to the ones obtained with the classification using the direct signals. Additionally, the number of columns of the unfolded matrix for each actuator can be reduced approximately 18 times. In order to provide a quantitative figure, the number of columns is reduced from 19200 samples with the use of direct signals to 1056 coefficients with the use of approximation coefficients, which results in a computational cost reduction.

Another important aspect is related to the treatment of the outliers. Although outliers are present in the three cases, the number is less when the approximation coefficients are used. This means that it is possible to perform a better classification by this approach. Additionally, it is important to observe that in all the cases the U-matrix representation allows an isolation of the outliers by the separation between the different areas. This separation represents the different zones delimited by boundaries, where the lighter colors depict these zones. The darker colors into these boundaries can be interpreted as the zones where the outliers are present into the map representation. This is an important result because this allows avoiding the creation of a new zone by the outliers. The U-Matrix realizes the emergence of structural features of the distances within the data space. Outliers as well as possible cluster structures can be recognized for high dimensional data spaces. However, the results obtained with the detail coefficients are not satisfactory when they are compared with the results obtained with the previous discussed approaches. In particular, it can be observed that the undamaged state cannot be properly separated from the damage state 1. This also holds between state four and six. It is also possible to observe that the distributions of the clusters in the map are different for all the three cases.

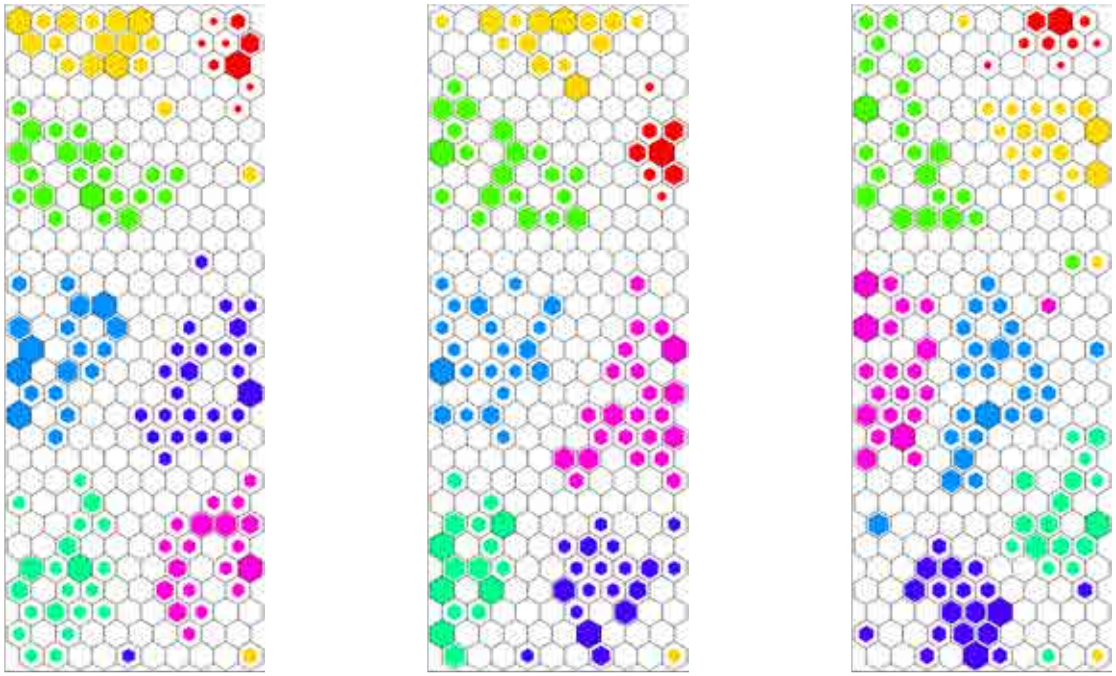

(a) (b) (c)

Figure 7.14: Cluster map for damage classification in the aircraft fuselage, using: (a) direct signals, (b) approximation coefficients and (c) detail coefficients.

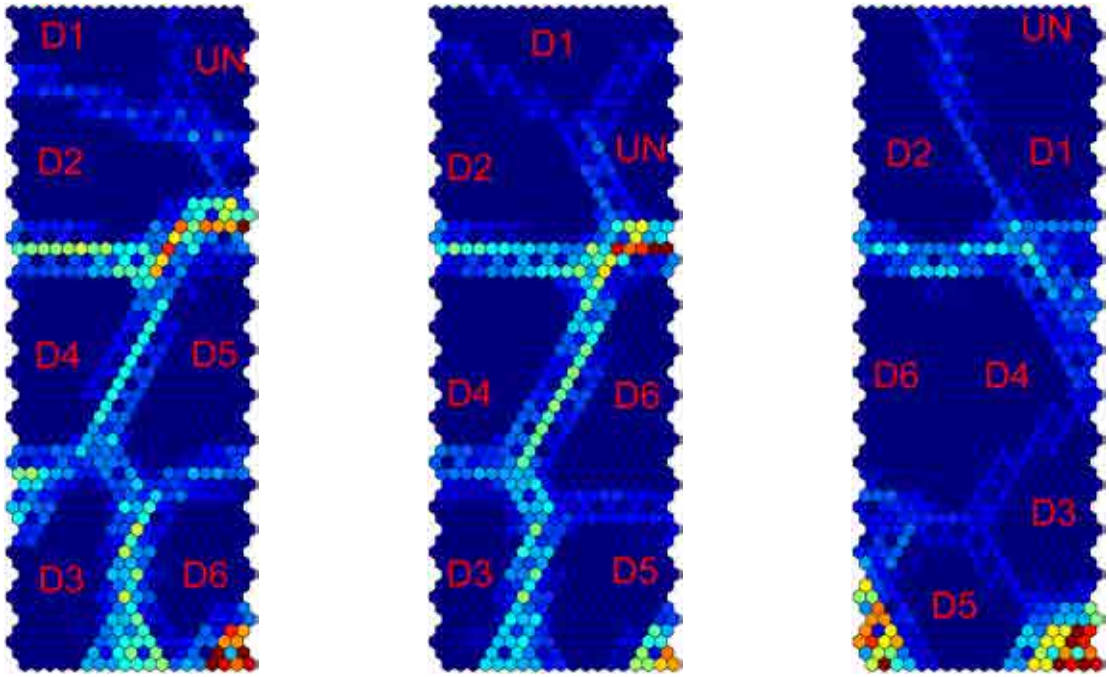

(a) (b) (c)

Figure 7.15: U-matrix for damage classification in the aircraft fuselage using: (a) direct signals, (b) approximation coefficients and (c) detail coefficients.

CFRP plate

Figures 7.16 and 7.17 depict the results obtained with the composite plate case. First, Figure 7.16 shows the clusters map using the direct signal, the approximation coefficients and the detail coefficients respectively. In a similar manner, Figure 7.17 shows the U-matrix using the direct signal, the approximation coefficients and the detail coefficients. As it is possible to observe by means of the separations between the groups in the Figure 7.17, a similar classification performance is obtained with the proposed approaches. In this case, seven clusters seem to have been well identified. Additionally, the boundaries are more clearly depicted compared with the previous example. Another significant difference is that there is no presence of outliers in the cluster map. The approach of the approximation coefficients provides good results and it is possible to replace the direct analysis of the signals by using these coefficients without losing reliability in the analysis.

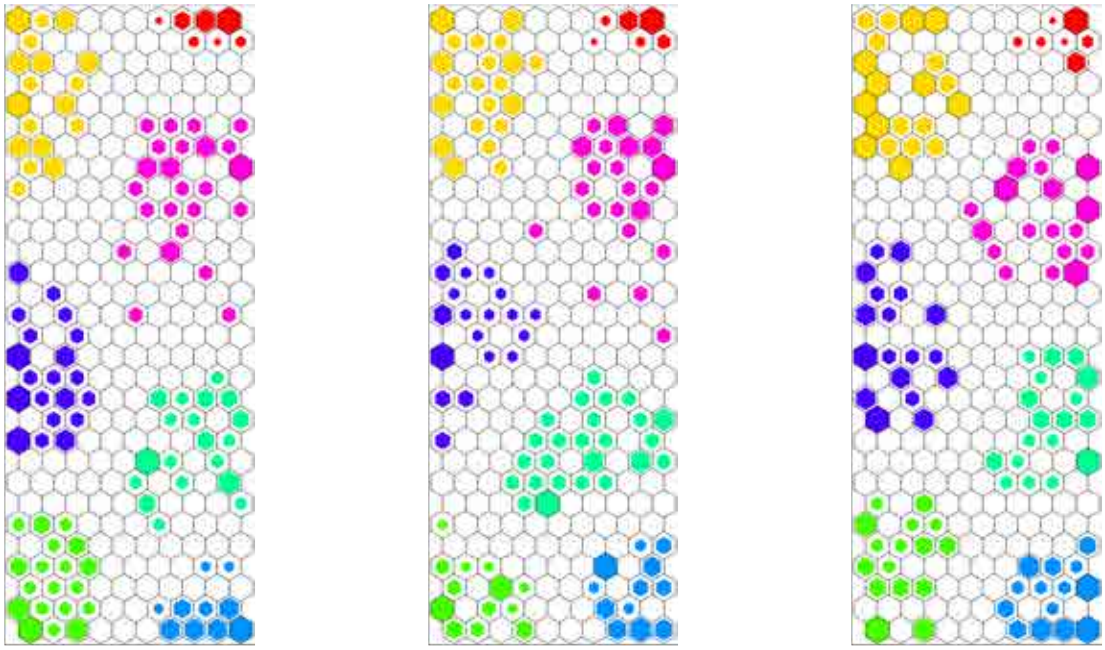

(a) (b) (c)

Figure 7.16: Cluster map for damage classification in the CFRP Plate using: (a) direct signals, (b) approximation coefficients and (c) detail coefficients.

Contrasting the fuselage case, in this particular case, the coefficients of the details also provide good results. This could probably be explained by higher harmonic generation of guided Lamb waves. It has been shown that nonlinear materials depict power-dependent transmission and selective generation of higher harmonics [34], [154]. This topic requires further research. In this case, the size of the unfolding matrix from each actuator with the direct signal is of 9600 samples $\times$ 150 experiments while using the approximation or details coefficients is of 584 coefficients 150 experiments. This implies a reduction in the unfolding matrix from each actuator of approximately 16 times less columns in each matrix. Compared with the previous example, the three cluster maps obtained by the different approaches have similar cluster distributions

into the cluster map. In contrast with the U-matrix, the results obtained in the CFRP Composite plate are more clearly separated. This can be explained by the fact that the aircraft fuselage is a more complex structure which contains stringers, ribs and rivets.

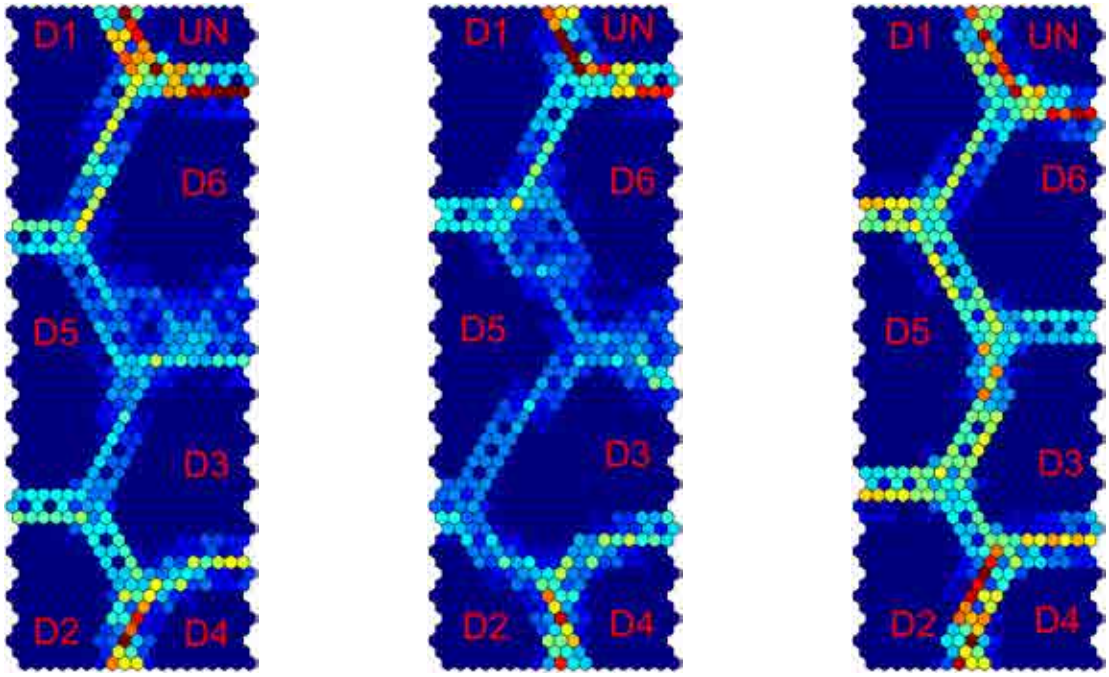

(a) (b) (c)

Figure 7.17: U-matrix for damage classification in the CFRP plate using: (a) direct signals, (b) approximation coefficients and (c) detail coefficients.

7.3.4 Damage classification using ICA

As was explained in the Section 5.3 any Multivariate Statistical Method that allows to represent the data by components can be used in the damage detection methodology for replacing PCA. Now in this subsection PCA is replaced by ICA in order to test the methodology and compare the results. This comparison was performed in a multilayered composite plate which corresponds to the structure described in Section 4.4.

Figures 7.18 and 7.19 show the results obtained by means of the cluster map and the U-matrix using PCA and ICA respectively, in both cases, the results are obtained by including the DWT to obtain the approximation coefficients.

The U-matrix shows similar results in both cases separating the different states. This can be seen at the separation boundaries depicted in lighter colors. Another important aspect is related to the treatment of the outliers that could be produced as a result of experimental errors and/or any type of noise source. By analyzing the cluster maps in Figures 7.18 and 7.19, it can be seen that outliers are only present in the ICA case. Additionally, it is important to observe that in this case the U-matrix representation allows an isolation of the outliers by the separation between the different areas. This is an important result because this allows avoiding

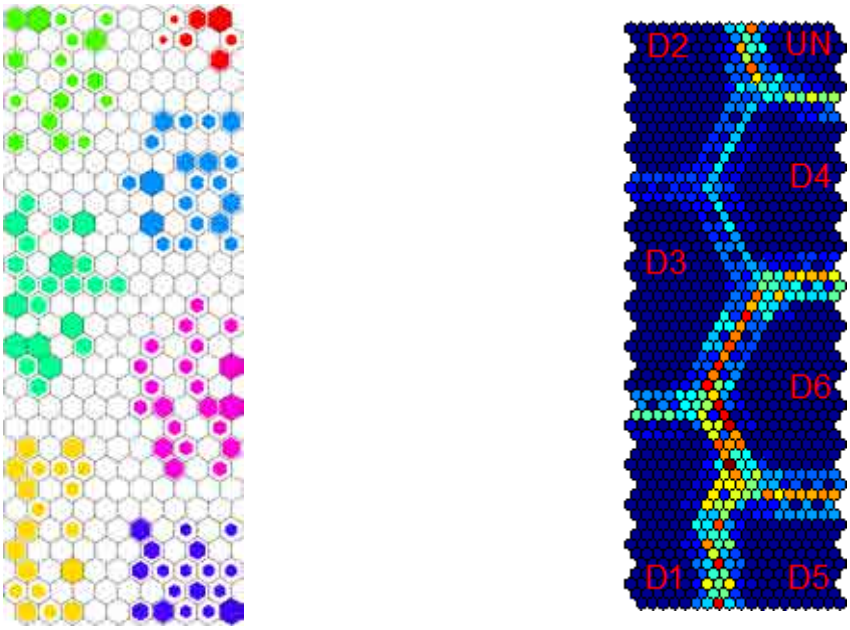

Figure 7.18: Damage classification using 3 Scores and Q-statistic. Figures (a) and (b) show the Cluster Map and the U-matrix using approximation coefficients from DWT and PCA.

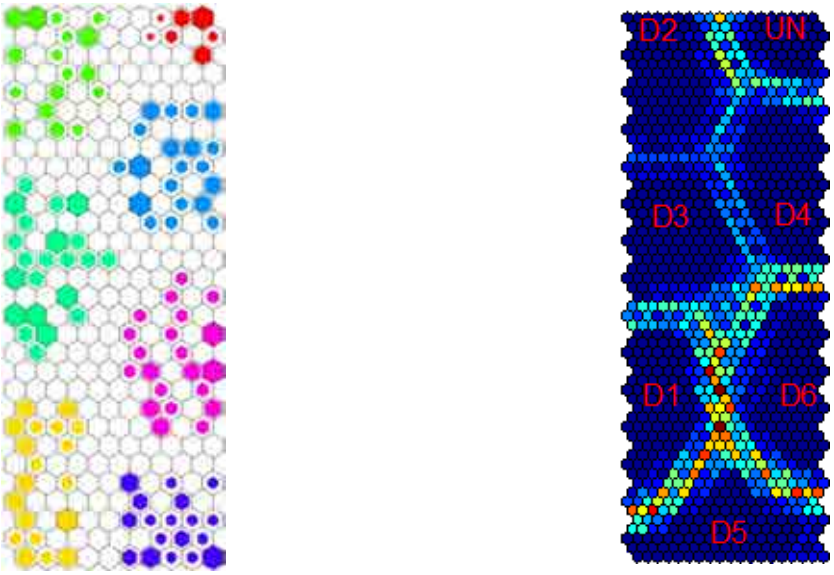

Figure 7.19: Damage classification using 3 Scores and SPE. Figures (a) and (b) show the Cluster Map and the U-matrix using approximation coefficients from DWT and ICA.

the creation of a new zone by the outliers. It can be seen how the U-Matrix recognizes the emergence of structural features of the distances within the data space. As a result, outliers as well as possible cluster structures can be recognized for high dimensional data spaces. It is also possible to observe that the distributions of the clusters in the map are different for all the cases. By analyzing the previous results, it can be seen that none of the methods is outperforming the other. This observation plays a critical role in the selection of the novelty detection algorithms. This is given by the fact that every algorithm has its own computational cost for the processing

of the input data to create the models. Regarding to the computational cost, PCA is the one providing the lowest cost followed by ICA. In contrast, ICA needs several algorithm runs in order to achieve optimal results, however, if the results are based on a "one-shoot" basis run, the results by ICA can significantly change. This is reflected by the changes of the values at the boundaries in the U-matrix, i.e. the values in some cases are smaller showing that the separation between the states are not strong, and in some other cases these values are higher presenting good separation between the groups. This result indicates some reservations about the use of ICA for the purpose of the detection and classification tasks.

7.3.5 Analysis of changes in temperature

To determine the effect of the temperature in the damage classification approach, some experiments were conducted using an oven with controlled temperature and an aluminum plate instrumented with 5 piezoelectric transducers. More details about the structure and the experiments can be found in Section 4.8.

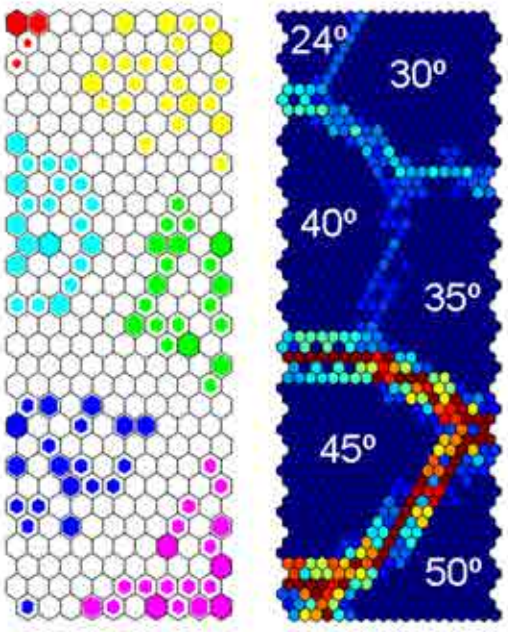

Figure 7.20: Classification of the different baselines at different temperatures using 2 scores and the Q-index.

To verify the sensitivity of the approach to the changes of the temperature and determine if it is possible to classify the different states of the structure, two studies were conducted. First, the classification of the different baselines at the different temperatures is evaluated. In particular, data from the structure under six different temperatures (24 °C, 30 °C, 35 °C, 40 °C, 45 °C and 50 °C) were used to evaluate the approach. For the evaluation, the cluster map and the U-Matrix are analyzed in order to find differences between the data from the healthy structure under different temperatures scenarios. The results are depicted in Figure 7.20. In this case, six clusters seem to have been well identified in the cluster map and the U-matrix. The analysis

of the cluster map shows that the data from the structure when the temperature is 24 °C are better organized, this can be observed by evaluating the number of output neurons occupied in the cluster map. In the U-matrix the boundaries represent the separation between the clusters and its color shows the differences between the clusters, in this sense darker colors implies big separations in the normalized map. As it is possible to observe by the colors in the boundaries, there are not big differences between the first four temperatures but this difference is increased with the last two temperatures. Another important aspect is related to the treatment of the outliers, as is shown in the cluster map presented in Figure 7.20, where there is an outlier in the data from the structure when the temperature is 45 °C. In this case, it is important to observe how the U-matrix allows an isolation of the outlier by the separation between the different areas. This separation represents the different zones delimited by boundaries, where the lighter colors depict these zones. The darker colors into these boundaries can be interpreted as the zones where the outliers are present into the map representation. This is an important result because this allows avoiding the creation of a new zone by the outliers. The U-Matrix realizes the emergence of structural features of the distances within the data space. Outliers as well as possible cluster structures can be recognized for high dimensional data spaces. The result of this first study is useful to demonstrate that there are differences between the data from the healthy structure in the different temperatures as was expected. Those differences were less significant among the first temperatures.

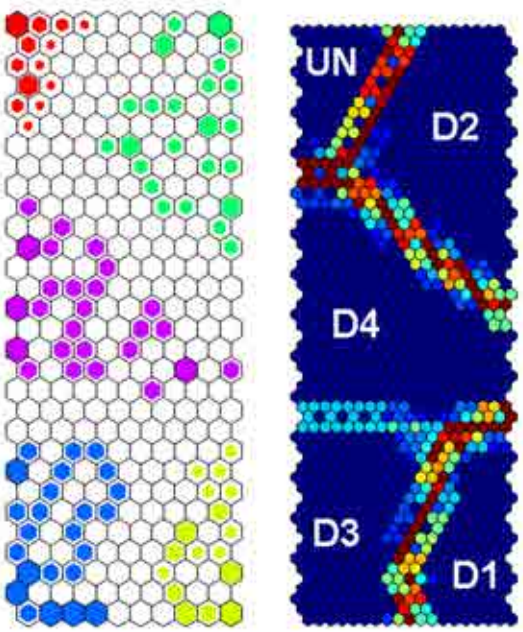

Figure 7.21: Classification of the different baselines at 24 C using 2 scores and the Q-index.

In a second study, the maps were trained using the data from five different states (healthy state and four damages). Damage on the tested plate was simulated by localized masses at different positions on the surface as was presented in the experimental setup section. Figures 7.21 to 7.26 show the classification results when the structure is subjected to 24 °C, 30 °C, 35 °C, 40 °C, 45 °C and 50 °C. In this case, six clusters seem to have been well identified. The

boundaries between the clusters in the U-matrix show that there is a clear separation between all the states. Additionally, according to the results in the cluster map there is no outliers.

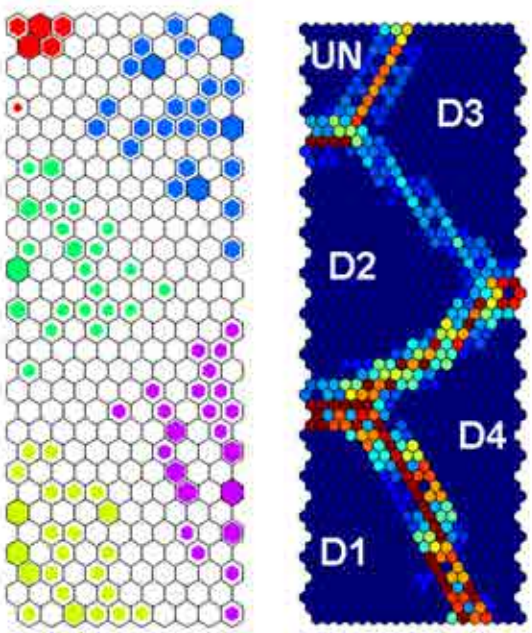

Figure 7.22: Classification of the different baselines at 30 C using 2 scores and the Q-index.

Figure 7.22 shows again that six clusters seem to have been well identified. Again the boundaries show clear separations between the different states. In difference with the result when the temperature is 24 °C, there is one data separated more than two output neurons in the cluster map from the rest of data in the undamaged state. This outlier is isolated by the separation between the undamaged sate and the damage 2. Other difference to remark is the distribution of the states in the cluster map and the U-matrix which is different to the distribution when the temperature is 24 °C.

Figure 7.23 shows the results when the temperature is 35 °C. These results again showed that six clusters seem to have been well identified. In difference, there is again a different distribution in the cluster map and the U-matrix compared with the data from the structure with 24 °C and 30 °C. As to the results with 30 °C the smallest differences between the clusters are between the damages 2 and 3. This can be seen by the lighter color in the boundary between these two clusters.

Figure 7.24 shows the results with 40 °C, as is shown there are five clusters well identified. Equally to the results obtained with 30 °C and 35 °C the boundary between the damage 2 and damage 3 is in lighter color, this means less differences between these damages. By evaluating the cluster map it is possible to see that there is one data separated by a distance of more than two output neurons from the rest of the data; this possible outlier is isolated in the U-matrix by the boundary line between the D4 and D1.

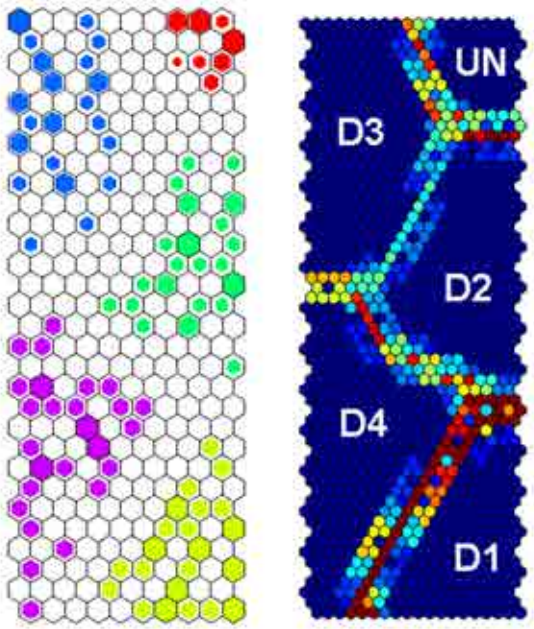

Figure 7.23: Classification of the different baselines at 35 C using 2 scores and the Q-index.

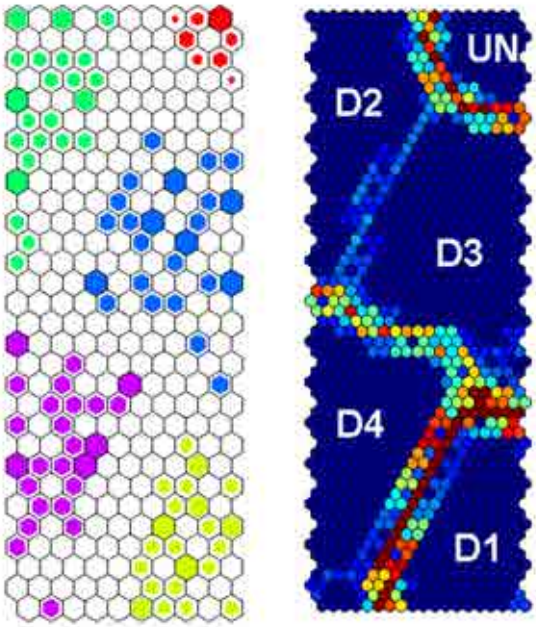

Figure 7.24: Classification of the different baselines at 40 C using 2 scores and the Q-index.

Figure 7.25 shows the results with 45 °C, again, are shown five clusters clearly separated in the cluster map and the U-matrix. Equally to the results obtained with 30 °C, 35 °C and 40 °C the boundary between the damage 2 and damage 3 is in lighter color. It is worth underlining that, while the data from the damage 4 and damage 3 are scattered compared with the other damages, the U-matrix allows equally a good classification of these states.

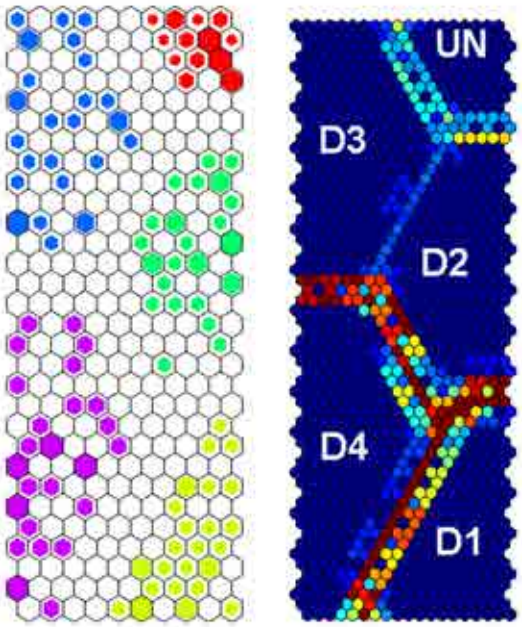

Figure 7.25: Classification of the different baselines at 45 C using 2 scores and the Q-index.

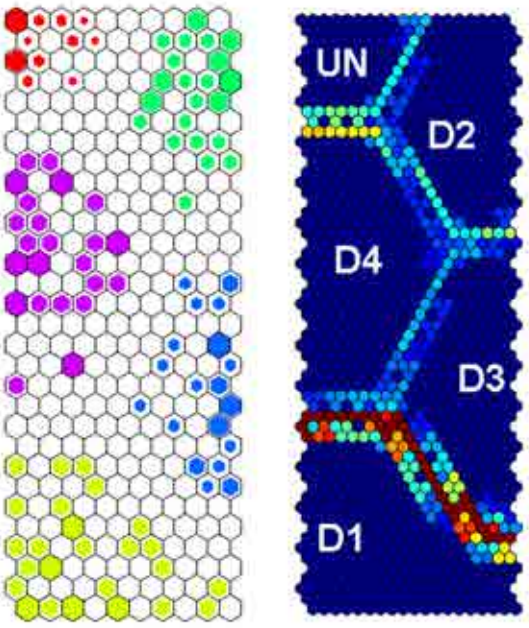

Figure 7.26: Classification of the different baselines at 50 C using 2 scores and the Q-index.

In difference with the previous results, with 50 °C (Figure 7.26) the lighter boundary are between the data from damage 4 and 3. Equally, five states are clearly separated and the classification of all the states is possible. Comparing the results in the classification from all the temperatures studied, it is possible to assert that in all the cases the classification is possible for all the states with a good treatment of the outlier. This treatment presents good results in the sense that there is no creation of a new cluster. The undamaged state in all the temperatures

is clearly separated from the rest of the damages in spite of the number of output neurons in the cluster map is different for each temperature.

7.4 Discussion

This chapter has proposed an approach for structural damage classification through the integration of: a multiactuator system (several PZT's working as actuator and sensors in several phases), a statistical reference model based on Principal Component Analysis, a damage index and a Self Organizing Map as classification tool to combine and contrast the information obtained from each actuator phase. The approach has been experimentally analyzed showing good results classifying different states of the structure in three different specimens with different materials, properties and sizes showing the robustness of the approach.

Results indicate that the use of the approach enables one to detect and classify damages even when the structure is subjected to a range of temperature changes. In the specific case presented, the preprocessing with DWT, the use of two scores and the Q-index by each phase and the data fusion by means of a Self-Organizing Map presented the best result in the classification. The detection can be performed when the new data in the cluster map or in the U-matrix is separated from the undamaged state. According to the results, in all the cases evaluated, the undamaged state is clearly distinguished and the detection is possible. In addition, with the application of this approach, the problem of evaluate all the phases to define the existence of a damage, as was defined in Chapter 5, specially, in large structures instrumented with several PZT transducers is solved. Now, the solution implies only the evaluation of the cluster map or the U-matrix obtained by data fusion.

In the classification, each cluster represents one state of the structure. As was shown, the classification was possible in all the cases (different temperatures) with similar results. There are some changes in the final distribution in the cluster map and the U-matrix, mainly because the organization in these plots depends on the input data, but these changes do not alter the final result of the classification.

In the same manner, the methodology has been tested with partners from the Siegen University with excellent results using Hierarchical Nonlinear PCA in different structures, such as a simplified aircraft composite skin panel with reversible damages [175], [174] and a pipe with real damages [173], showing the utility of the approach. All these results allow to ensure that is possible to replace the use of PCA by other multivariate statistical method in the methodology and obtain good results and that it is independent of the properties of the structure such as shape or material.

Chapter 8

CONCLUSIONS AND FUTURE RESEARCH

8.1 Observations and concluding remarks

This thesis has contributed with the development of a structural health monitoring system based on pattern recognition techniques for tackling the SHM problem in aeronautical structures. This development was focused on damage detection, localization and classification. From the application of this system several advantages were obtained as shown by the results throughout this manuscript.

In general, several conclusions can be drawn from this thesis. They are organized in six subsections: instrumentation and data acquisition, preprocessing, model building, damage detection, damage localization and finally, damage classification.

8.1.1 Instrumentation and data acquisition

Starting from the instrumentation level, it is possible to conclude that the use of the Piezoelectric Transducers (PZT's) is a viable solution for structural inspection. They provide the following advantages:

- By its nature of transducer, they can work either as actuators or sensors
- They can work in a wide range of frequencies
- They can be easily attached to any structure and they are available in different sizes and presentations.
- The price is relatively low compared with other sensors normally used in NDT inspection and SHM applications.

As it has been shown in this thesis, an active piezoelectric system which consists of several PZT transducers attached to the structure under test, was used in several actuator

phases. In each actuator phase, one PZT transducer is used as actuator to excite the structure and the rest are used as sensors to obtain the signals from different points of the structure. This configuration allows to perform a global and robust inspection compared with the basic inspection performed by a pair of piezoelectric transducers by working in pitch-catch mode. In the other hand, it is not tied to the use of a data acquisition equipment from a specific company to perform the experiments. This means that it is possible to use any equipment that meets the requirements to inspect the structure (generation of signals defined by the user in the order of KHz and data acquisition). A proof of this statement is that as shown in Chapter 4, three different equipment from different companies were used in this work to inspect the structures. The results showed that in all the cases it was possible to detect, localize and classify damages.

A strong advantage about the use of the proposed methodologies is that they can be used indistinctly with other kind of transducers working in a similar configuration. This is possible because all the proposed approaches just need the vibrational time responses for the different actuation phases.

8.1.2 Data preprocessing

According to the obtained results, it is possible to conclude that an adequate preprocessing of the original data adds some advantages to the methodologies such as:

First, the normalization allowed to scale the data set using the mean and standard deviation of all measurements. This step provides the opportunity to treat in the same manner all the data from each sensor, it is really important since data from different sensors have different magnitudes and scales. These differences depend on factors such as the distance from the actuator, the type of material in which the signal is propagated, stiffeners, and others.

Second, the unfolding of the original data allowed to organize them to perform a multivariate analysis, allowing to analyze the variability in each experiment, summarizing the information in the data with respect both the sensor and the time variation.

Finally, the use of the DWT allowed to improve the computational efficiency. It was included in the preprocessing step with the corresponding result of the reduction in the computational cost by decreasing the size of the unfolding matrices for each phase. Equally, the classification of the data set from different structural states was improved. Due to the fact that DWT decomposes the signal in details and approximations, a study was performed to evaluate which coefficients presented better results. This study showed that the approximation coefficients can be used in place of the direct signal collected in the experiments and in some cases outperform the traditional PCA features in securing the separability of the data classes and allowing a lower dimensional representation. Though DWT was not included in the analysis for damage localization, results are expected to be similar to those obtained in the damage detection and localization with the corresponding time reduction.

8.1.3 Data driven baseline modeling

After reviewing the literature and considering the previous experience of the author and advisors, PCA and ICA were selected as techniques to build a baseline data driven model using the healthy structure. The use of multivariate approaches allowed to perform a robust analysis extracting the information from the data of all sensors in each actuation phase, and to project it onto a lower dimensional space. In the case of PCA this new reduced space is defined by the principal components, while in the ICA case is done by the independent components.

When PCA is used, an analysis of the variances retained in the components allowed to define the optimal number of principal components required for building the PCA models. In some cases, it was possible to reduce the dimension to 2 principal components allowing to obtain a good representation of the data with less computational cost. In the ICA case, there is no way to determine which component contains the most relevant information. To solve this problem and perform the reduction of data, PCA was previously applied using the analysis of the retained variance.

The application of PCA and ICA as multivariate statistical methods to create a model by each phase presented several advantages:

- These baselines must be calculated only once using the data from the structure when this is known as healthy.
- These baselines can be used in the three methodologies without any change. As was showed throughout the thesis, the damage detection methodology is the basis for the classification and localization tasks.
- These baselines are a reduced representation of the original data, therefore, the computational cost is also reduced.

8.1.4 Damage detection

The methodology presented in this thesis allowed to detect damages using PCA and ICA with similar results. The advantage of this methodology is its simplicity, since to determine the state of a structure only few steps are required: to collect new data, preprocess these data and project them into the models. These projections by itself can be used to detect damages by each actuator phase. The detection can be performed by analyzing the differences in the score plots between the undamaged state and the new data by each phase.

The contribution of this thesis to solve the damage detection problem is the use of four damage detection indices. Although two of these indices were known in SHM (Q and T^2), this thesis introduce new alternatives. The other indices (ϕ and I^2) are new in the SHM field and was shown that in some cases the results are better. In general, it should be emphasized that the detection of damages can be performed by using any of these five features (scores, T^2, Q, ϕ and I^2) independently.

The performance of the damage detection methodology using the projections and the indices were tested in different structures. In particular, results from aircraft turbine blade and the aircraft wing skeleton revealed that the use of the scores and the damage indices allowed in most cases the detection of the damages. Additionally, the approaches allowed to separate and distinguish damages among them in most of the cases. These results allow to affirm that the use of the scores and damage indices have potential for real applications and can be used in a combined way to evaluate the state of a structure.

In general, the results showed that the score plots are not very useful when the variances contained in the principal components are not significant. In these cases, the use of a combined analysis with the damage indices can be used for detecting damages with better results.

8.1.5 Damage localization

A novelty system for the localization of damages was developed. The approach combined some important elements such as:

(i) A piezoelectric active system working in different actuation phases.

(ii) The damage detection methodology to reduce the original data, obtain the baseline models by each actuator phase and calculate the scores and damage indices.

(iii) The evaluation of the influence of every sensor to the damage index in each actuation phase. This influence can be calculated by means of contribution analysis methods, which are used to localize the origin of the change in the vibrational response (damage).

(iv) A data fusion technique to combine the results from each actuation phase in one result to offer one generalized diagnostic about the position of the damage. The region that contains the damage is obtained by finding the highest value area, for which the sum of the contributions obtained for each sensor to each index is calculated.

Five contribution analysis methods (CDC, PDC, ABC, DC, RBC) were introduced in SHM for calculating the contribution of each sensor to the index. Therefore, five different ways to localize damages by each damage index are available. In particular, it was found that using T^2 and Q index, the lowest contributions were obtained applying CDC method. Specifically, in the Q index case, the results obtained with the other methods presented similar results, but in the T^2 index case best results were obtained using ABC method. In the case of the ϕ and I^2 the results were similar to the obtained with T^2 index and Q index, showing that all the methods are useful to localize damages.

Results vary for each actuator. In this way, the use of data fusion allowed to consider the results from each actuator phase and obtain a simplified final diagnostic.

Although ICA was not used for damage localization, results are expected to be similar as those obtained ones by PCA.

8.1.6 Damage classification

It was shown that the damage detection methodology can be extended for damage classification. In the approach, a combination of: a multiactuator system working in several phases, PCA or ICA, the projections to the components, the damage indices, and a SOM properly configured were used.

The SOM was used as a classifier and data fusion tool to contrast the information obtained from every phase, allowing the properly classification of different states of each inspected structure (from the healthy structure to different damages defined across the structure).

To demonstrate the effectiveness of the approach, two clear stages in the methodology were performed: first, the baseline pattern building stage and second, the diagnosis stage using different data. The first stage demonstrated how the results are highly influenced by the inputs and the normalization method applied in the SOM. The information from the state of the structure was used to verify the quality of the classification and the best parameters of the approach: how many scores should be used, how many damage indices are necessary and the configuration of the SOM (structure, number of output clusters, normalization, etc). Additionally, it was shown that the T^2-index (although is a good index for damage detection by itself) can be avoided to reduce the number of inputs to the SOM. This result is potentially useful in future applications when working with structures instrumented with a large sensor network in order to optimize the computational cost. The second stage allowed assessing the effectiveness of the proposed approach by using new data from each state of the structure which were not included in the first stage.

Although all the steps can be generalized in the classification methodology to be used with any multivariate statistical method, some elements such as the definition of the number of components, type of normalization of the SOM input data and the size of the map should be evaluated for each specific case. Particularly, in most cases studied in this thesis, the normalization type $histC$ presented the best results allowing to obtain a better classification. This means that a better separation between vectors was obtained. Similarly, it was found that the size of the SOM must be greater than 4x4: a smaller SOM means overlapped clusters, while using a very big SOM generates too many empty clusters which adds uncertainty to the classification.

In addition, it was shown how the SOM algorithm by means of the U-matrix detects and isolates the outliers allowing the identification of the different structural states in different zones. The results obtained from the structures showed that, in spite of the possible noise in the experimental setup and the complexity of the structure, it was possible to classify and detect damages doing a proper management of the outliers in the final representation (U-matrix). The U-matrix allows to identify the sparser regions between the maps and to isolate the outliers. Furthermore, the possible presence of high order harmonics in the spectrum of the transmitted signals could be an indication of nonlinearity inside the material which potentially may lead to significant enhancement in the sensitivity to structural defects.

One of the challenges in structural health monitoring is the variability caused by variation in operational and environmental conditions, producing changes in the signals propagated through of the structure therefore. The results can generate false indications of damages. To avoid these false alarms, the methodologies need robustness. This feature was evaluated inspecting an aluminium plate using different changes in the temperature. As result, it was demonstrated that the detection and classification was possible in all the cases.

8.2 General conclusions

Results showed the real practical potential of the proposed methodologies for detection, localization and classification. This statement is supported by the fact that they can work properly with any type of structure regardless of whether it is a simple aluminum plate or a more complex part of an aircraft as a fuselage or a wing, which contain stiffeners in two directions. Additionally, the results in each SHM level (detection, localization and classification) demonstrated that the goal is achieved independently of the type of material of the structure, temperature changes, data acquisition system, etc. Although the inspection was performed under controlled laboratory conditions, the results showed a potential use in real applications.

The applicability of the methodologies is enhanced by the following elements:

- The multi-actuator architecture. Since the final diagnosis is performed by analyzing the results from the different actuator phases, it is possible to evaluate the abnormalities from different points of view, this means, from different sensors in different locations of the structure.
- The preprocessing step. This step allows to normalize and organize the signals in each actuation phase in order to perform an adequate multivariate analysis of the data.
- The model building step. The use of multivariate statistical methods allows to obtain a baseline data driven model in a reduced dimension space.
- The use of damage indices. These indices allows to identify abnormalities in the data to define the presence of damages by comparing the data from different structural states with the undamaged state.
- The data fusion. This step is really important in the presentation of the final results since it allows to give one general diagnosis by combining the analysis from the different actuation phases. This implementation provides a degree of reliability to the methodologies.

8.3 Future work

This thesis has contributed to SHM but many open issues still remain. The following subjects are outlined as future works specifically related to the system developed in this thesis.

8.3.1 Tests with different damages

In the majority of the cases in this thesis, the damages have consisted in adding masses at specific locations. Although they are not real structural damages, they have allowed to evaluate the methodologies without irreversibly damaging the available experimental specimens. Future evaluations would be interesting to be performed with real typical damages.

8.3.2 Variation of the environmental conditions

Since a structure in normal operating conditions undergoes temperature variations and different forces by the environmental conditions, it is necessary to test the methodologies using more complex structures subjected to different loads and environmental conditions (variation in temperature, random vibration, humidity, etc.) to continue the validation of the proposed methodologies.

Additionally, it is necessary to work in the development of more robust baseline models. To achieve this objective, the data from the structure under different environmental conditions when it is known as healthy need to be considered in the PCA modeling.

8.3.3 Sensor distribution Optimization

A good alternative to improve the results is related to the fact of an optimized sensor distribution. In this sense, the study and development of a methodology to determine the optimal location and the number of the sensors according to each structure is needed.

8.3.4 Sensor fault detection

The methodologies presented in this work assumed that the signals from the sensors were always right and there was no sensor failure. In real applications, this assumption is not ensured all the time since the sensors and the structures are subjected to changes in environmental conditions and different loads. To solve this problem, the active piezoelectric system needs to incorporate a validation procedure to ensure the properly functioning.

8.3.5 Validation using more complex structures

Although the results from the experiments in two composite plates were included, it is necessary to perform more experiments with more complex structures and different materials in order to validate the scope of the methodologies.

As applications of composite materials in aeronautic and aerospace structures is growing, it is very important to continue testing all these techniques to determine how they affect the results depending on the class of material. Of course it is expected that all the results will be different, but it is important to determine if this variation improves or gets worse results. Following this direction, the author started to work at the end of this thesis and some new contributions to journals and conferences are still in process with partners from Siegen University in Germany

and the DTU Wind Energy, RISØ Campus in Denmark, where other composite materials including sandwich composite materials were inspected using real damages such as cracks and delamination.

8.3.6 Evaluation of different statistical methods

The methodologies presented in this thesis allow to use any multivariate statistical method to reduce data and to calculate the components and indices. As a preliminary result, the damage classification methodology was also tested in collaboration with partners of Siegen University by using Hierarchical Non-Linear PCA with excellent results. These results have not been included in this thesis since they are still under further studies.

Appendix A

PUBLICATIONS

As results of the current thesis were obtained the next contributions to books, journals and relevant conferences on the area:

A.1 Book chapters

1. **D.A. Tibaduiza, L.E. Mujica, J. Rodellar. Structural Health Monitoring based on principal component analysis: damage detection, localization and classification. In: Advances in Dynamics, Control, Monitoring and Applications, Universitat Politècnica de Catalunya, Departament de Matemàtica Aplicada III, p. 8-17, 2011. ISBN: 978-84-7653-539-4**.

A.2 Journals

1. **D.A. Tibaduiza, L.E. Mujica, J. Rodellar. Comparison of several methods for damage localization using indices and contributions based on PCA. Journal of Phisycs: Conference Series, 305 012013 doi:10.1088/1742-6596/305/1/012013, 2011**.

2. **D.A. Tibaduiza, L.E. Mujica, J. Rodellar. Damage Classification in Structural Health Monitoring using Principal Component Analysis and Self Organizing Maps. Accepted for publication in Structural Control and Health Monitoring, 2012**.

3. **D.A. Tibaduiza, M.A. Torres Arredondo, L.E. Mujica, J. Rodellar, C.P. Fritzen. A study of Two Unsupervised Data Driven Statistical Methodologies for Detecting and Classifying Damages in Structural Health Monitoring. Submitted to Mechanical Systems and Signal Processing, 2012**.

4. **M.A. Torres Arredondo, D.A. Tibaduiza, L.E. Mujica, J. Rodellar, C.P. Fritzen. Data Driven Multivariate Algorithms for Damage Detection and Classification: Evaluation and Comparison. Submitted to Structural Health Monitoring An International Journal. 2012**.

A.3 Conferences

1. **M.A. Torres Arredondo, D.A. Tibaduiza, L.E. Mujica, J. Rodellar, C.P. Fritzen. Damage Assesment in a Stiffened Composite Panel Using Non-Linear Data Driven Modelling and Ultrasonic Guided Waves. Presented in: 4th International Symposium on NDT in Aerospace. Ausburg-Germany. November 2012**.

2. **M.A. Torres Arredondo, I. Buethe, D.A. Tibaduiza, J. Rodellar, C.P. Fritzen. Damage Detection and Classification in Pipework Using Acousto-Ultrasonic and Probabilistic Non-Linear Modelling. Presented in: Workshop on Civil Structural Health Monitoring (CSHM-4). Berlin-Germany. November 2012**.

3. **D.A. Tibaduiza, L.E. Mujica, M. Anaya, J. Rodellar, A. Güemes. Principal Component Analysis vs Independent Component Analysis for Damage Detection. Presented in: The 6th European Workshop on Structural Health Monitoring. Dresden-Germany, July 2012**.

4. **D.A. Tibaduiza, L.E. Mujica, M. Anaya, J. Rodellar, A. Güemes. Independent Component Analysis for Detecting Damage on Aircraft Wing Skeleton. Presented in: EACS 2012-5th European Conference on Structural Control. Genoa-Italy, June 2012**.

5. **D.A. Tibaduiza, L.E. Mujica, J. Rodellar. Comparison of Several Methods for Damage Localization Using Indices and Contributions Based on PCA. Presented in: The 9th International Conference on Damage Assessment of Structures. Oxford-UK, July 2011**.

6. **D.A. Tibaduiza, L.E. Mujica, J. Rodellar. Structural Health Monitoring based on Principal Component Analysis: damage detection, localization and classification. Presented in: The Workshop on Control Dynamics, Monitoring and Applications.Caldes de Montbuì-Barcelona, February 2011**.

7. **D.A. Tibaduiza, L.E. Mujica, M. Anaya, J. Rodellar. Combined and I indices based on Principal Component Analysis for damage detection and localization. Presented in: The 8th International Workshop on Structural Health Monitoring. Stanford-USA, September 2011**.

8. **D.A. Tibaduiza, L.E. Mujica, A. Güemes, J. Rodellar. Active Piezoelectric System using PCA. Presented in: The Fifth European Workshop on Structural Health Monitoring. Sorrento-Italy, June 2010**.

9. **L.E. Mujica, D.A. Tibaduiza, J. Rodellar. Data-Driven Multiactuator Piezoelectric System for Structural Damage Localization. Presented in: The Fifth World Conference on Structural Control and Monitoring (5WCSCM). Tokyo-Japan, July 2010**.

Appendix B

STRUCTURAL HEALTH MONITORING LABORATORY

B.1 Commercial Solutions

In terms of companies that provide solutions to end users of SHM, there exist many systems that include custom solutions for specific applications, or sale of equipments by separate to configure according to the needs. Most of these companies are oriented to the civil engineering sector [71].
In general terms, SHM systems usually includes three components. These are:

- a sensor and actuator system to produce the excitation and/or measure the response of the structure
- The hardware to acquire and pre-processing the collected signals. It depends of the kind and number of sensors, the kind of structure material and the excitation signal, among others.
- The software with the different techniques according to the own application (damage detection, impact detection, loads monitoring, etc.)

B.1.1 Sensor and actuator systems

There are different ways to apply and collect signals in structures. Nowadays several kind of sensors are used in SHM [126], among them, the most used are: piezoelectrics transducers ([66],[73], [183], [130]) , Optical Fibre ([141],[169],[36], [106],[122]) and Strain sensors ([110] ,[106], [25]). On the other hand, they can be used in the structure in different manners. For instance, the sensors can be neither attached to the surface or integrated within the structure. As an example of this sensors, Accellent inc offers the SMART Layer®sensors. These sensors are a thin, flexible and ultra-lightweight dielectric film with an array of durable networked piezoelectric sensors (see figures B.1 and B.2). This layer can be adapted to any structure with complex geometry.

Figure B.1: Smart Layer sensors [3].

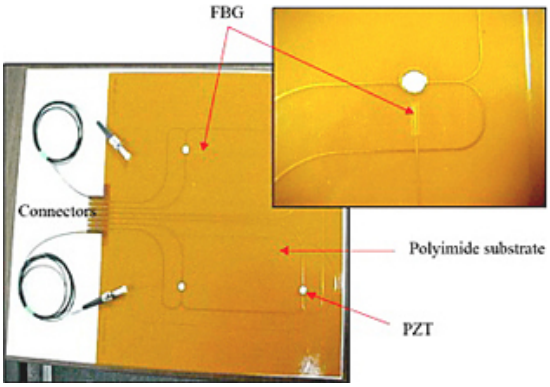

Figure B.2: Smart Layer sensors [3].

B.1.2 Hardware to acquire and pre-processing the collected signals

This hardware includes all the essential hardware to inspect the structures and depending on the needs of the application can contain elements to generate signals and acquire signals. Additionally, elements for transporting the signals from the sensors to the acquisition systems and for transforming these signals into a interpretable set of data such as filters, amplifiers, etc. Of course, the selection of a good hardware depends of the sensors and the application, since it is necessary to consider features such as frequencies, amplitude, kind of signal to apply, sample rate, etc. Some examples of hardware vendors are TiePie engineering, Trek, and National Instruments. The first company for instance, is the distributor of the Handyscopes HS4 and HS5 which are a high resolution oscilloscope and generator [16]. The company Trek offers many different piezo drivers and amplifiers which can work in a wide range of frequencies and voltages [18]. National Instruments offers different equipment for data acquisition such as the NI CompactRIO or the PXI chassis and software as Labview for developing applications. These equipments can be configurated according to the needs of the application, one example can be found in [168] where using Labview, System Identification and Advanced Signal Processing Toolkits as software and PXI-4472B, PXI-6652, PXI-8187, PXI-6602 as hardware developed an application for the monitoring of the Donghai Bridge in China. Using this system it is possible to calculate the extent of damages and deterioration using the frequency response from more than 500 sensors including acelerometers and FBG optical sensors spread across each segment of the bridge. Other application reported using national instruments equipment [144] included the use of Labview, DIAdem and Labview Signal Express as software and NI 9237, NI 9205, CompactRIO, NI CompactDAQ, NI 9219, NI 9211 as hardware in order to monitor by long- and short-term a range of structural systems during and after construction.

B.1.3 Software

The specialized software for SHM should consider and include: (i) pre-processing data techniques for de-noising, smoothing, normalization, etc; (ii) feature extraction and feature selection methods for reducing the dimensionality of the problem and (iii) a strategy for apply SHM levels in the strict sense. In commercial scale, there is no specialized software for Structural Health Monitoring although as shown below there are some integrated solutions with specialized software associated to a specific hardware.

Integrated systems

Currently there are some companies that offers some specific solutions for SHM involving sensors, hardware and software. For instance, Acellent technologies provide complete integrated systems with a specialized software and hardware for impact detection and detection, localization and quantification of damages [2]. Specifically for damage detection in composite structures, the company offers a system which consists of SMART Layer sensors, Portable ScanGenie hardware, SmartComposite software (see figure B.3). According to the information in the company web page, "this system is ideal for monitoring large composite structures such as aircraft wings, fuselage, wind blades, and pressure vessels. The system identifies damages such as delaminations, disbonds, and matrix cracking. It identifies the onset of damage in the structure and also quantifies the damage size."

Figure B.3: Composite Damage Detection System [3].

For impact monitoring, ***Acellent*** (see figure B.4) has a system to detect and monitor this type of defects in real time, including the measure of the force and location of an impact using a threshold. This system consists on the SMART Layer, IMGenie hardware, and AIM software. Some applications of this system include: Thermal protection system, Smart bumper for automobiles and Rocket motor testing.

Hot spots are specific geometric locations in a structure that are particularly prone to damage during operation and under variable loading conditions. ***Accelent*** offers a system that can be used for monitoring different kinds of joints, bearing/race assemblies, engine disks, and other vulnerable components [3]. This system consists of SMART Layer sensors, ScanSentry hardware, SmartPatch software(see figure B.5).

Figure B.4: Impact Monitoring System [3].

Figure B.5: Hot-Spot Monitoring [3].

The company ***Digitexx*** Data System offers different solution for real-time SHM for monitoring different kind of structures with a width-range of sensors. Some of these solutions are the portable systems PDAQ and the Digitexx RTMS. The last is a multi-channel real-time data acquisition and structural analysis system with manual and event-driven triggering (see figure B.6). This systems has 10 channels and a sampling rate of up to 1,000 samples per second burst and features as broadcasting data to remote locations, localized recording, local and remote data retrival and event-driver notifications [9].

Figure B.6: Digitexx SHM system [9].

Digitexx also offers the Digitexx's Server Software which broadcast and publishes real-time data directly to remote client locations. The architecture can be seen in the figure B.7.

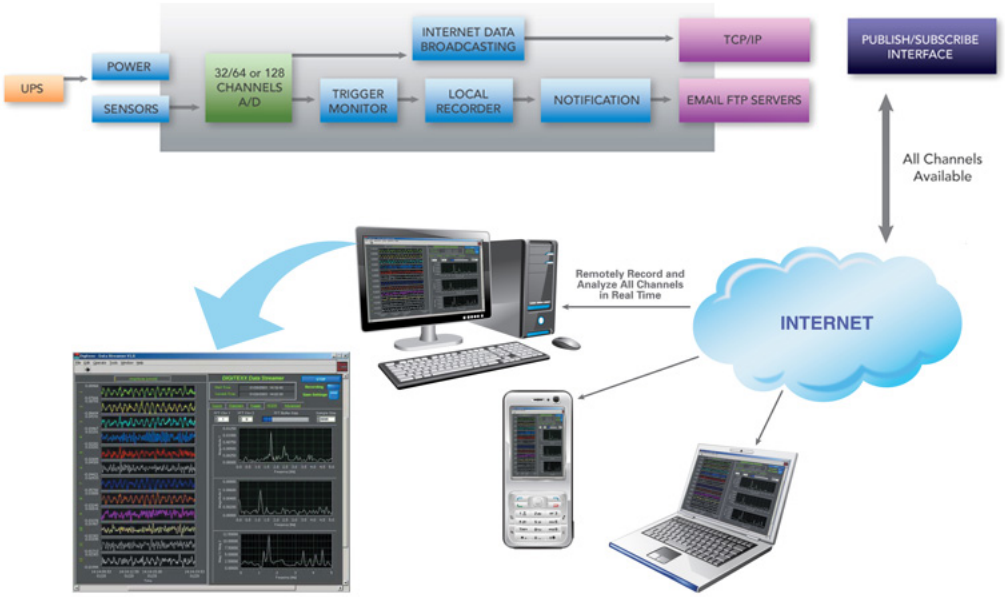

Figure B.7: Digitexx software for SHM [9].

The company ***CONDITION ENGINEERING- Condition & Structural Health Monitoring Solutions*** [8] has a system called SensorRope, it is used to automatically assess the conditions that lead to potential in-service failure of earthen infrastructure. This is a real-time system for diagnostic and to produce alerts if a dangerous condition occurs or is predicted to occur and can be used for local monitoring and widespread monitoring (see Figures B.8 and B.9).

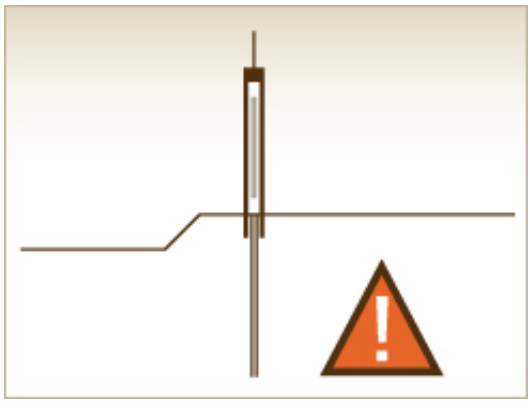

Figure B.8: SensorRope [8]

Figure B.9: SensorRope application [8].

The company ***MAGEBA*** [12] provides Robo®Control (see figures B.10, B.11 and B.12), this system is used to detect the absence of machine specifications at the component and conveys these to a central computer. Using this system it is possible to obtain data such as loads, movements, stresses and vibrations of any part of a structure. All the data are processed and made available through internet.

Figure B.10: Robo®Control mageba [12].

Figure B.11: Robo®Control mageba [12].

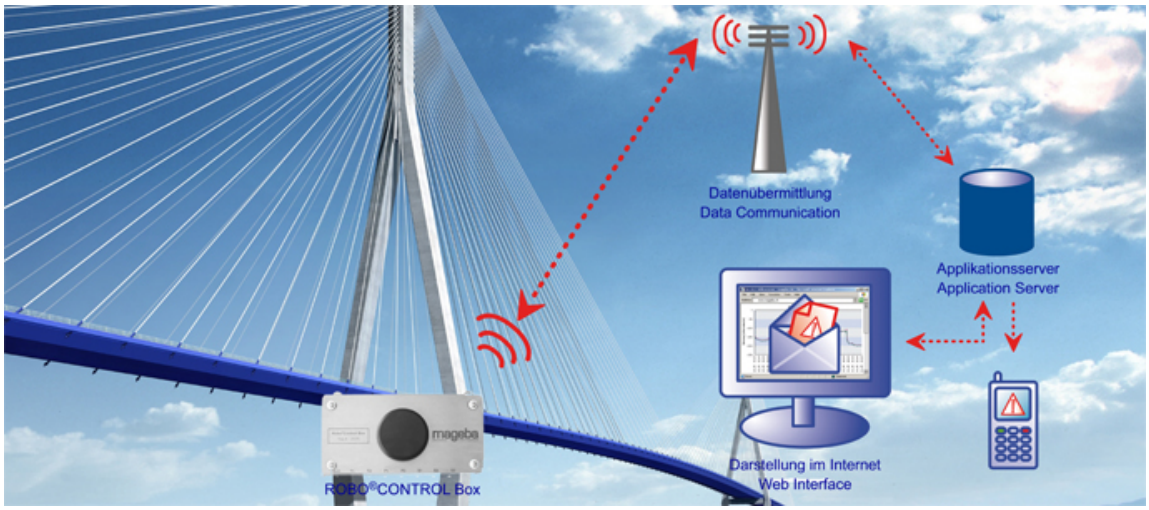

Figure B.12: Robo®Control general scheme [12].

Bridge Diagnostics Inc.[7] offers a system that include the use of a wide variety of wireless or hard wired sensors and two variety of systems for SHM, one of them for diagnostic and dynamic testing which can be used for wireless load testing and high-speed loggers to capture live loads. The other system is for tracking slow responses such as temperature-induced loads, concrete crack width opening, and pier rotations due to scour (figures B.13 and B.14).

The company ***FIBERPRO*** [11] offers specialized systems in Fiber Bragg sensors. One of his products is the Fiber Bragg Grating Interrogation (FBGI) which includes a laser and sensors modules (Figure B.15), among their application, it is possible to perform monitoring of large structures; overheat detection and special temperature monitoring as surveillance &

Figure B.13: Diagnostic & Dynamic Testing Systems[7].

Figure B.14: Long Term Data Collection systems[7].

safety systems; temperature profile monitoring in lakes, sea, rivers etc; and strain distribution monitoring for soil instabilities, ground slides and earthquake, etc. [17].

Figure B.15: Fiber Bragg Grating Interrogation (FBGI) [11].

Virginia Technologies, INC.[20] offers an embedded corrosion instrument (Figure B.16) that provides early warning of conditions that damage steel reinforcement leading to cracking, spalling, and other deterioration of concrete structures.

Figure B.16: Embedded corrosion monitoring [20].

Strainstall company [15] offers solutions for monitoring of marine systems on board, onshore and offshore. Some of them are: **STRESSALERT** which enhances vessel safety by maintaining a log of hull stresses throughout the life of a ship, and warning the master in real-time of any overstress or bow slamming (see Figure B.17). This is achieved by continuous measurement of the hull using deck-mounted long baseline strain gauges and a bow accelerometer to provide displays of bending moments, alarms when unsafe levels of stress are experienced, detection of bow slamming and long-term monitoring of fatigue.

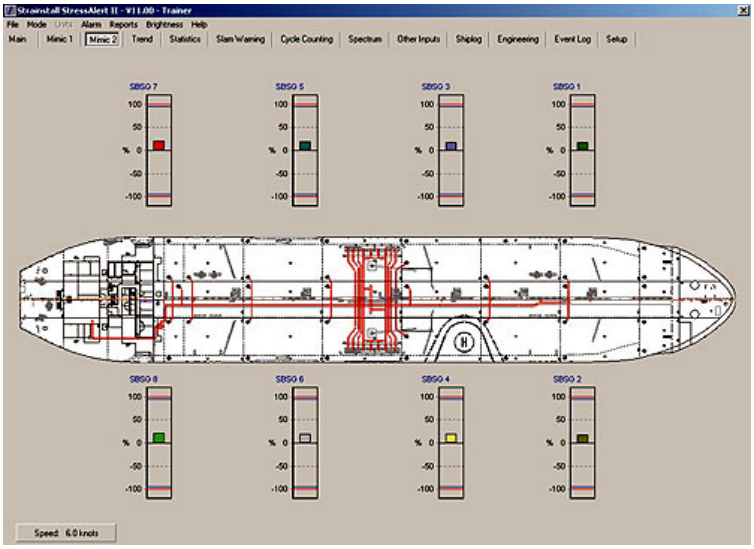

Figure B.17: Stressalert software [15].

Physical Acoustics Corporation [14] offers solution using acoustic emission (AE) among others (see Figure B.18). They offers also the **Sensor Highway II system** which supports 16 high speed AE monitoring channels, the input range of sensors is $\pm 10V$ and it has alarm and remote web based monitoring.

Figure B.18: Sensor Highway II [14].

As has been shown throughout this section, there are several companies that offer specific solutions for SHM, but these solutions are ever linked to the software and the hardware of a specific company and do not allow to improve the software or add new elements from another company. To solve this problem and create an open and reconfigurable hardware and software it is neccesary to define a new system based on elements commercially available. The next section presents a new proposal developed in the CoDAlab Group which uses Labview as software and a PXI chassis which can be configurated according to the application.

B.2 Structural Health Monitoring Laboratory of the CoDAlab Group

The Structural Health Monitoring laboratory of the CoDAlab group was designed by the author with his advisors in 2009. The acquisition of the elements was supported by the "Ministerio de Ciencia e Innovación" of Spain through the coordinated research project DPI2008-06564-C02, and the implementation was performed in collaboration with the PhD. student Fahit Gharibnezhad who is currently working in the group in the same area [171].
This laboratory allows to inspect structures by means of a signal generator, a switch matrix and a digitizer card; which are inserted in a PXI chassis and can be configurated depending of the needs of each experiment. In general, the SHM laboratory contains:

- A chasis of National Instruments (NI-PXI 1033): This chasis contains 5 slots, in each slot it is possible to add cards of National Instruments, for instance, generation cards, acquisition cards, switches cards and other elements. The chassis can be connected with a laptop using the PXI port by an express card.
- A NI PXI-5114 card, it is a 8-bit Digitizer/oscilloscope of 250MS/s with 40mV to 40V input ranges.

- A card NI PXI-5412, it is an arbitrary waveform generator with 14-bit resolution and 100 MS/s sampling rate.
- A Crosspoint Matrix Switch card. Using this card, it is possible to define until 4×32 matrix configuration. It is useful because depending of size of the structure and the number of sensors it is possible to reconfigure the number of terminals to use.
- A laptop, to connect the chassis and to execute the algorithms of acquisition and processing data.
- A wideband power amplifier to amplify the signals to apply to the sensors.
- A shelf to hang-up the elements to test.

In a general way, each experiment is performed as follows:

1. The instrumented structure is suspend using elastic ropes to isolate it from environment disturbances.
2. By mean of the switch module, one of all PZT transducers attached to the surface is chosen as the one which works as actuator .
3. An excitation signal is applied to the structure (vibrational input) throught the chosen PZT and using the NI-generator card.
4. The excitation signal is amplified using a wideband power amplifier before to apply to the structure.
5. The vibrational responses at different points are recorded by using the rest of PZTs (sensors) and the digitizer card.
6. Actuator and sensors are changed using the switch module, and the steps 2 to 4 are repeated. These changes and repetitions are automatically applied by the algorithms developed in Labview.
7. Data in text based format is saved and organized.
8. The structure is damaged (real or simulated damages) and the experiments are repeated (steps 2 until 6).
9. The strategies based on PCA to compare the vibrational responses of the current and healthy structures are applied.

Figure B.19: Laboratory in SHM.

Bibliography

[1] 20 airbus a380s inspected for cracks. $http : //articles.cnn.com/2012 - 01 - 25/travel/travel\_airbus-a380-cracks\_1\_airbus-a380s-cracks-noncritical?_s = pm : travel$, January 25 2012.

[2] Acellent technologies. $http : //64.105.143.179/software.asp$. feb. 10, 2012, 2012.

[3] Acellent technologies, inc. a structural health monitoring company. $www.acellent.com$, July 2012.

[4] Aena aeropuertos. $http : //www.aena.es/csee/satellite?pagename = estadisticas/home$, June 2012.

[5] Aircraft inspections. $http : //navyaviation.tpub.com/14022/css/14022_196.htm$, July 2012.

[6] Aircraft inspections. $http : //www.faa - aircraft - certification.com/aircraft - inspections.html$, July 2012.

[7] Bridge diagnostics inc. (bdi). $http : //www.bridgetest.com/products$, July 2012.

[8] Condition engineering-condition & structural health monitoring solutions. $http : //www.conditionengineering.com/sensorropedms.html$, July 2012.

[9] Digitexx data systems, inc. $http : //www.digitexx.com/rtms\_real - time\_monitoring\_system/$, July 2012.

[10] Federal aviation administration (faa). $http : //www.faa.gov/airports/airport - \_safety/safety\_management\_systems/$, July 2012.

[11] Fiberpro. $http : //www.fiberpro.co.kr/$, july 2012.

[12] Mageba. $http : //www.mageba.ch/en/dyn\_output.html?content.void = 734\&377358f92a0711c9084722b87392a9f3$, July 2012.

[13] Ndt resource center. $http : //www.ndt - ed.org/educationresources/$, July 2012.

[14] Physical acoustics corporation. $http : //www.pacndt.com/products/remote\%20 - monitoring/civil\_structures.pdf$, July 2012.

[15] Strainstall. $http : //www.ship-technology.com/contractors/controls/strainstall2/$, July 2012.

[16] Tiepie engineering . $http://www.tiepie.com/en$. nov. 20, 2012, November 2012.

[17] tradekorea.com. $http://www.tradekorea.com/e-catalogue/fiberpro/product-detail/p00041884/fiber\%20bragg\%20grating\%20interrogation\%20(fbgi).html$, July 2012.

[18] Trek. $http://www.trekinc.com/$. nov. 20, 2012., Nov 2012.

[19] The usa ś 2005-2009 multi-year hornet procurement contract. $http://www.defenseindustrydaily.com/the-usas-2005-2009-multi-year-hornet-procurement-contract-03882/$, July 2012.

[20] Virginia technologies, inc. $http://www.vatechnologies.com/eciindex.htm$, July 2012.

[21] A.P. Adewuyi and Z.S. Wu. Vibration-based structural health monitoring technique using statistical features from strain measurements. *ARPN Journal of Engineering and Applied Sciences*, 4:38–47, 2009.

[22] C. Alcala and J. Qin. Reconstruction-based contribution for process monitoring. *Automatica*, 45:1593–1600, 2009.

[23] C. Alcala and S.J. Qin. Unified analysis of diagnosis methods for process monitoring. In *7th IFAC Symposium on Fault Detection, Supervision and Safety of Technical Processes. Barcelona, Spain.*, 2009.

[24] D. N. Alleyne and P. Cawley. The interaction of lamb waves with defects. *IEEE Transcation on Ultrasonics, Ferroelectrics, and Frequency Control*, 39(3):381–397, 1992.

[25] A. Amditis, D. Bairaktaris, M. Bimpas, S. Camarinopolos, S. Frondistou-Yannas, V. Kalidromitis, M. Pozzi, J. Santana, N. Saillen, Y. Stratakos, T. Torfs, D. Ulieru, B. Wenk, and D. Zonta. Wireless sensor networks for seismic evaluation of concrete buildings. In *Fifth European Workshop on Structural Health Monitoring*, 2010.

[26] M.A. Torres Arredondo and C.P. Fritzen. On the application of digital signal processing techniques and statistical analysis for the localization of acoustic emissions. In *5th European Workshop in Structural Health Monitoring, EWSHM 2011, Sorrento, Italy: DEStech Publications, Inc.*, 2010, pp. 1017-1022.

[27] M.A. Torres Arredondo and C.P. Fritzen. A viscoelastic plate theory for the fast modelling of lamb wave solutions in ndt/shm applications. *ULTRAGARSAS (ULTRASOUND)*, 66:7–13, 2011.

[28] M.A. Torres Arredondo, C.P. Fritzen, and C. Yang. On the application of bayessian analysis and advanced signal processing techniques for the impact monitoring of smart structures. In *8th International Workshop in Structural Health Monitoring, IWSHM 2011, Stanford, CA: DEStech Publications, Inc.*, 2011, pp. 1062-1069.

[29] M. Azarbayejani. *Optimal Sensor Placement in Structural Health Monitoring (SHM) with a Field Application on a RC Bridge*. PhD thesis, The University of New Mexico, 2009.

[30] M. Azarbayejani, A.I. El-Osery, K.K. Choi, and M. M. Reda Taha. A probabilistic approach for optimal sensor allocation in structural health monitoring. *Smart Mater. Struct*, 17, 2008.

[31] S.G. Azevedo, J.E. Mast, S.D. Nelson, E.T. Rosenbury, H.E. Jones, T.E McEwan, D.J Mullenhoff, R. E. Hugenberger, R. D. Stever, J. P. Warhus, and M. G. Wieting. Hermes: A high-speed radar imaging system for inspection of bridge decks. nondestructive evaluation techniques for aging infrastructure and manufacturing. In *SPIE 294(6), 195204.*, 1996.

[32] A. Baker. *Composite Materials for Aircraft Structures*, chapter Indroduction and overview, pages 1–21. AIAAA Education Series, 2004.

[33] N. Bakhary, H. Hao, and A. Deeks. Neural network based damage detection using substructure technique. In *5th Australian Congress on Applied Mechanics (ACAM 2007), Brisbane, Australia*, December 2007.

[34] C. Bermes, J.Y. Kim, J. Qu, and L.J. Jacobs. Experimental characterization of material nonlinearity using lamb waves. *Applied Physics Letters*, 90(2):021901–3, 2007.

[35] D. Bernal. Damage detection from correlations in kalman filter innovations: Difficulties from variability in the noise statistics. In *Fifth European Workshop on Structural Health Monitoring. Sorrento-Italy*, 2010.

[36] D.C. Betz, G. Thursby, B. Culshaw, and W. Staszewski. Acousto-ultrasonic sensing using fiber bragg gratings. *Smart Materials and Structures*, 12:122–128, 2003.

[37] P. De Boe and J.C. Golinval. Principal component analysis of piezo-sensor array for damage localization. *Structural Health Monitoring: An International Journal*, 2(2):137–144, 2003.

[38] C. Brand and C. Boller. Identification of life cycle cost reductions in structures with self-diagnostic devices. In *NATO RTO Symposium on on Design for Low Cost Operation and Support. Otawa, Canada. Pp. 1-8*, 1999.

[39] J.M.W. Brownjohn. Structural health monitoring of civil infrastructure. *Phil. Trans. R. Soc. A*, 365:589–622, 2007.

[40] M. Chandrashekhar and R. Ganguli. Structural damage detection using modal curvature and fuzzy logic. *Structural Health Monitoring. An international journal*, 8:267–282, 2009.

[41] C.C. Chang and Z. Sun. Locating and quantifying structure damage using spatial wavelet packet signature. In Shih-Chi Liu, editor, *Smart Structures and Materials 2003: Smart Systems and Nondestructive Evaluation for Civil Infrastructures*, volume 5057, pages 97–105. SPIE, 2003.

[42] P. C. Chang, A. Flatau, and S.C. Liu. Review paper: Health monitoring of civil infrastructure. *Structural Health Monitoring*, 2:257–267, 2003.

[43] C. C. Chiang, J.R. Lee, and H.J. Shin. Structural health monitoring for a wind turbine system: a review of damage detection methods. *Measurement Science and Technology*, 19, 2008.

[44] J-H. Chou and J. Ghaboussi. Genetic algorithm in structural damage detection. *Computers & Structures*, 79(14):1335–1353, jun 2001.

[45] R.R. Coifman and M.V. Wickerhauser. Entropy-based algorithms for best basis selection. *IEEE Transactions on Information Theory*, 38(2):713–718, 1992.

[46] P.T. Coverley and W.J. Staszewski. Impact damage location in composite structures using optimized sensor triangulation procedure. *Smart Materials and Structures*, 12:795–803, 2003.

[47] N. Dervilis, R. Barthorpe, W. Staszewski, and K. Worden. Structural health monitoring of composite material typical of wind turbine blades by novelty detection on vibration response. *Key Engineering Materials*, 518:319–327, 2012.

[48] L.A. Dobrzanski, M. Sroka, and J. Dobrzanski. Application of neural networks to classification of internal damages steel working in creep service. *Journal of Achievements in Materials and Manufacturing Engineering*, 20:Issues 1–2. 2007. Pp. 303–306, 2007.

[49] S. Doebling, F. Hemez, and W. Rhee. Statistical model updating and validation applied to nonlinear transient structural dynamics. In *European Cost F3 Conference on System Identification & Structural Health Monitoring. Madrid*, 2000.

[50] S.W. Doebling, C.R. Farrar, and M.B. Prime. A summary review of vibration-based damage identification methods. *The Shock and Vibration Digest*, 30(2):91–105, 1998.

[51] K. Dragan, M. Mcgugan, S. Klimaszewski, T. Uhl, B. F. Sorensen, K.K. Borum, and K. Martyniuk. Structural integrity monitoring of wind turbine composite blades with the use of nde and shm approach. In *Fifth European Workshp on Structural Health Monitoring. Sorrento-Italy*, 2010.

[52] R. Dua, S.E. Watkins, D.C. Chandrashekhara, and F. Akhavan. Detection and classification of impact-induced damage in composite plates using neural networks. In *IJCNN 01. International Joint Conference on Neural Networks*, 2001.

[53] W. Fan and P. Qiao. Vibration-based damage identification methods: A review and comparative study. *Structural Health Monitoring*, 10(1):83–111, 2011.

[54] C. Farrar and D. Jauregui. Comparative study of damage identification algorithms applied to a bridge: I.experiment. *Smart Mater. Struct*, 7:704–719, 1998.

[55] C. Farrar and N. Lieven. Damage prognosis: the future of structural health monitoring. *Phil. Trans. R. Soc. A*, 365:623–632, 2007.

[56] C. R. Farrar, S. W. Doeblng, and D. A. Nix. Vibration-based structural damage identification. *Philosophical Transactions: Mathematical, Physical & Engineering Sciences*, 359(1778):131–149, 2001.

[57] C. R. Farrar and K. Worden. An introduction to structural health monitoring. *Phil. Trans. R. Soc. A*, 365:303–315, 2007.

[58] C.R. Farrar, F. Hemez, G. Park, A.N. Robertson, H. Sohn, and T.O. Williams. A coupled approach to developing damage prognosis solutions. *Key Engineering Materials*, 245-246:289–306, 2003.

[59] C.R. Farrar, H. Sohn, and G. Park. A statistical pattern recognition paradigm for structural health monitoring. In *9th ASCE Specialty Conference on Probabilistic Mechanics and Structural Reliability*, 2004.

[60] S.D. Fassois. Statistical time series methods for structural health monitoring. In *8 th International Conference on Damage Assessment on Structures (DAMAS). Beijing, China*, 2009.

[61] S.D. Fassois and J.S. Sakellariou. Time-series methods for fault detection and identification in vibrating structures. *Phil. Trans. R. Soc.*, 365:411–448, 2007.

[62] A. Fernandez, A. Guemes, C.P. Fritzen, and G. Mengelkamp. Comparison of health monitoring systems with fiber bragg grating and piezoelectric sensors. In *Third European Workshop on Structural Health Monitoring*, 2006.

[63] E.B. Flynn and M.D. Todd. A bayesian experimental design approach to structural health monitoring. In *Fifth European Workshop on Structural Health Monitoring*, 2010.

[64] E.B. Flynn and M.D. Todd. Optimal placement of piezoelectric actuators and sensors for detecting damage in plate structures. *Intelligent Material Systems and Structures*, 21(1):265–274, 2010.

[65] M.I. Friswell, J.E.T. Penny, and S.D. Garvey. A combined genetic and eigensensitivity algorithm for the location of damage in structures. *Computers and Structures*, 69(5):547–556, dec 1998.

[66] H. Fukunaga, N. Hu, and F.K. Chang. Structural damage identification using piezoelectric sensors. *International Journal of Solids and Structures*, 39(2):393, jan 2002.

[67] U. Galvanetto, C. Surace, and A. Tassoti. Structural damage detection based on proper orthogonal decomposition: Experimental verification. *AIAA Journal*, 46, No.7:1624–1630, 2008.

[68] U. Galvanetto and G. Violaris. Numerical investigation of a new damage detection method based on proper orthogonal decomposition. *Mechanical System and Signal Processing*, 21:1346–1361, 2007.

[69] R. Ganguli. A fuzzy logic system for ground based structural health monitoring of a helicopter rotor using modal data. *Journal of Intelligent Material Systems and Structures*, 12:397–407, 2001.

[70] R. Garziera, M. Amabili, and L. Collini. Structural health monitoring techniques for historical buildings. In *IV Conferencia Panamericana de END Buenos Aires*, 2007.

[71] A. Gastineau, T. Johnson, and A. Schultz. Bridge health monitoring and inspections- a survey of methods. Technical Report MN/RC 2009-29, Department of Civil Engineering. University of Minnesota., 2009.

[72] V. Giurgiutiu. Lamb wave generation with piezoelectricwafer active sensors for structural health monitoring. In *SPIE's 10th Annual International Symposium on Smart Structures and Materials and 8th Annual International Symposium on NDE for Health Monitoring and Diagnostics*, 2-6 March 2002, San Diego, CA.

[73] V. Giurgiutiu, A. Zagrai, and J.J. Bao. Piezoelectric wafer embedded active sensors for aging aircraft structural health monitoring. *Structural Health Monitoring*, 1:41–61, 2002.

[74] N. Godin, S. Huguet, R. Gaertner, and L. Salmon. Clustering of accoustic emission signals collected during tensile tests on unidirectional glass/polyester composite using supervised and unsupervised classifiers. *NDT&E International*, 37:253–264, 2004.

[75] J.C. Golinval, P.De Boe, A.M. Yan, and G. Kerschen. Structural damage detection based on principal component analysis of vibration measurements. In *58th Meeting of the Soc. for Mach. Failure Prevention Tech, Virginia Beach*, 2004.

[76] D. Gorinevsky, G. Gordon, S. Beard, A. Kumar, and F. Chang. Design of integrated shm system for commercial aircraft applications. In *Fifth International Workshop on Structural Health Monitoring, Stanford, CA.*, September 2005.

[77] K. Gryllias, I. Koukoulis, C. Yiakopoulos, I. Antaniadis, and C. Provatidis. Morphological processin of propoer orthogonal modes for crack detection in beam structures. *Journal of Mechanics of Materials and Structures*, Vol 4. No. 6:1063–1088, 2009.

[78] M. Gul and N. Catbas. Structural health monitoring and damage assessment using a novel time series analysis methodology with sensor clustering. *Journal of Sound and Vibration*, 330:1196–1210, 2011.

[79] M.F. Gunter, A. Wang, R.P. Fogg, S.E. Starr, K.A. Murphy, and R.O. Claus. Fiber optic impact detection and location system embedded in a composite material. In MA. (Eds. Claus R.O. Rogowsky, R.S.)Boston, editor, *Meeting on Fiber Optic Smart Structures and Skins V*, pages 262–269, 1993.

[80] K.H. Law H. Sohn. Application of load-dependent ritz vectors to bayesian probabilistic damage detection. *Probabilistic Engineering Mechanics*, 15:139–153, 2000.

[81] G. Hackmann, Sun F, N. Castaneda, C. Lu, and S. Dyke. A holistic approach to decentralized structural damage localization using wireless sensor networks. *Computer Communications*, 2012.

[82] H.T. Hann, B. Wilkerson, and J. Stuart. An artificial neuronal network for low-energy impact monitoring. *Journal of Thermoplastic Composite Materials*, 7:344–351, 1994.

[83] H. Hao and Y. Xia. Vibration-based damage detection of structures by genetic algorithm. *Journal of Computing in Civil Engineering*, 16(3):222–229, 2002.

[84] J.P.T. Higgins and S.G. Thompson. Quantifying heterogenity in a meta-analysis. *Statistics in medicine*, 21:1539–1558, 2002.

[85] BC Hoskin and AA Baker. *Composite Materials for Aircraft Structures*. New York: American Institute of Aeronautics and Astronautics;, 1896.

[86] A. Hot, G. Kerschen, E. Foltete, and S. Cogan. Detection and quantification of non-linear structural behavior using principal component analysis. *Mechanical System and Signal Processing*, 26:104–112, 2012.

[87] Y. Huan, F. Ghezzo, P. Rye, and S. Nemat-Nasser. Pasive damage detection in composite laminates with integrated sensing networks. In *SPIE*, 2008.

[88] A. Hyvrinen, J. Karhunen, and E. Oja. *Independent Component Analysis*. New York: Wiley. ISBN 978-0-471-40540-5, 2001.

[89] International Civil Aviation Organization (ICAO). State of global aviation safety 2011. $http://www.icao.int/safety/documents/icao_state-of-global-safety_web_en.pdf$.

[90] D. J. Inman and B. L. Grisso. *Adaptative Structures: Engineering Applications*, chapter Adaptative Structures for Structural Health Monitoring, pages 1–30. John Wiley & Sons, Ltd, 2007.

[91] M. Iskandarani. Application of neural network to damage classification in composite structures. *LATEST TRENDS on COMPUTERS*, I:109–113, 2010.

[92] A. Iwasaki, A. Todoroki, Y. Shimamura, and H. Kobayashi. An unsupervised statistical damage detection method for structural health monitoring (applied to detection of delamination of a composite beam). *Smart Materials and Structures*, 13, 2004.

[93] J. Jaques, D.E. Adams, D. Doyle, and W. Reynolds. Using impact modulation to identify loose bolts in a satellite structure. In *Fifth European Workshop on Structural Health Monitoring*, 2010.

[94] H. D. Jeong, H. J. Shin, and J. Rose. Detection of defects in a thin steel plate using ultrasonic guided wave. $http://www.ndt.net/article/wcndt00/papers/idn020/idn020.htm$, July 2012.

[95] J.Kullaa. Distinguishing between sensor fault, structural damage, and environmental or operational effects in structural health monitoring. *Mechanical Systems and Signal Processing*, 25:2976–2989, 2011.

[96] I.T. Jolliffe. *Principal Component Analysis*. Springer, 2002.

[97] S. Kabir, P. Rivard, and G. Ballivy. Neural-network-based damage classification of bridge infrastructure using texture analysis. *Canadian Journal of Civil Engineering*, V 35:(Report), Source Issue: 3, March 2008.

[98] S. Kaski, J. Nikklia, and T. Kohonen. Methods for interpreting a self-organized map in data analysis. In *6 th European Symposium of Artificial Neuronal Networks (E)SANN98. Brussels, Belgium, pp. 185-190*, 1998.

[99] Y. Kawano, T. Mikami, and F. Katsuki. Health monitoring of a railway bridge by fiber optic sensor (sofo). In *Fifth European Workshop on Structural Health Monitoring. Sorrento-Italy.*, 2010.

[100] G. Kerschen, P. De Boe, J.C. Golinval, and K. Worden. Sensor validation using principal component analysis. *Smart Materials and Structures*, 14:36–42, 2005.

[101] T. Kohonen. *Self Organizing Maps*. Springer, 2001.

[102] P. Kolakowski, L.E. Mujica, and J. Vehí. Two approaches to structural damage detection: Vdm vs cbr. *Journal of Intelligent Material Systems and Structures*, 16:63–79, 2006.

[103] P. Kraemer, I. Buethe, and C.-P. Fritzen. Damage detection under changing operational and environmental conditions using self organizing maps. In *SMART 11, Saarbruecken, Germany*, 2011.

[104] J.N. Kudva, N. Munir, and P.W. Tan. Damage detection in smart structures uisng neuronal networks and finite-element analysis. *Smart Materials and Structures*, 1:108–112, 1992.

[105] G. Park K. Farinholt L. Bornn, C. Farrar. Structural health monitoring with autoregressive support vector machines. *Journal of Vibration and Acustics*, 131:Issue 2, 021004, 2009.

[106] K. Lau, L. Yuan, L. Zhou, J. Wu, and C. Woo. Strain monitoring in frp lamintaes and concrete beams using fbg sensors. *Composite Structures*, 51:9–20, 2001.

[107] B. Leao, J. Gomes, R. Galvao, and T. Yoneyama. Aircraft flap and slat systems health monitoring using statistical process control techniques. In *Aerospace Conference IEEE.*, pages 1–8, 2009.

[108] J. W. Lee, J. D. Kim, C. B. Yun, J. H. Yi, and J. M. Shim. Health monitoring method for bridges under ordinary traffic loadings. *Journal of Sound and Vibration*, 257:247–264, 2002.

[109] Y. Lei, A.S. Kiremidjian, K.K. Nair, J.P. Lynch, K.H. Law, T.W. Kenny, E. Carryer, and A. Kottapalli. Statistical damage detection using time series analysis on a structural health monitoring benchmarck problem. In *9 th Conference on Applications of Statistics and Probability in Civil Engineering, San Francisco, CA. USA.*, 2003.

[110] Z.X. Li, T.H.T. Chan, and J.M. Ko. Fatigue analysis and life prediction of bridges with structural health monitoring data: Part i methodology and strategy. *International Journal of Fatigue*, 23:45–53, 2001.

[111] Y. Ling and S. Mahadevan. Integration of structural health monitoring and fatigue damage prognosis. *Mechanical System and Signal Processing*, 28:89–104, 2012.

[112] T.H. Loutas, A. Panopoulou, D. Roulias, and V. Kostopoulos. Intelligent health monitoring of aerospace composite structures based on dynamic strain measurements. *Expert Systems with Applications*, 39:8412–8422, 2012.

[113] J. Lynch and K. Loh. A summary review of wireless sensors and sensor networks for structural health monitoring. *The Shock and Vibration Digest*, 38(2):91–128, 2006.

[114] Torres Arredondo M.-A., M.M., Ramirez Lozano, and C.-P. Fritzen. *DispWare Toolbox - A scientific computer program for the calculation of dispersion relations for modal-based Acoustic Emission and Ultrasonic Testing.* University of Siegen, Siegen, Germany, 2011.

[115] S. Mallat. *A Wavelet Tour of Signal Processing*. Acedemic Press, 2nd edition, 1999.

[116] S.G. Mallat. A theory for multiresolution signal decomposition: the wavelet representation. *IEEE Transactions on Pattern Analysis and Machine Intelligence*, 11(7):674–693, 1989.

[117] G. Manson. Identifying damage sensitive, environmental insensitive features for damage detection. In *3rd. Int. Conf. Identification in Engineeing Systems. University of Wales Swansea, UK,*, 2002.

[118] G. Manson, K. Worden, K. Holford, and R. Pullin. Visualisation and dimension reduction of acoustic emission data for damage detection. *Journal of Intelligent Material Systems and Structures*, 12:529–536, 2001.

[119] C. Mares and C. Surace. An application of genetic algorithms to identify damage in elastic structures. *Journal of Sound and Vibration*, 195(2):195–215, aug 1996.

[120] J.M. Menéndez, A. Fernández, and A. Güemes. Shm with embedded fibre bragg gratings and piezoelectric devices. In *Third Europan Workshop on Structural Health Monitoring*, 2006.

[121] D. Merkl and A. Rauber. Cluster connections - a visualization technique to reveal cluster boundaries in self-organizing maps. In *9 th Italian Workshop of Neuronal Nets (WIRN97): Springer*, 1997.

[122] M. Mieloszyk, K. Majewska, A. Zak, and W. Ostachowicz. A wing for small aircraft application with an array of fibre bragg grating sensors. In *Fifth European Workshop on Structural Health Monitoring*, 2010.

[123] B. Mnassri, E. El Adel, and M. Ouladsine. Fault localization using principal component analysis based on a new contribution to the squared prediction error. In *16th Mediterranean Conference on Control and Automation Congress Centre, ajaccio, France. June 25-27*, 2008.

[124] L.E. Mujica, J. Rodellar, A. Fernandez, and A. Güemes. Q-statistic and t^2-statistic pca-based for damage assessment in structures. *Structural Health Monitoring. An international Journal*, 10, No. 5:539–553, 2011.

[125] L.E. Mujica, J. Rodellar, and J. Vehí. A case based reasoning approach for damage assessment in smart structures. In *III ECCCOMAS Thematic Conference on Smart Structures and Materials. Gdansk, Poland.*, July 2007.

[126] L.E. Mujica, J. Rodellar, and J. Vehí. A review of impact damage detection in structures using strain data. *International Journal of COMADEM*, 13(1):3–18, 2010.

[127] L.E. Mujica, J. Rodellar, J. Vehí, K. Worden, and W. Staszewski. Extended pca visualization of system damage features under enviromental and operational variations. In *Smart Structures and Materials & Nondestructive Evaluation and Health Monitoring. San Diego, California, USA.*, March 2009.

[128] L.E. Mujica, M. Ruiz, X. Berjaga, and J. Rodellar. Multiway partial least square (mpls) to estimate impact localization in structures. In *7 th IFAC Symposium on Fault Detection, Supervision and Safety of Technical Process. Barcelona-Spain*, 2009.

[129] L.E. Mujica, M. Ruiz, A. Gemes, and J. Rodellar. Contribution plots on pca based indices for damage identification on structures. In *Proc of the 4th. ECCOMAS Thematic Conference on Smart Structures and Materials. Porto, Portugal*, 2009.

[130] L.E. Mujica, D.A. Tibaduiza, and J. Rodellar. Data-driven multiactuator piezoelectric system for structural damage localization. In *Fifth World Conference on Structural Control and Monitoring. Tokio-Japan*, July 2010.

[131] L.E. Mujica, J. Vehí, J. Rodellar, and P. Kolakowski. A hybrid approach of knowledge-based reasoning for structural assessment. *Smart Materials and Structures*, 14:1554–1562, nov 2005.

[132] L.E. Mujica, J. Vehí, J. Rodellar, and P. Polakowsky. Damage identification by using soft-computing techniques. In *Smart Materials and Structures-AMAS Workshop-SMART'03. Jadwisin*, September 2003.

[133] L.E. Mujica, J. Vehí, M. Ruiz, M. Verleysen, W. Staszewski, and K. Worden. Multivariate statistics process control for dimensionality reduction in structural assessment. *Mechanical Systems and Signal Processing*, 22:155–171, 2008.

[134] L.E. Mujica, J. Vehí, W. Staszewski, and K. Worden. Impact damage detection in aircraft composites using knowledge-based reasoning. *Structural Health Monitoring, an International Journal*, 7(3):215–230, 2008.

[135] Y. Nitta and A. Nishitani. Structural health monitoring methodology consisting of two stages with different purposes. In *13 th World Conference on Earthquake Engineering. Vancouver, B.C., Canada*, August 2004.

[136] P. Nomikos and J.F. MacGregor. Monitoring batch processes using multiway principal component analysis. *AIChE Journal*, 40(8):1361–1375, aug 1994.

[137] P. Panetsos, E. Ntotsios, C. Papadimitriou, D.C Papadioti, and P. Dakoulas. Health monitoring of metsovo bridge using ambient vibrations. In *Fifth European Workshop on Structural Health Monitoring. Sorrento-Italy*, 2010.

[138] C. Papadimitriou, D.C Papadioti, and E. Ntotsios. Structural damage identification using a bayesian model selection framework. In *Fifth European Workshop on Structural Health Monitoring. Sorrento-Italy.*, 2010.

[139] G. Park and D. Inman. Structural health monitoring using piezoelectric impedance measurements. *Philosophical Transactions of The Royal Society*, 365:373–392, 2007.

[140] G. Park, S.G. Taylor, K.M. Farinholt, and C.R. Farrar. Shm of wind turbine blades using piezoelectric active sensors. In *Fifth European Workshop on Structural Health Monitoring*, 2010.

[141] S. W. Park, D.H. Kang, H.J. Bang, S.O. Park, and C.G. Kim. Strain monitoring and damage detection of a filament wound composite preassure tank using embedded fiber bragg grating sensors. *Key Engineering Materials*, 321-323:182–185, 2006.

[142] A. Raghavan and Carlos E. S. Cesnik. Review of guided-wave structural health monitoring. *The Shock and Vibration Digest*, 39:91–114, 2007.

[143] L. J. Ren, X. C. Jiang, G.H. Sheng, and W.W. Yang. State inspection for transmission lines based on independient component analysis. *Journal of Shanghai Jiaotong University (Science)*, 14:129–132, 2009.

[144] Elstner Associates Inc. Richard Lindenberg Wiss, Janney. Performing structural health monitoring with modular ni hardware and software.

[145] C. Riveros. Structural health monitoring methodology for simply supported bridges: Numerical implementation. *Revista Facultad de Ingeniera Universidad de Antioquia*, 039:42–55, 2007.

[146] J. Rose. Dispersion curves in guided wave testing. *Materials Evaluation*, pages 20–22, 2003.

[147] J.L. Rose. *Ultrasonic waves in solid media*. Cambridge University Press, Cambridge, 1999.

[148] A. Rytter. *Vibration Based Inspection of Civil Engineering Structures*. PhD thesis, Department of Building Technology and Structural Engineering. Aalborg University, Denmark, 1993.

[149] M. Salehi, S. Ziaei-Rad, M. Ghayour, and M.A. Vaziri-Zanjani. A frequency response based structural damage localization method using proper orthogonal decomposition. *Journal of Mechanics*, Vol. 27 No. 2. DOI: 10. 1017/ jmech.2011.17:Pp. 157–166, June 2011.

[150] A. Salehian. Identifying the location of a sudden damage in composite laminates using wavelet approach. Master's thesis, Worcester Polytechnic Institute, 2003.

[151] P.M. Schindler, R.M. May, R.O. Claus, and J.K. Shaw. Location of impacts in composite panels by embedded fibre optic sensors and neuronal network processing. In CA. (Spillman W.B.) San Diego, editor, *SPIE Conference: Smart Structures and Materials Symposium; Smart Sensing, Processing and Instrumentation*, volume 2444, pages 481–490, 1995.

[152] M. Scholz. *Approaches to Analyse and Interpret Biological Profile Data*. PhD thesis, Max Planck Institute of Molecular Plant Physiology, Potsdam University, 2006.

[153] G. Serino and M. Spizzuoco. The health monitoring system of an isolated religious building in italy. In *Fifth European Workshop on Structural Health Monitoring*, 2010.

[154] I.V. Shadrivov, A.B. Kozyrev, D.W. Van der Weide, and Y.S. Kivshar. Tunable transmission and harmonic generation in nonlinear metamaterials. *Applied Physics Letters*, 93(16)::161903–3, 2008.

[155] Q. Shan and G. King. Fuzzy techniques for impact locating and magnitude estimating. *Insight - Non-Destructive Testing and Condition Monitoring*, 45(3):190–195, mar 2003.

[156] J.S. Sirkis, J.K. Shaw, T.A. Berkoff, A.D. Kersey, E.J. Fribele, and R.T. Jones. Development of an impact detection technique using optical fiber sensor ans neuronal networks. In J.S.) (Edited by Sirkis, editor, *SPIE on SMART Structures and Materials Symposium; Smart Sensing, Processing, and Instrumentation . Orlando, FL.*, volume 2191, pages 158–165, 1994.

[157] H. Sohn, C. Farrar, and N. Hunter. Structural health monitoring using statistical pattern recognition techniques. *Journal of Dynamic Systems, Measurement and Control*, 123:706–711, 2001.

[158] H. Sohn, C. R. Farrar, N. Hunter, and K. Worden. Applying the lanl statistical pattern recognition paradigm for structural health monitoring to data from a surface-effect fast patrol boat. Technical Report LA-13761-MS, Los Alamos National Laboratory, 2001.

[159] H. Sohn, K. Worden, and C.R. Farrar. Statistical damage classification under changing environmental and operational conditions. *Journal of Intelligent Material Systems and Structures*, 13(9):561–574, 2002.

[160] H. Song, L. Zhong, and B. Han. *Advanced Data Mining and Applications*, chapter Structural Damage Detection by Integrating Independent Component Analysis and Support Vector Machine, pages 670–677. Springer Berlin / Heidelberg, 2005.

[161] A. Sophian, G. Y. Tian, D. Taylor, and J. Rudlin. A feature extraction technique based on principal component analysis for pulsed eddy current ndt. *NDT&E International*, 36:37–41, 2003.

[162] W.J. Staszewski. Advanced data preprocessing for damage identification based on pattern recognition. *The International Journal of System and Science, Special issue on Intelligent Fault detection*, 31(11):1381–1396, nov 2000.

[163] W.J. Staszewski, C. Biemans, C. Boller, and G. Tomlinson. Impact damage detection in composite structures using passive acousto-ultrasonic sensors. *Key Engineering Materials*, 221-222:389–400, 2002.

[164] W.J. Staszewski and K. Worden. *Health Monitoring of Aerospace Structures*, chapter Signal Processing for Damage Detection, pages 164–206. Wiley, 2004.

[165] W.J. Staszewski, K. Worden, R. Wardle, and G.R. Tomlinson. Fail-safe sensor distributions for impact detection in composite materials. *Smart Materials and Structures*, 9:298–303, 2000.

[166] A. Subasi. Application of adaptive neuro-fuzzy inference system for epileptic seizure detection using wavelet feature extraction. *Computers in Biology and Medicine*, 37(2):227–244, 2007.

[167] Z. Sun and C.C. Chang. Statistical wavelet-based method for structural health monitoring. *Journal of Structural Engineering*, 130:1055–1062, 2004.

[168] Yonglin Zhan JUST ONE Technology. Structural health monitoring of the donghai bridge using labview and pxi. $http://sine.ni.com/cs/app/doc/p/id/cs-12706$.

[169] R.C. Tennyson, W.D. Morison, and E. Christians. Application of fiber optic sensors for impact damage detection on space. In *5 th International Workshop on Structural Health Monitoring*, 2005.

[170] D. A. Tibaduiza, L. E. Mujica, A. Güemes, and J. Rodellar. Active piezoelectric system using pca. In *Fifth European Workshop on Structural Health Monitoring*, 2010.

[171] D.A. Tibaduiza, F. Gharibnezhad, L.E. Mujica, and J. Rodellar. Design and validation of structural health monitoring system for aeronautical structures. $http://decibel.ni.com/content/docs/doc-11446$.

[172] D.A. Tibaduiza, L.E. Mujica, and J. Rodellar. Comparison of several methods for damage localization using indices and contributions based on pca. *Journal of Physics: Conference Series*, 305 012013 doi:10.1088/1742-6596/305/1/012013, 2011.

[173] M.A. Torres, I. Buethe, D.A. Tibaduiza, J. Rodellar, and C.P. Fritzen. Damage detection and classification in pipework using acousto-ultrasonics and probabilistic nonlinear modelling. In *Workshop on Civil Structural Health Monitoring (CSHM-4), Berlin-Germany*, 2012.

[174] M.A. Torres, D.A. Tibaduiza, L.E. Mujica, J. Rodellar, and C.P. Fritzen. Damage assessment in a stiffened composite panel using non-linear data-driven modelling and ultrasonic guided waves. In *4 th International Symposium on NDT in Aerospace. Ausburg, Germany*, 2012.

[175] M.A. Torres, D.A. Tibaduiza, L.E. Mujica, J. Rodellar, and C.P. Fritzen. Data-driven multivariate algorithms for damage detection and classification: Evaluation and comparison. *Submitted to Structural Control and Health Monitoring*, 2012.

[176] M.A. Torres-Arredondo and C.P. Fritzen. Characterization and classification of modes in acoustic emission based on dispersion features and energy distribution analysis. In *International Conference on Structural Engineering Dynamics, ICEDyn 2011, Tavira, Portugal*, 2011.

[177] I. Trendofilova, V. Lenaerts, G. Kerschen, J.C. Golinval, and H. Van Brusssel. Detection, localization and identification of nonlinearities in structural dynamics. In *ISMA International Conference on Noise and Vibration Engineering*, 2000.

[178] E.D. Uebeyli. Adaptive neuro-fuzzy inference system employing wavelet coefficients for detection of ophthalmic arterial disorders. *Expert Systems with Applications*, 34(3):2201–22, 2008.

[179] A. Ultsch. *Information and Classification-Concepts, Methods and Applications*, chapter Self-Organizing neuronal networks for visualization and classification. Springer, 1993.

[180] J. Vesanto, J. Himberg, E. Alhoniemi, and J. Parhankangas. *SOM Toolbox for Matlab 5*. Helsinki University of Technology: Helsinki, Finland, 2000.

[181] Z. Wang, J. Chen, G. Dong, and Y. Zhou. Constrained independent component analysis and its application to machine fault diagnosis. *Mechanical Systems and Signal Processing*, 25:2501–2512, 2011.

[182] Z. Wang and K.C.G. Ong. Autoregresive coefficients based hotellings t^2 control chart for structural health monitoring. *Computers and Structures*, 86:1918–1935, 2008.

[183] D. Weems, H.T. Hahn, E. Granlund, and I.G. Kim. Impact detection in composite skin panels using piezoelectric sensors. In *In American Helicopter Society 47th Annual Forum Proceedings*, pages 643–652, 1991.

[184] J. Westerhuis, T. Kourti, and J. MacGregor. Comparing alternative approaches for multivariate statistical analysis of batch process data. *Journal of Chemometrics*, 13:397–413, 1999.

[185] S. Wildy, A. Kotousov, and J. Codrington. New passive defect detection technique. In *5 th Australasian Congress on Applied Mechanics, ACAM 2007. Brisbane, Australia*, 2007.

[186] S. Wold, P. Geladi, K. Esbensen, and J. Ohman. Multiway principal component and pls analysis. *Journal of Chemometrics*, 1:41–56, 1987.

[187] H. Woo and H. Sohn. Parameter estimation of the generalized extreme value distribution for structural health monitoring. *Probabilistic Engineering Mechanics*, 21, Issue 4:366–376, 2006.

[188] K. Worden and G. Manson. The application of machine learning to structural health monitoring. *Phil. Trans. R. Soc. A*, 365:515–537, 2007.

[189] K. Worden, G. Manson, and N.R.J Fieller. Damage detection using outliers analysis. *Journal of Sound and Vibration*, 229:647–667, 2000.

[190] K. Worden and W.J. Staszewski. Impact location and quantification on a composite panel using neural networks and a genetic algorithm. *Strain*, (36):61–70, 2000.

[191] K. Worden, W.J. Staszewski, and J.J. Hensman. Natural computing for mechanical systems research: A tutorial overview. *Mechanical Systems and Signal Processing*, 25(1):4–111, 2011.

[192] X. Xu, F. Xiao, and S. Wang. Enhanced chiller sensor fault detection, diagnosis and estimation using wavelet analysis and principal component analysis methods. *Applied Thermal Engineering*, 28:226–237, 2008.

[193] A.M. Yan, G. Kerschen, P. De Boe, and J.C. Golinval. Structural damage diagnosis under varying environmental conditions part i: A linear analysis. *Mechanical Systems and Signal Processing*, 19(4):847–864, July 2005.

[194] A.M. Yan, G. Kerschen, P. De Boe, and J.C. Golinval. Structural damage diagnosis under varying environmental conditions part ii: Local pca for non-linear cases. *Mechanical Systems and Signal Processing*, 19(4):865–880, July 2005.

[195] T. Yan, K. Holford, D. Carter, and J. Brandon. Classification of accoustic emission signatures using a self-organization neuronal network. *Journal of Acoustic Emission*, 17(1-2):49–59, 1999.

[196] K.C. Yap and D.C. Zimmerman. The effect of coding on genetic algorithm based structural damage detection. In *Proceedings of the 16th International Modal Analysis Conference*, number 1, pages 165–171, Santa Barbara, CA, feb 1998. Society for Experimental Mechanics, Inc, Bethel.

[197] Lin Ye, Ye Lu, Z. Su, and G. Meng. Functionalized composite structures for new generation airframes: a review. *Composites Science and Technology*, 65:1436–1446, 2005.

[198] H. Yue and S.J. Qin. Reconstruction-based fault identification using a combined index. *Ind. Eng. Chem. Res.*, 40:4403–4414, 2001.

[199] C. Zang, M.I. Friswell, and M. Imregun. Structural damage detection using independent component analysis. *Structural Health Monitoring. An International Journal*, 31(1):69–83, 2004.

[200] C. Zang and M. Imregun. Structural damage detection using artificial neural networks and measured frf data reduced via principal component projection. *Journal of Sound and Vibration*, 242(5):813–827, 2001.

[201] Y. Zhang, C. Zhou, and Z. Li. Piezo paint acoustic emission sensor and its application to online structural health prognosis. In *Fifth European Workshop on Structural Health Monitoring*, 2010.

[202] W. Zhou, D. Chakraborty, N. Kowali, A. Papandreou, D. Cochran, and A. Chattopadhyay. Damage classification for structural health monitoring using time-frequency feature extraction and continuous hidden markov models. In *Signals, System and Computers, 2007. ACSSC 2007. Conference Record of the Forty-First Asilomar Conference on*, 2008.

[203] Y. Zhou, S. Tang, C. Zang, and R. Zhou. *Advances in Information Technology and Industry Applications*, chapter An artificial inmune pattern recognition approach for damage classification in structures, pages 11–17. Springer Berlin Heidelberg, 2012.